



universität  
wien

# MASTERARBEIT

„Investigation of the Role of PTEN and  
the Alternative Activation of Macrophages in Pulmonary Fibrosis“

Verfasserin

Julia Barbara Kral, BSc

angestrebter akademischer Grad

Master of Science (MSc)

Wien, 2012

Studienkennzahl lt. Studienblatt: A 066 877

Studienrichtung lt. Studienblatt: Genetik und Entwicklungsbiologie

Betreuerin / Betreuer: o.Univ.Prof.Dr. Thomas Decker



## Danksagung

Ich möchte mich ganz herzlich bei allen bedanken, die mich beim Erarbeiten und Erstellen dieser Arbeit und bei meinem Studium unterstützt haben.

Für die Chance an diesem spannenden Projekt zu arbeiten und für das Leiten durch und die Betreuung während des Projekts, möchte ich mich ganz besonders bei meinem Supervisor Priv. Doz. Dr. Gernot Schabbauer bedanken.

Ein großes Dankeschön möchte ich auch an Ao. Univ.-Prof. Dr. Sylvia Knapp aussprechen, für ihre Supervision, die hilfreichen Tipps und dafür, dass ich die Möglichkeit hatte mit ihrem Team zusammenzuarbeiten.

Mein besonderer Dank richtet sich an Dr. Joanna Warszawska und Mag. Emine Sahin für die Einschulung in die Labortechniken, ihre praktische Unterstützung, ihr Zuhören und die inspirierenden Diskussionen. Ein ganz besonderer Dank gilt allen Teammitgliedern für ihre Einschulung und Mitwirkung.

Abschließend will ich mich bei meiner Familie und bei meinen Freunden bedanken. Besonders gilt dieses Dankeschön meinen Eltern Barbara und Dipl.Ing. Wolfgang Kral für die Unterstützung und Begleitung durch das Studium. Für die moralische Unterstützung, das Zuhören und die Geduld, sage ich mich bei meinem lieben Lebensgefährten Alexander Pointner herzlichen Dank.

**Vielen lieben Dank!!!**



## 1. Abstract

Pulmonary fibrosis is characterized by a dysregulated wound healing response accompanied by the pathological replacement of functional tissue by connective tissue. This process leads to the malfunction of the lung and therefore mortality is considerably high. Suitable treatment options are scarce and the development of new therapies is needed.

Increasing evidence of the contribution of innate immunity in pulmonary fibrosis awakened our interest in the impact of myeloid phosphatase and tensin homolog deleted in chromosome ten (PTEN) in this disease. The bleomycin induced pulmonary fibrosis model showed that myeloid PTEN deficient mice developed more severe disease progression than their wild-type littermates. One of the identified differences was the increase in IL-4, a potent inducer of alternative activation of macrophages, in the conditional PTEN knockout mice. Therefore we wanted to elucidate possible changes in the alternatively activated phenotype of macrophages and possible pro-fibrotic consequences. PTEN deficiency led to an elevated expression of Arginase 1 and FIZZ, while YM1 and MRC1 were decreased after stimulation with IL-4 or IL-13. Additionally Arginase 1, an important enzyme for collagen synthesis, was induced by bleomycin and increased in myeloid PTEN knockout mice. Thus we assume that the phosphoinositide 3-kinase (PI3K), which action is inhibited by PTEN, is a putative mediator of alternative activation of macrophages and consequently exhibit a negative influence on pulmonary fibrosis.



## 2. Zusammenfassung

Unkontrollierter Wundheilungsprozess in der Lunge kann zu pulmonaler Fibrose führen. Dabei kommt es zu einer pathologischen Vermehrung des Bindegewebes, wodurch es zur geminderten Lungenfunktion kommt und im Extremfall zum Tod führen kann. Auf Grund des Mangels an adequaten Behandlungsmethoden, besteht die Notwendigkeit, den Mechanismus genauer aufzuklären. Die enorme Bedeutung des angeborenen Immunsystems an fibrotischer Pathogenese weckte unser Interesse, mehr über die Funktion der myeloid exprimierten Phosphatase PTEN (Phosphatase and Tensin homolog) zu wissen. Durch Bleomycin induzierte Lungenfibrose konnten wir zeigen, dass der myeloide Knockout von *pten* in Mäusen zu einer schwereren Fibrose führte, im Vergleich zu Wildtypmäusen. Zusätzlich stellten wir eine erhöhte Expression von IL-4 fest, welches ein wichtiges Zytokin für die Differenzierung zu alternativ aktivierten Makrophagen darstellt. Die Rolle von PTEN in der Differenzierung zu alternativ aktivierten Makrophagen, wurde durch die Stimulierung von alveolären Makrophagen mit IL-4 und IL-13 getestet. Der Mangel an PTEN bewirkte eine erhöhte Expression von Arginase 1 und FIZZ, während YM1 und MRC1 in geringem Ausmaß gebildet wurden. Um deren Relevanz für Bleomycin induzierte Lungenfibrose zu deklarieren, wurde die Expression von Arginase 1 während der Krankheit untersucht. Dabei wurde entdeckt, dass deren Expression durch Bleomycin induziert wurde und in den myeloiden PTEN knockout Mäusen erhöht war. Das lässt den Schluss zu, dass die Phosphoinositol 3-kinase (PI3K), welche durch PTEN inhibiert wird, die alternative Aktivierung von Makrophagen, sowie die Fibrogenese beeinflusst.



# Table of Contents

<b>1. Abstract</b> .....	<b>1</b>
<b>2. Zusammenfassung</b> .....	<b>3</b>
<b>3. Abbreviations</b> .....	<b>9</b>
<b>4. Introduction</b> .....	<b>13</b>
4.1. Immune System .....	13
4.1.1. Innate Immune System.....	13
4.1.2. Adaptive Immune System .....	15
4.1.3. Cytokines and Chemokines.....	16
4.1.4. Phosphoinositide 3-kinase Pathway.....	16
4.1.5. Arginase 1 .....	19
4.2. Plasticity of Immune Cells.....	21
4.2.1. Macrophages.....	21
4.2.2. Dendritic Cells .....	26
4.2.3. T Helper Cells.....	27
4.3. Fibrosis.....	29
4.3.1. From Acute to Chronic Inflammation to Fibrosis .....	30
4.3.2. Mechanism of Fibrosis.....	32
4.3.3. Bleomycin Induced Lung Fibrosis .....	35
4.4. Aim of the Study.....	36
<b>5. Materials and Methods</b> .....	<b>37</b>
5.1. Mice.....	37
5.2. Genotyping.....	37
5.2.1. Murine Tissue Lysis.....	37
5.2.2. Polymerase Chain Reaction PCR .....	38
5.2.3. Gel Electrophoresis .....	39
5.3. In Vivo Experiments .....	40
5.3.1. Anesthesia .....	40
5.3.2. Fibrosis Induction .....	41
5.3.3. Clinical Fibrosis Scoring .....	41
5.3.4. Bronchoalveolar Lavage.....	41
5.3.5. Lung Homogenization.....	42

## Table of Contents

5.3.6.	Preparation of Single Cell Suspensions of Murine Lungs .....	43
5.4.	In Vitro Experiments.....	44
5.4.2.	Isolation of Alveolar Macrophages .....	44
5.4.3.	Stimulation of Alveolar Macrophages <i>In Vitro</i> .....	45
5.5.	Analytical Methods.....	45
5.5.1.	Histology .....	45
5.5.2.	Hematoxinilin and Eosin Stain .....	46
5.5.3.	Sirius Red Stain.....	47
5.5.4.	Quantification of Histological Sections .....	48
5.5.5.	Hydroxyproline Measure.....	48
5.5.6.	RNA Isolation with TRIzol.....	49
5.5.7.	Reverse Transcription .....	50
5.5.8.	Quantitative Polymerase Chain Reaction (qPCR) .....	51
5.5.9.	SDS-PAGE .....	52
5.5.10.	Western Blot .....	55
5.5.11.	Enzyme Linked Immunosorbent Assay (ELISA) .....	55
5.5.12.	Cytospin.....	57
5.5.13.	Antibody Staining for Flow Cytometry .....	58
5.6.	Statistical Analysis .....	59
<b>6.</b>	<b>Results .....</b>	<b>61</b>
6.1.	Establishment and Validation of the Bleomycin Induced Pulmonary Fibrosis Model .....	61
6.2.	PTEN Deficient Alveolar Macrophages Display a Decreased Inflammatory Response.....	65
6.3.	Myeloid PTEN Deficiency Promotes Fibrotic Response in Bleomycin Induced Lung Injury .....	66
6.4.	Cytokines Linked to Inflammation and Fibrosis are Partly Elevated in Myeloid PTEN Deficient Mice.....	71
6.5.	IL-4/ IL-13 Stimulation Leads to Enhanced PI3K Activity in PTEN Deficient Alveolar Macrophages .....	74
6.6.	The Phenotypic Analysis of Naïve Lung Macrophages Deficient for PTEN .....	74
6.7.	IL-4 or IL-13 Stimulated PTEN Deficient Macrophages Display a M2 like Phenotype.....	77

6.8. In Vitro Stimulation with IL-4/ IL-13 Leads to Increased Levels of Arginase 1 in PTEN Deficient Alveolar Macrophages .....	80
6.9. Arginase 1 Expression is Increased in Myeloid PTEN Deficient Mice Post BLM Treatment.....	81
6.10. Myeloid Cells are Responsible for the Expression of Arginase 1 in BLM Induced Pulmonary Fibrosis .....	82
6.11. Myeloid Arginase 1 deficient mice have a reduced loss of weight due to BLM application.....	83
6.12. Cytokine Profile of Myeloid Arginase 1 Deficient Mice in Pulmonary Fibrosis .....	84
<b>7. Discussion and Perspectives.....</b>	<b>87</b>
<b>8. List of Figures.....</b>	<b>95</b>
<b>9. List of Tables .....</b>	<b>98</b>
<b>10. Curriculum Vitae.....</b>	<b>99</b>
<b>11. Literature.....</b>	<b>101</b>



### 3. Abbreviations

Akt	Protein kinase B (PKB)
AP1	Activator protein 1
Arg1	Arginase 1
BLM	Bleomycin
C57BL/6J	C57 Black 6 mice from the Jackson Laboratory
CCL	Chemokine (C-C motif) ligand
CD	Cluster of differentiation
CpG ODN	Cytosine phosphodiester guanine oligodeoxynucleotides
Cre	Cyclization recombination
CXCL	Chemokine (C-X-C motif) ligand
DCs	Dendritic cells
DNA	Deoxyribonucleic Acid
dNTPs	Deoxyribonucleotide Triphosphate
ECM	Extracellular matrix
EGF	Epithelial growth
ELISA	Enzyme-linked Immunosorbent Assay
FcγR	Fragment , crystalline receptor for immunoglobulin G
Foxp3	Forkhead box P3
FR	Folate receptor
GR	Galactose receptor
GSK-3β	Glycogen synthase kinase 3β
H&E staining	Hematoxylin and eosin staining
H3K27	Histon 3 Lysine 27
H3K4	Histon 3 Lysine 4
i.n.	Intranasal
i.p.	Intraperitoneal
i.t.	Intratracheal
i.v.	Intravenous
Ig	Immune globulin
IL	Interleukin
INF-γ	Interferon γ
iNOS	Inducible nitric-oxide synthase (NOS2)
IPF	Idiopathic pulmonary fibrosis
IRF4	Interferon regulatory factor 4

## Abbreviations

JMJD3	<i>Jumonji</i> domain containing 3
LAP	Latency- associated protein
LPS	Lipopolysaccharide
LysM	Lysozym M
M1	Phenotype of classically activated macrophages
M2	Phenotype of alternatively activated macrophages
MCP-1	Monocyte chemoattractant protein 1 (CCL2)
MDSCs	Myeloid derived suppressor cells
MHCII	Major Histocompatibility Complex II
MIP-1 $\alpha$	Macrophage inflammatory protein 1 $\alpha$ (CCL3)
MMP	Matrix metalloprotease
MR	Mannose receptor
NFAT	Nuclear factor of activated T-cells
NF- $\kappa$ B	Nuclear factor 'kappa-light-chain-enhancer' of activated B-cells
NO	Nitric oxide
NOS	Nitric oxid synthase
OAT	Ornithine amino transferase
ODC	Ornithine decarboxylase
PAMPs	Pathogen- associated molecular patterns
PCR	Polymerase Chain Reaction
PDGF	Platelet derived growth factor
PDK	Phosphoinositde- dependent kinase
PI3K	Phosphoinositde 3-kinase
PPAR- $\gamma$	Peroxisome proliferator-activated receptor
PPR	Pattern recognition receptor
PtdIns	Phosphatidylinositols
PtdIns (4)P	Phosphatidylinositol 4-phosphate
PtdIns (4,5)P2	Phosphatidylinositol 4,5-bisphosphate (PIP2)
PtdIns(3,4,5)P3	Phosphatidylinositol (3,4,5)-trisphosphate (PIP3)
PTEN	Phosphatase and tensin homolog deleted on chromosome 10
qPCR	Quantitative Real Time Polymerase Chain Reaction
RNA	Ribonucleic Acid
ROR $\gamma$ t	Orphan Nuclear Receptor
ROS	Reactive oxygen species
RT	Room temperature
SAC	<i>Staphylococcus aureus</i> Cowan's antigen

SDS-PAGE	Sodium Dodecyl Sulfate Polyacrylamid Gel electrophoresis
SHIP	SH2 domain- containing inositol phosphatase
SR	Scavenging receptor
STAT6	Signal transducer and activator of transcription
Syk	Spleen tyrosine kinase
TAM	Tumor associated macrophage
TCR	T-cell receptor
Tfh cell	T follicular helper cell
TH1-Cells	T helper cell type 1
TH2-Cells	T helper cell type 2
TLR	Toll Like Receptor
TNF	Tumor necrosis factor
TRAF6	TNF receptor associated factors 6
TREG-Cells	Regulatory T cells
TSLP	Thymic stromal lymphopietin
VEGF	Vascular endothelial growth factor
$\alpha$ -SMA	Alpha smooth muscle actin



## 4. Introduction

### 4.1. Immune System

The immune system comprises all molecules, proteins, cells and tissues, which are involved in host defense and healing. Furthermore it has to recognize invaders and to distinguish between host and pathogens in order to spare the host and to eliminate the pathogen. The mammalian immune system can be divided into two arms: the innate and the adaptive immunity (Beutler 2004).

#### 4.1.1. Innate Immune System

The first challenge that pathogens have to meet and to overcome is the barrier provided by epithelial cells or the mucus in the gastrointestinal, respiratory and genitourinary tract, produced by the epithelium. If pathogens succeed in breaking through these initial barriers, the innate immune system has additional defense mechanisms composed of cellular and humoral components. The cells – neutrophils, basophils, eosinophils, mast cells, macrophages, monocytes and dendritic cells – participating in the innate immune response derive from the hematopoietic stem cell through the myeloid arm (Chaplin 2003).

Neutrophils are important for bacterial clearance because they phagocytose bacteria and produce reactive oxygen species (ROS) to kill them. In addition they generate cytokines such as tumor necrosis factor (TNF) and interleukin 12 (IL-12) and thereby contribute to tissue remodeling and repair (Chaplin 2003).

In the blood stream circulating monocytes will differentiate into macrophages, if they enter a tissue. There they are important in phagocytosis of microbes and bacterial and viral moieties opsonized with antibodies or factors of the complement system (described below). They eliminate the pathogens via nitric oxide (NO) and stimulate T-cell response via the production of cytokines as will be further explained below. Macrophages can present antigens of pathogens to T helper cells via class I and class II major histocompatibility complex (MHC) molecules, in addition to dendritic cells, which are more skilled in antigen presentation (Chaplin 2003).

Eosinophils and basophils produce cytokines and influence the inflammatory environment. They are mainly involved in the defense against parasites – such as helminthes – and in allergic reactions eosinophils and mast cells (Beutler 2004).

The innate immune cells sense pathogens with a limited number of germline encoded receptors (Chaplin 2003). These receptors are called pattern recognition receptors (PRRs). Examples are the Toll-like receptors (TLRs) that can bind pathogen-associated microbial patterns (PAMPs). PAMPs are molecular moieties, which are characteristic for related groups of microbes. More precisely PRRs bind specific molecules instead of patterns (Beutler 2004). The great advantages of the PAMPs are that a related group of microorganisms express the same PAMPs, which are absent in the host. Moreover these molecules are crucial for the microbial survival, thus microbes require them. In this respect PAMPs are great weak points for the innate immune system to target lots of various microorganisms with the appropriate PRRs (Medzhitov 2007). In this way the innate immune system is able to react immediately on pathogens. In humans ten TLRs are known and in mice eleven. After sensing the pathogen the immune cells produce reactive nitrogen intermediates (RNI) and reactive oxygen species (ROS), for instance superoxid ( $O_2^-$ ) and hydrogen peroxide ( $H_2O_2$ ) within the phagosome to eliminate invaders (Beutler 2004; Biswas and Mantovani 2010).

Soluble proteins and bioactive molecules support the innate immune cells. These humoral factors are either permanently present in the blood flow or are released by the immune cells during an immune response (Chaplin 2003). Members of the protein family the collectins – for example mannose-binding protein – and the pentraxin – for instance C-reactive protein – bind microbes via a mannosyl residue or supposable lectin-like interactions, respectively (Beutler 2004). Binding of the mannose-binding protein induces the activation of the complement system. The complement system comprises serum and cell surface proteins, which undergo a cascade of proteolytic cleavage of zymogens after activation. Three routes of activation are known: the classical pathway, the mannose binding lectin pathway and the alternative pathway, which are triggered by antigen-antibody complexes, mannan- containing microbes and microbial components, respectively. The complement activation can lead to mast cell degranulation, edema and the recruitment of immune cells; moreover microbes can be killed via the complement membrane attack complex that induces cell lysis (Chaplin 2003).

Additional humoral factors are antimicrobial peptides. There are two main families in mammals: the defensins expressed by neutrophils and the cathelicidins produced by the epithelium. These peptides can breakup bacterial membranes by an unknown mechanism (Beutler 2004).

### 4.1.2. Adaptive Immune System

The adaptive immunity is maintained mainly by conventional T- and B- lymphocytes and gets activated by the antigen presentation of innate immune cells. In contrast to the cells of innate immune system, cells of the adaptive immunity adjust their T-cell receptor or B-cell receptor diversity according to the pathogen. Somatic recombination of variable and constant gene fragments, insertion of non-templated nucleotides and gene conversion lead to the establishment of a great variety of completely new assembled receptor. The B-cell receptor can be additionally modified by somatic hypermutations (Medzhitov 2007).

Lymph nodes and spleen drain most of the body's tissue fluids and the blood, respectively and lymphocytes move among the lymph nodes. Antigen-presenting cells – such as dendritic cells – of the innate immune system migrate into the lymph node once they processed an antigen. In the lymph node they present their antigen towards conventional lymphocytes, which are specific for this antigen. The presentation leads to the differentiation of the lymphocyte into an effector cell dependent on the antigen. Cytokines and chemokines instruct the lymphocyte about their differentiation and the site of infection, respectively (Medzhitov 2007). Thus the lymphocyte with the best adapted receptor or immunoglobulin has to proliferate to provide enough effector cells and antibodies. Therefore the adaptive immune response begins after the innate immune cells have reacted (Chaplin 2003). After the initiation of the T-cell response and the clonal expansion, the contraction phase is triggered. This phase is characterized by the apoptosis of effector T-cells to regain homeostasis. Only a small subpopulation survives and forms memory T-cells with an extended life span. The persistence of a low level of memory T-cells is maintained by constant T-cell proliferation and apoptosis. It is believed that MHC and T-cell receptor (TCR) interaction as well as IL-15 and IL-17 are required for this homeostasis (Schluns and Lefrancois 2003). In addition to the memory T-cell memory B-Cells are developed. The great advantage of memory cells provide is that the host can induce more rapid and more specific immune responses against the same microbe at second infection (Chaplin 2003).

Conventional T-cells ( $\alpha\beta$  T cells) most derive from the hematopoietic stem cell and differentiate in the thymus to mature T lymphocytes. Different types of effector T- cells can be identified such as T helper cells (discussed later). Cytotoxic T-cells are capable to identify infected host cells – for example by a virus – via the major histocompatibility complex class I (MHCI). Recognized infected host cells are eliminated by cytotoxic T-cells, while healthy host cells are spared. This process is known as self-tolerance. The T

helper cells recognize pathogens via MHC II and are required for the maturation of B-cells and induce class switching and somatic mutations through cytokines (Chaplin 2003).

Conventional B-cells (B2 cells) originate from the hematopoietic stem cell and mature in the bone marrow, in contrast to T-cells. B-cells can differentiate to plasma cells and produce antibodies, which are the humoral part of the adaptive immune system (Chaplin 2003). Activation of B-cells is mediated by the binding of unprocessed antigen to the B-cell receptor, which is assembled of immunoglobulin heavy and light chains (Harwood and Batista 2008).

In addition to the conventional T- and B- lymphocytes innate-like lymphocytes support the adaptive immune system. B1 cells, marginal-zone B cells, natural-killer T cells and parts of  $\gamma\delta$  T cells are examples. They vary from the conventional cells in their receptor, which is assembled in a similar way, but less randomly and limited (Medzhitov 2007).

#### **4.1.3. Cytokines and Chemokines**

Cytokines are secreted proteins, which are released during an inflammatory response by various immune, epithelial and endothelial cells. They serve as communication tools between the respective cells and are very important for modulating the innate and adaptive immune response (Krishnamoorthy and Honn 2006). They function via binding to cell surface receptors and induce intracellular signal transduction (Chaplin 2003). An essential part of the cytokines responsible for immune reaction is the chemokine family. Chemokines bind to receptors of the seven transmembrane G-protein coupled receptor family and recruit inflammatory cells – such as neutrophils – via chemotaxis to the site of infection. They participate mainly in mediating inflammation, angiogenesis and homeostasis. (Krishnamoorthy and Honn 2006)

#### **4.1.4. Phosphoinositide 3-kinase Pathway**

The phosphoinositide 3-kinases (PI3K) are conserved signal transducing heterodimeric enzymes composed of a catalytic and a regulatory subunit. According to their structure PI3Ks can be divided into the three classes I, II and III. This thesis will only focus on the class I PI3K, which consists of one of the catalytic subunits p110 $\alpha$ , p110 $\beta$  or p110 $\delta$  and one of the regulatory subunits p85 $\alpha$ , p85 $\beta$  or p55 $\gamma$  (Domin and Waterfield 1997).

The PI3K pathway plays a major role in the regulation of growth, proliferation, survival and migration of cells. Growth factors, inflammatory components, hormones, antibodies and antigens can induce the activation of the PI3K pathway (Marone, Cmiljanovic et al. 2008). In resting cells the activity of the PI3K is suppressed by the catalytic subunit. Activation of the PI3K through growth factors is triggered by the direct contact of the regulatory subunit with the phosphotyrosine residues of the growth factor receptors or its adaptor proteins. This event leads to the translocation of the PI3K toward the plasma membrane in close proximity to its substrates (Cantley 2002). The activated PI3K phosphorylates the 3-hydroxyl group of phosphatidylinositols (PtdIns), PtdIns (4)P and PtdIns (4,5)P<sub>2</sub> (PIP<sub>2</sub>), whereby PIP<sub>2</sub> is the preferred substrate in vivo (see Figure 1) (Vanhaesebroeck, Leever et al. 2001). Phosphorylation of PIP<sub>2</sub> generates PtdIns(3,4,5)P<sub>3</sub> (PIP<sub>3</sub>), which induces the translocation of the serine-threonine kinase protein kinase B (PKB, Akt) toward the plasma membrane. This kinase is recruited to the plasma membrane through its pleckstrin- homology (PH)- domains, which bind the PIP<sub>3</sub> (Marone, Cmiljanovic et al. 2008). PH- domains of different proteins are able to distinguish between PtdIns(3,4)P<sub>2</sub>, PtdIns(3,4,5)P<sub>3</sub> and other lipids and thus provide the specificity of the PI3K pathway (Fruman and Cantley 2002). At the plasma membrane different kinases can activate Akt. For example the phosphoinositide- dependent kinase 1 (PDK1) and PDK2 phosphorylate Akt at Thr308 and at the Ser473, respectively and thereby activate the kinase. Activated Akt can activate or inhibit in turn various target proteins via phosphorylation and thus regulates cell cycle progression, survival and metabolism (Marone, Cmiljanovic et al. 2008).

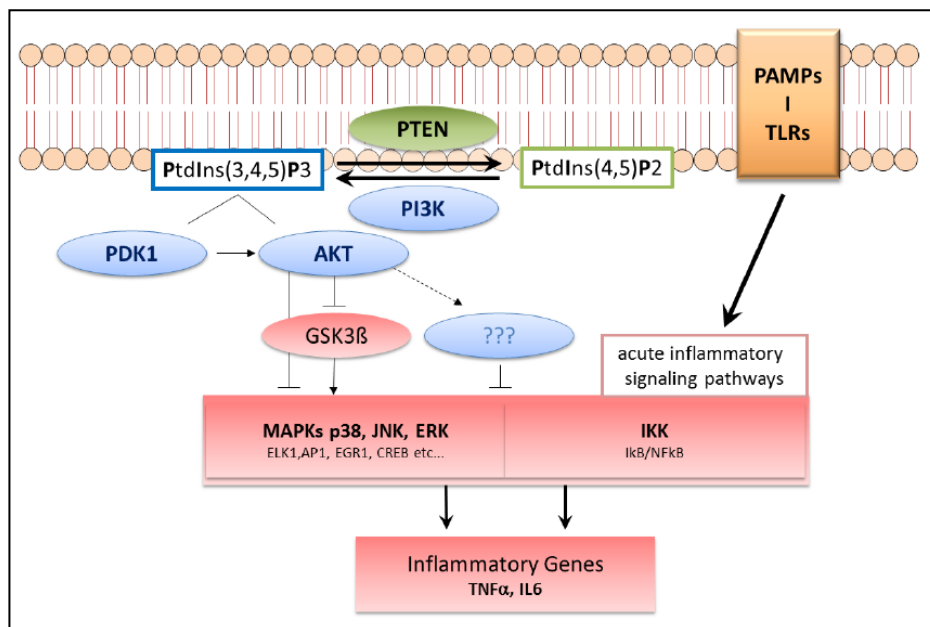


**Figure 1: Phosphoinositide 3-kinase pathway.** Modified from (Gunzl and Schabbauer 2008)

PI3K signaling in mammalian immune cells can be induced by cytokines, chemokines, immunoglobulins and antigens. Proliferation, differentiation, survival, chemotaxis, phagocytosis and degranulation can be modulated by this signaling pathway. For example PI3K augments the B-cell receptor mediated  $\text{Ca}^{2+}$  increase in B-Cells via the recruitment of Phospholipase C  $\gamma 2$  (PLC $\gamma 2$ ) to the plasma membrane due to its PH-domain (Fruman and Cantley 2002). Moreover the membrane compound lipopolysaccharide (LPS) of gram negative bacteria can activate the PI3K pathway via the TLR4/MyD88 signaling. The LPS mediated signaling induces the phosphorylation of Akt (Laird, Rhee et al. 2009).

For osteoclasts and dendritic cells the TNF family member TRANCE (RANKL) is an important functional regulator and acts via the induction of Akt through TNF receptor associated factors 6 (TRAF6), c-Src and the PI3K signaling pathway (Wong, Besser et al. 1999). The PI3K inhibitor wortmannin suppresses the production of  $\text{PIP}_3$  in neutrophils in response to the stimulation with the chemotactic protein formyl peptide. Indicating a role of the PI3K in chemotaxis (Okada, Sakuma et al. 1994).

The knockout of the three regulatory subunits of the class I PI3K p85 $\alpha$ , p85 $\beta$  or p55 $\gamma$  is perinatal lethal and exhibits dramatic necrosis of hepatocytes and brown fat tissue as well as calcification of the cardiac tissue (Fruman, Mauvais-Jarvis et al. 2000).

The activity of PI3K is counteracted by two phosphatases: the SH2 domain-containing inositol phosphatase (SHIP) and the phosphatase and tensin homolog deleted in chromosome ten (PTEN). SHIP and PTEN dephosphorylate  $\text{PIP}_3$  to  $\text{PtdIns}(3,4)\text{P}_2$  and  $\text{PtdIns}(4,5)\text{P}_2$ , respectively. In this context PTEN is a tumor suppressor gene and mutated in different kinds of tumors (Marone, Cmiljanovic et al. 2008).

PTEN consists of the phosphatase and C2 domains, which are capable of binding lipids. PTEN dephosphorylates the 3-position of the inositol ring and its predominantly target *in vivo* is the  $\text{PI}(3,4,5)\text{P}_3$ . Additionally it removes phosphate residues of  $\text{PI}(3)\text{P}$  and  $\text{PI}(3,4)\text{P}_2$ .

The activation state of PTEN can be regulated via phosphorylation. Phosphorylation of PTEN potentially induces a closed, more stable conformation with decreased competence to bind its substrates. The PI3K downstream kinase glycogen synthase kinase 3 $\beta$  (GSK-3 $\beta$ ) can phosphorylate the Ser362 and Thr366 of PTEN and thus down regulate the catalytic activity of PTEN. Phosphorylation by GSK-3 $\beta$  is promoted by a previous phosphorylation of PTEN by CK2. This inhibition provides a negative feedback loop of the PI3K signaling (Gericke, Munson et al. 2006).

#### 4.1.5. Arginase 1

A second important pathway during an immune response is the metabolism of L-arginine. The two for the substrate competing enzymes the Arginase 1 (Arg1) and the inducible nitric-oxide synthase (iNOS, NOS2) are responsible for the conversion of L-arginine in murine myeloid cells (Bronte and Zanovello 2005).

Arg1 hydrolyses the amino acid to L-ornithine and urea. L-ornithine is further converted into polyamines and L-proline by the ornithine decarboxylase (ODC) and the ornithine aminotransferase (OAT), respectively (see Figure 2). Polyamines are small cationic molecules and support cell growth and differentiation while L-proline is important for the collagen synthesis therefore suggesting an involvement in fibrosis (Bronte and Zanovello 2005). The enzymes argininosuccinate synthase and the argininosuccinate lyase are able to recycle L-arginine from L-citrulline (Munder 2009).

Two isoforms of Arginase are known. The Arg1 is expressed in the cytosol of hepatocytes and participates in the urea cycle. IL-4, IL-13 (Munder, Eichmann et al. 1999) and TGF- $\beta$  (Boutard, Havouis et al. 1995) can stimulate the Arg1 expression in myeloid cells in mice. The transcription factors signal transducer and activator of transcription 6 (STAT6) and STAT1 are the main players in the transcriptional activation of Arg1. The second isoform Arg2 is constitutively found in the mitochondria of renal cells, neurons, macrophages and enterocytes (Bronte and Zanovello 2005). In contrast to murine leukocytes in human only granulocytes express Arginase 1 constitutively. Stimulation with IL-4 and IL-10 failed to increase Arginase 1 expression. Additionally the localization is different, because human granulocytes store Arginase 1 in azurophil granules and exhibit fungicidal properties (Munder, Mollinedo et al. 2005).

The nitric-oxide synthase (NOS) is composed of the oxygenase and reductase domain and its cofactors (6R)-5,6,7,8-tetrahydrobiopterin (BH4), haem, flavin-adenine dinucleotide (FAD) and flavin mononucleotide (FMN). In addition calmodulin is required for the conversion of L-arginine to L-citrulline and nitric oxide (NO). NO can be further used to produce superoxide ( $O_2^-$ ), hydrogen peroxide ( $H_2O_2$ ) or peroxynitrites ( $ONOO^-$ ), which induce damage to lipids, proteins and DNA (deoxyribonucleic acid) (Bronte and Zanovello 2005).

In murine macrophages, neutrophils, eosinophils, dendritic cells (DCs) and natural killer cells iNOS is present, however two further isoforms of NOS are known. NOS1 or nNOS and NOS3 or eNOS are expressed in the neuronal tissue and endothelial cells, respectively. In addition they exhibit differences in their regulation, intracellular localization

and catalytic features. Binding of LPS, IFN- $\gamma$ , IL-1, TNF, IFN- $\alpha$  or IFN- $\beta$  to their receptors lead to the expression of iNOS via different transcription factors, for example the nuclear factor 'kappa-light-chain-enhancer' of activated B-cells (NF- $\kappa$ B), activator protein 1 (AP1), IFN-regulatory factor 1 and STAT1 (Bronte and Zanovello 2005).

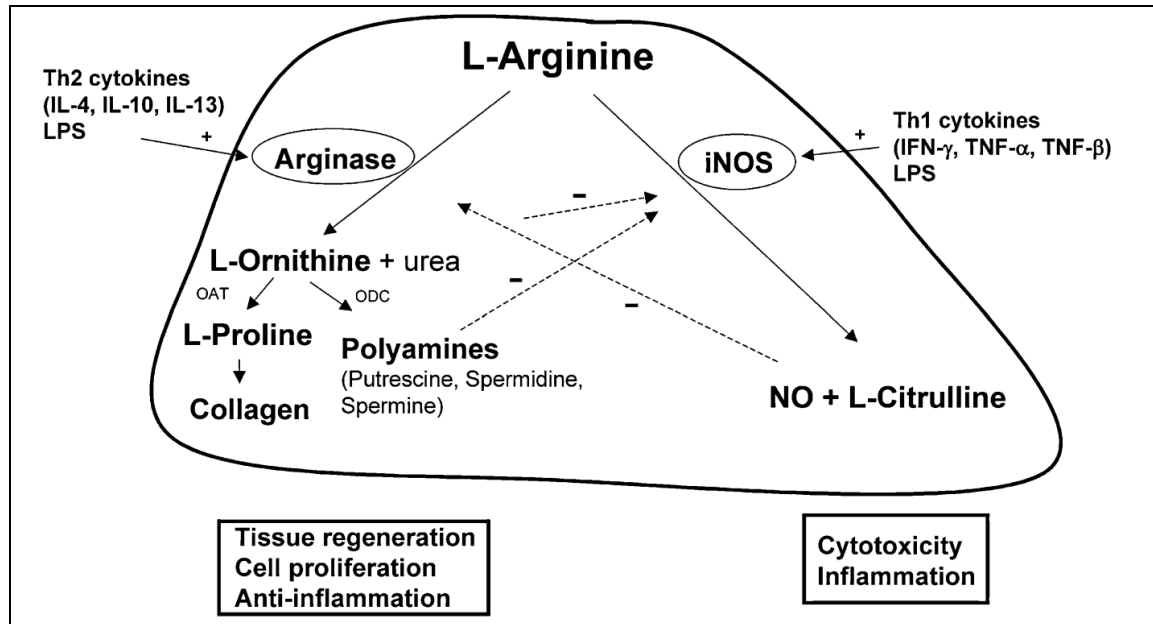


**Figure 2: L-arginine conversion by Arginase versus iNOS in murine myeloid cells (Munder 2009).**

Due to the differential activation Arg1 and iNOS by type 2 (such as IL-4, IL-13) and type 1 (for instance IFN- $\gamma$ ) cytokines, they can be used as marker for alternative (M2) or classically (M1) activation of macrophages, respectively (as will be further explained below). In contrast, LPS was shown to induce both enzymes, although it is considered as inducer of a T helper cell type 1 (TH1) response (Bronte and Zanovello 2005).

Arg1 activity can cause a depletion of L-arginine in its microenvironment. This effect down regulates the expression of CD3 $\zeta$  (cluster of differentiation 3 $\zeta$ ) of the TCR, thus blocks T-cell proliferation (Bronte and Zanovello 2005). The precise mechanism remains to be identified. Lack of amino acids can inhibit translation of messenger ribonucleic acid (mRNA), due to uncharged transfer RNAs (tRNAs) (Baniyash 2004).

Stimulation of Arg1 and iNOS at the same time does not negatively influence each other, but the diminution of L-arginine shifts the production from mainly nitric oxide towards mainly superoxide by iNOS (Bronte and Zanovello 2005).

## **4.2. Plasticity of Immune Cells**

A very important way how the immune system provides adequate host defense, without self-damage, is the phenotypical and functional adaptation of immune cells according to the immune reaction. Cell types of the immune system – such as T-Cells – form various subpopulations – for example TH1 cells – with differences in their phenotype and function. Combined stimuli – for instance cytokines – induce their differentiation and can even lead to the conversion from one subtype into another. The next sections will deal with the plasticity of macrophages, DCs and T helper cells (Galli, Borregaard et al. 2011).

### **4.2.1. Macrophages**

Macrophages are derived from the myeloid progenitors of the hematopoietic stem cells and differentiate in most cases directly through monocytes in the blood to specific tissue macrophages by entering the tissue, such as alveolar macrophages (AMs), Kupffer cells or osteoclasts. Therefore they are characterized according to their anatomical location. Activation of macrophages initiates a change in expression of pattern-recognition receptors resulting in different functional phenotypes, known as macrophage plasticity. Different microbial molecules can lead to a mixture of macrophages that vary in their capacity of phagocytosis and cytokine expression. The two best known functional phenotypes which are also the extremes of a spectrum are the classically activated macrophage (M1) and the alternatively activated macrophage (M2) (Biswas and Mantovani 2010). Further functional phenotypes are regulatory macrophages, tumor associated macrophages (TAMs) and myeloid derived suppressor cells (MDSCs) (Galli, Borregaard et al. 2011). TAMs share some features with M2 polarized macrophages and promote tumor progression, for example by suppressing adaptive immune responses (Biswas and Mantovani 2010). MDSCs are considered to have similar function like TAMs (Galli, Borregaard et al. 2011).

#### **Classically Activated Macrophages**

The M1 phenotype is characterized by the elevated expression of major histocompatibility complex II (MHCII) and the costimulator CD86, interferon  $\gamma$  (INF- $\gamma$ ) receptor and TLRs (see Figure 3). Damage associated molecular patterns, pathogen associated molecular patterns (Galli, Borregaard et al. 2011) and the TH1 cytokine INF- $\gamma$  induce a polarization of macrophages towards M1 phenotype (Biswas and Mantovani 2010). This is achieved by the INF- $\gamma$  receptor stimulating IRF/STAT signaling via IRF-5 and STAT1 and by the TLR4 through NF- $\kappa$ B and IRF-3 (Sica and Mantovani 2012). In a

feedback loop M1 macrophages mainly communicate with TH1-Cells by releasing IL-12 and the chemokines CXCL 9 (chemokine (C-X-C motif) ligand 9) and CXCL 10 and thereby inducing inflammation (Biswas and Mantovani 2010).

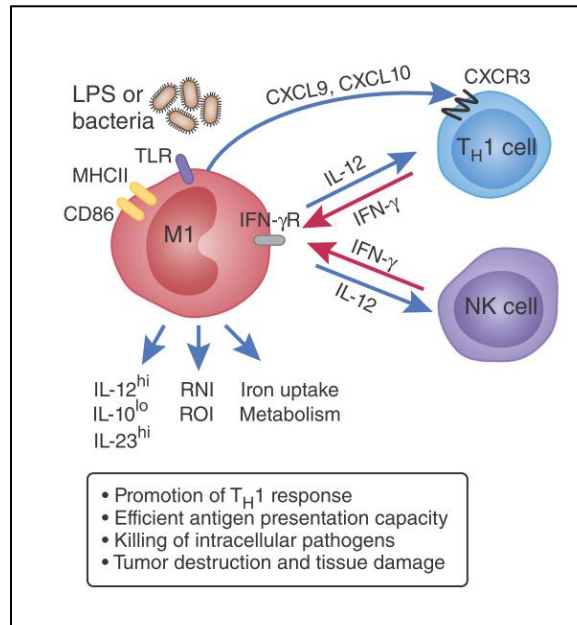


**Figure 3: Phenotypical characterization of M1 macrophages and its communication with Th1 cells and NK cells.** Reactive nitrogen intermediates (RNI), reactive oxygen intermediates (ROI). (Biswas and Mantovani 2010)

Their main function is the phagocytosis of microbes, and further to present their antigens to lymphocytes and to eliminate the pathogens (Biswas and Mantovani 2010). In the lysosome of the macrophages reactive nitrogen intermediates and reactive oxygen intermediates are produced. After microbial uptake the lysosome can fuse with the phagosome. In the phagosome these intermediates harm the pathogen (Desjardins, Celis et al. 1994; Biswas and Mantovani 2010). Thus classical activated macrophages are very important for the clearance of intracellular pathogens (Sica and Mantovani 2012).

An additional feature of M1 macrophages is that they sequester iron by repressing ferroportin (Biswas and Mantovani 2010), which transports iron into the serum (Schimanski, Drakesmith et al. 2005) and inducing H ferritin (Biswas and Mantovani 2010), an intracellular storage molecule (Ratledge and Dover 2000). In contrast to other nutrients – such as glucose, nitrogen or phosphate – the essential iron is inaccessible for pathogens in the host. This is possible because iron is bound to the glycoprotein

transferrin in the blood and the aerobic condition push free iron in the ferric oxidation state and thus it is insoluble (Bachman, Miller et al. 2009). Therefore pathogens have developed mechanisms for iron uptake, for example siderophores. Siderophores are tiny hydrophobic molecules that bind soluble iron with much greater affinity than mammalian proteins (Ratledge and Dover 2000).

### **Alternatively Activated Macrophages**

The expression of scavenging (SR), folate (FR), mannose (MR) and galactose (GR) receptors, CD23 (Biswas and Mantovani 2010), and CD163 (Gordon 2003) characterizes alternatively activated macrophages (M2) (see Figure 4) (Biswas and Mantovani 2010). Additional markers are IL-1 decoy receptor and IL-1RA, which neutralize the pro-inflammatory effects of IL-1 (Gordon 2003). *In vitro* studies showed that IL-4 induces proliferation on a low level (Gordon 2003) and the expression of MHC class II (Gordon 2003). IL-4 can promote the fusion of monocytes and macrophages to giant multinucleated cells – which for example have a role in removing foreign particles (McInnes and Rennick 1988), by supporting cell adhesion through an increased expression of E-cadherin (Sica and Mantovani 2012). Moreover Arginase 1 expression is elevated compared to classically activated macrophages, and thus induces a higher generation of ornithine and polyamines and therefore is an additional hallmark (Biswas and Mantovani 2010).

Two more M2 indicators are Ym1 and FIZZ1. Ym1 (in human known as chitinase-3-like protein 3 (CHI3L3)) belongs to the mammalian chitinase-like protein family and is STAT6 dependent induced during TH2 responses. Ym1 has evolutionary lost its ability to bind chitin and thus its chitinolytic activity (Reese, Liang et al. 2007). FIZZ (found in inflammatory zone 1, resistin-like molecule  $\alpha$  (Relm  $\alpha$ )) is a cysteine-rich protein secreted by macrophages, endothelial and epithelial cells (Gordon and Martinez 2010). Based on FIZZ deficient mice studies have shown that the lack of FIZZ increases pulmonary inflammation and fibrosis, and promotes M2 differentiation of macrophages. *In vitro* recombinant FIZZ is able to inhibit type 2 cytokines of T-cells (Nair, Du et al. 2009).

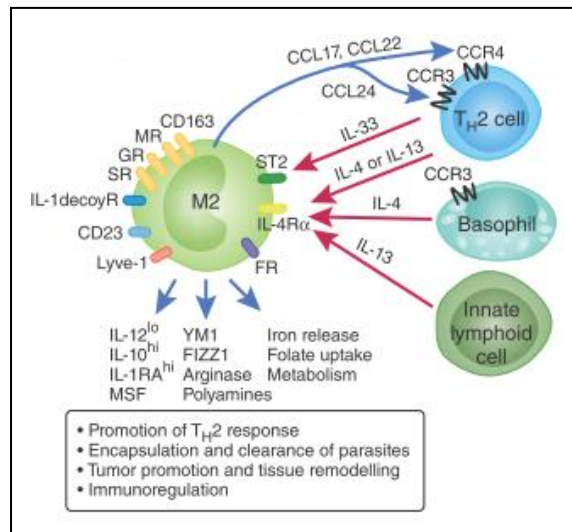


**Figure 4: Phenotypical characterization of M2 macrophages and its communication with TH2 cells, basophils and innate lymphoid cells. (Biswas and Mantovani 2010)**

M2 polarized macrophages attract TH2-Cells by the release of CCL17 (chemokine (C-C motif) ligand - 17), CCL22 and CCL24, which conversely promote a M2 phenotype by the secretion of IL-4, IL-13 or IL-33. Furthermore basophils and innate lymphoid cells release IL-4 and IL-13 promoting M2 polarization, respectively. Similarly to TH2 cells they are also recruited by CCL17, CCL22 and CCL24. Another characteristic of alternatively activated macrophages is the low production of IL-12 and the increased in IL-10, which has an anti-inflammatory effect and is additionally an important communication molecule between T<sub>REG</sub>-Cells and macrophages. Macrophages can recruit T<sub>REG</sub>-Cells by the secretion of CCL22 (Biswas and Mantovani 2010).

B-cells can influence the activation of macrophages either through antibodies, immune complexes or via cytokines. Immune globulins (Ig) are able to bind the fragment crystalline receptor for immunoglobulin G (FcγR) of macrophages and restrain TLR4 and type I interferon signaling through the spleen tyrosine kinase (Syk). The FcγRIIb triggers the formation of prostaglandin E<sub>2</sub>, thus reduces the expression of the pro-inflammatory cytokines IL-6 and TNF. Immune complexes are immune globulins that are bound to antigens (Shmagel and Chereshev 2009). Together with IL-1 or LPS, immune complexes can induce a M2 like phenotype, characterized by a low expression of IL-12 and a high production of IL-10 and CCL1, which interacts with eosinophils, polarized TH2-Cells and T<sub>REG</sub>-cells via CCR8 (Biswas and Mantovani 2010).

M2 macrophages participate in the immune reactions against helminthes and in allergic reactions. In the gut, alternatively activated macrophages stimulate clearance of extracellular parasites (Galli, Borregaard et al. 2011). Based on their characteristic to dampen immune responses and to support tissue remodeling, they are considered to have anti-inflammatory and immune regulatory effects. Alternatively activated macrophages produce IL-8, epithelial growth factor (EGF), vascular endothelial growth factor- A (VEGF-A) and VEGF-C and thus induce angiogenesis and lymphangiogenesis. In this context they sustain tumor progression, in contrast to M1 polarized phagocytes (Biswas and Mantovani 2010).

M2 macrophages differ in their iron metabolism from M1 cells, because they promote the upregulation of ferroportin. This leads to an increase in the iron levels in the plasma and supports cell proliferation (Biswas and Mantovani 2010).

An additional feature of macrophages is their participation in wound healing. Following platelet degranulation macrophages are attracted and secrete cytokines, chemokines, matrix metalloproteinases (MMPs) and the tissue inhibitor of metalloproteinases (TIMPs). In this regard they influence the remodeling of the extracellular matrix (Galli, Borregaard et al. 2011).

IL-4 induced gene expression starts with the binding to the type I IL-4 receptor – composed of IL4R $\alpha$  or IL4R $\gamma$ c – or to the type II IL-4 receptor – composed of IL-4R $\alpha$  or IL13R $\alpha$ 1. In contrast, IL-13 can only act through type II IL-4 receptor. This difference in receptor binding provides them a variation in their impact. Downstream effects of the activation of IL-4 receptors induce STAT6 signaling through diverse Janus kinases. STAT6 leads to the expression of peroxisome proliferator-activated receptor  $\gamma$  (PPAR- $\gamma$ ) and together they activate M2 associated genes. Further IL-4 triggers the activation of *jumonji* domain containing 3 (JMJD3), a histone demethylase, which stimulates the expression of Arg1, Ym1 and FIZZ. JMJD3 acts through methylating the histone 3 at the lysine 4 (H3K4) and demethylating H3K27 in their promoter region, thus inducing gene expression. In addition JMJD3 inhibits the Toll-like receptor 4 signaling, by stimulating the transcription factor interferon regulatory factor 4 (IRF4), which attaches to the adaptor molecule MyD88. IRF4 plays also an important role in the regulation of Arg1, Ym1 and FIZZ (Biswas and Mantovani 2010).

#### 4.2.2. Dendritic Cells

Dendritic cells derive from hematopoietic stem cells and are professional antigen presenting cells. Novel findings indicate that DCs originate from the common myeloid precursor (CMP) as well as from the common lymphoid progenitor (CLP). Both progenitors can differentiate into macrophage-DC progenitors (MDP), which give rise to different DC populations (Figure 5) (Kushwah and Hu 2011). 26 diverse DC populations are characterized according to their expression markers. They were isolated from lymphoid and non-lymphoid tissue (Miller, Brown et al. 2012).

An additional possibility to characterize DCs is the differentiation between steady-state conventional DCs and non-conventional DCs. In contrast to steady-state conventional DCs, non-conventional DCs emerge during inflammation. Both types include different subtypes (Kushwah and Hu 2011).

Conventional steady-state DCs include migratory DCs, which reside in the peripheral tissues and migrate toward the lymph nodes after antigen uptake. For example, in the lung three different subtypes are known, which are present in the intraepithelial network or in the lamina propria of the conducting airways. In addition to the migratory DCs conventional steady-state DCs consist of lymphoid DCs, which are found in the lymphoid organs (Kushwah and Hu 2011).

Non-conventional DCs comprise plasmacytoid DCs and monocyte-derived DCs. Plasmacytoid DCs are not restricted to lymphoid or peripheral organ. They are able to rapidly produce INF- $\gamma$ , maintain tolerance and are involved in autoimmune responses. Monocyte-derived DCs are located in the peripheral tissues and appear under steady-state conditions as well as during inflammation (Kushwah and Hu 2011).

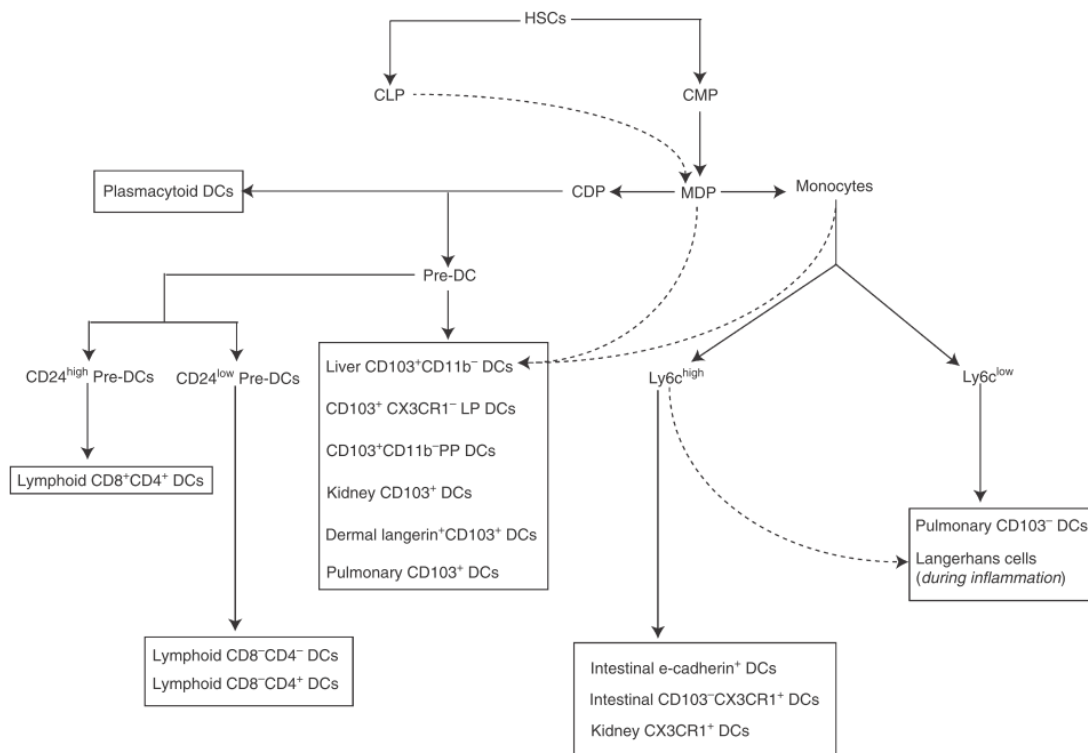


**Figure 5: Differentiation pathways of dendritic cells. (Kushwah and Hu 2011)**

### 4.2.3. T Helper Cells

Naïve CD4<sup>+</sup> T helper cells emerge from the lymphoid progenitor and can differentiate into various subsets. These subpopulations are characterized by their cytokine expression pattern and their corresponding effector functions. Frequently, single cells of a lineage fail to produce all representative cytokines of their lineage, instead every cell express a few and together they specify the population. These cytokine expression differences may be mediated by nuclear factor of activated T-cells (NFAT) and epigenetic factors. There are four TH cell lineages TH1, TH2, TH17 and T<sub>REG</sub>-cells. A few more lineages – such as TH3, TH9 or T follicular helper cells (Tfh cells) – are discussed, but supposedly they are only subsets of the four named previously (Zhu and Paul 2010).

#### TH1 Cells

Immune responses against intracellular pathogens are mainly triggered by TH1 cells. The cytokines IL-12 and INF- $\gamma$  are responsible for the differentiation of T helper cells toward TH1. Further involved in the differentiation are the transcription factors STAT4 and interferon regulatory factor (IRF-1), because the lack of these transcription factors leads to

the absence of TH1 cells. IRF-1 modulates the expression of IL-12 of antigen presenting cells and thus contributing to TH1 differentiation. An additionally involved transcription factor is T-box expressed in T cells (T-bet) of the T-box family. In contrast to STAT4 and IRF-1, T-bet is restricted to thymocytes and TH1 lymphocytes and is regulated by the signaling of the T cell receptor. T-bet is potent in the activation of the INF- $\gamma$  transcription and in the inhibition of IL-4 and IL-5 expression (Szabo, Kim et al. 2000).

The hallmark of TH1 cells is the production of INF- $\gamma$ , which activates macrophages and polarizes them toward M1 macrophages. In addition they are able to produce LT $\alpha$ , IL-2 and TNF $\alpha$ . TH1 cells can change their phenotype into a TH2 phenotype in response to IL-4. This effect is only possible *in vitro*, if they were primed for one round; at later stages they maintain their expression pattern (Zhu and Paul 2010).

### **TH2 Cells**

TH2 cells are the main actors in the immune reaction against extracellular pathogens, parasites and in allergies. IL-4 together with IL-2, IL-7 and the thymic stromal lymphopoietin (TSLP) triggers TH2 polarization through GATA3 and STAT5 and is sustained by GATA3 and Gfi-1 (Zhu and Paul 2010). GATA3 is strongly expressed during the development of TH2 cells and diminished in TH1 cells. Binding of GATA3 to the GATA Site of the IL-5 promoter is necessary for the expression of the type 2 cytokine IL-5 (Zhang, Cohn et al. 1997). An additional transcription factor c-Maf, which is specific for TH2 cells, can together with NFAT and NIP45 (NFAT interacting protein 45) stimulate B lymphoma cells to produce IL-4 (Hodge, Chun et al. 1996). The lack of c-Maf leads to restrained expression of IL-4, whereas other TH2 cytokines, such as IL-5, IL-10 and IL-13 are still present (Kim, Ho et al. 1999).

Mature TH2 cells express IL-4, IL-5, IL-10 and IL-13 (probably also IL-25), which induce IgE generation and recruit eosinophils. Similar to TH1 cells, TH2 cells can turn into TH1 cells after exposure to IL-12, if they are primed only once *in vitro*. In later stages of maturation they lose this plasticity. Stimulation with TGF- $\beta$  leads to a repression of IL-4 and an induction of IL-9 (Zhu and Paul 2010). Retroviral expression of T-bet reverses the TH2 polarization into TH1 polarization, indicated by the drop of IL-4 and IL-5 production and the initiation of INF- $\gamma$  expression (Szabo, Kim et al. 2000).

### **TH17 cells**

TH17 cells participate in the immune reaction against fungi and extracellular bacteria. TGF- $\beta$  together with IL-6, IL-21 and IL-23 induce the differentiation of naïve CD4<sup>+</sup> T cells into TH17 cells, by the activation of the transcription factors retinoic acid receptor orphan nuclear receptor (ROR $\gamma$ t) / STAT3. The maturation leads to the production of IL-17a, IL-17f, IL-21 and IL-22. Subsets of TH17 cells are found to generate IL-9 or IL-10. TH17 cells show the greatest plasticity among the TH cell lineages. Even after several rounds of TH17 priming they are able to express – additional to their IL-17 production – INF- $\gamma$  or IL-4, after exposure to IL-12 or IL-4, respectively (Zhu and Paul 2010).

### **T<sub>REG</sub>-Cells**

Naturally occurring regulatory T cells originate from the thymus in the presence of IL-2 and TGF- $\beta$ . Additionally CD28 co-stimulation and self-recognition support their development. Further IL-2, TGF- $\beta$  and stimulation of the TCR can prime naïve T helper cells to develop into inducible regulatory T cells in the periphery. The transcription factors forkhead box P3 (Foxp3) and STAT5 trigger their maturation. Isolated populations of T<sub>REG</sub>-Cell are composed of both the naturally occurring regulatory T cells and the inducible regulatory T cells. Possible they exhibit same functions. They mediate self-tolerance, dampen immune responses and possibly promote them. Until now no markers have been found to discriminate them. T<sub>REG</sub>-Cells also feature plasticity; a lack of lymphocytes induces a decline of Foxp3 and an increase of IL-17 and INF- $\gamma$  (Zhu and Paul 2010).

## **4.3. Fibrosis**

Fibrosis is considered as the pathological replacement of functional tissue by connective tissue. Well known initiators of fibrosis are viral infections, radiotherapy, chemotherapeutic drugs, aerosolized toxins (Wynn 2011) or alcohol (Lieber 1999). In contrast there are still unidentified trigger factors such as in idiopathic pulmonary fibrosis (IPF) (Wynn 2011). The process of fibrosis often starts with alveolar epithelial cell lesion in pulmonary fibrosis (Moore and Hogaboam 2008) or with chemical injury in the liver due to its drug metabolizing activities (Mehendale 2005). Subsequently inflammatory cells infiltrate the organ and stimulate fibroblast hyperplasia. Their maturation into myofibroblasts leads to an extensive collagen and extracellular matrix (ECM) deposition, which results in impaired tissue function due to destruction of the tissue architecture. This results in an ineffective gas exchange in the lungs (Moore and Hogaboam 2008). The liver

develops cirrhosis and shows portal hypertension with reduced perfusion and nodules of regenerating hepatocytes. Finally fibrosis results in malfunction of the organ due to the replacement of functional tissue by connective tissue. (Bataller and Brenner 2005).

#### **4.3.1. From Acute to Chronic Inflammation to Fibrosis**

Development of fibrosis has often been connected to dysregulation of wound healing. The process of wound healing is important to restore epithelial and endothelial function, especially the barrier function and the inhibition of blood loss. The process can be divided in three distinct phases; starting with the injury, followed by the inflammation and ending up with the tissue repair (see Figure 6).

In the injury phase inflammatory mediators are produced by the damaged epithelial and endothelial cells. These mediators activate the coagulation cascade and recruit platelets, leading to the formation of a fibrin clot and platelet aggregation. In order to induce leukocyte migration to the site of damage, platelet degranulation occurs, leading to vasodilatation of the blood vessels and enhanced permeability of the endothelium. Additionally the basement membrane composed of ECM components has to be degraded by leukocytes by means of MMPs such as MMP-2 and MMP-9 to perform extravasation. Moreover MMPs and their inhibitors (TIMPs) are important for the clearance of inflammatory cells and for the instruction to which extent collagen has to be deposited.

In the inflammatory phase the leukocytes, which have entered the site of damaged cells create chemokine gradients to recruit additional immune cells. Macrophages phagocyte damaged and dead cells and remove pathogens in case they exist. Moreover neutrophils, eosinophils and lymphocytes are recruited, release cytokines and promote inflammation (Wilson and Wynn 2009). Further endothelial cells are encouraged for cell division and migration toward the lesion and angiogenesis is promoted (Wynn 2008).

The wound healing process ends with the rebuilding of functional tissue. Wound contractions by myofibroblasts, and the fibrin rich scaffold, which directs epithelial and endothelial cells, help to reach this aim. Essential in this phase is the passage from increased collagen deposition towards a steady-state collagen production. This effect is achieved by apoptosis of fibroblasts, decay of inflammation and clearance of leukocytes (Wilson and Wynn 2009).

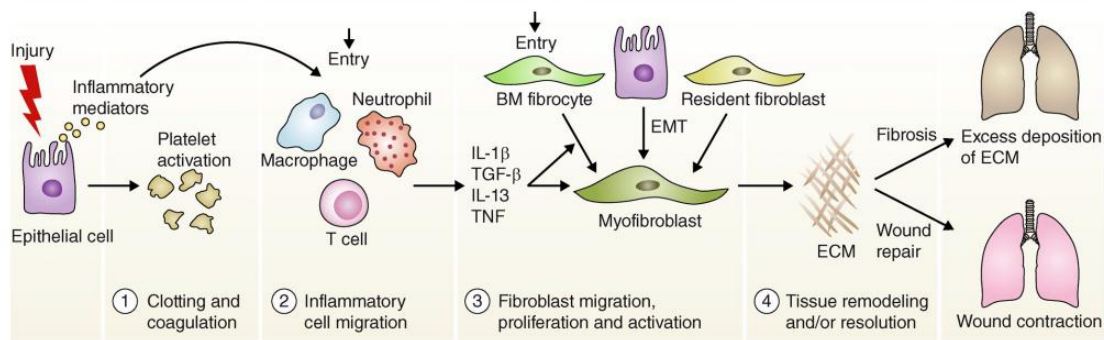


**Figure 6: Phases of wound healing response and their possible contribution to fibrosis. (Wynn 2011)**

According to the literature dysregulation of the wound healing response can result in chronic inflammation and further in fibrotic disease and is possible the main reason for this disease (Wilson and Wynn 2009). In comparison to normal wound healing, where the three phases are in sequence, inflammation and tissue remodeling take place synchronously in fibrosis (Wynn 2008). Even factors of the injury phase are involved in the fibrotic progression. The X-box binding protein-1 and thrombin are found increased in patients suffering from IPF, indicating an enhanced clotting and an important role of the platelets in this disease. Moreover thrombin induces the differentiation of fibroblasts into alpha smooth muscle actin ( $\alpha$ -SMA) - positive myofibroblasts, which are the main source for collagen in fibrosis. In addition maladjustment of MMPs and TIMPs can contribute to increased ECM degradation and thus elevated collagen deposition (Wilson and Wynn 2009).

The inflammatory response and the involved cells have a disputed role in fibrosis. On the one hand at the beginning of chronic disease inflammation can reduce the fibrotic outcome and on the other hand at later time points fibrotic progression can be supported through the production of the pro-fibrotic cytokines IL-13 and TGF- $\beta$ . In contrast macrophages and T<sub>REG</sub>-cells can also contribute to attenuate fibrotic process at later stages, by removing fibroblasts and down-regulating TGF- $\beta$ , respectively (Wilson and Wynn 2009).

In fibrotic tissue the last phase of wound healing, the tissue repair, often sustains. Retardation of fibroblast clearance is often noticed. One possibility could be their insensibility toward apoptotic inducers, but the precise mechanism remains to be clarified (Wilson and Wynn 2009). Instead of resolution of the wound healing process fibroplasia occurs and mesenchymal tissue is substituted by connective tissue, which is unable to carry out originally tissue function (Wynn 2004). All these effects lead to the

predominance of collagen synthesis over its degradation with an increase of total collagen and malfunction of the tissue (Wynn 2008).

#### **4.3.2. Mechanism of Fibrosis**

The development of fibrosis is a complex mechanism, influenced and accompanied by many factors, such as myofibroblasts, cytokines and chemokines (Wynn 2008).

Myofibroblasts play a major role in the pathogenesis of fibrosis, because they are the main source of collagen. They derive from various fibroblasts, for example residential fibroblasts of the tissue. Moreover epithelial and endothelial cells can give rise to fibroblasts via epithelial- mesenchymal transition and endothelial- mesenchymal transition, respectively. Additional bone marrow stem cells can differentiate into a fibroblast- like cells, the fibrocytes, which circulate in the blood. The specific functions in fibrosis of the different subpopulation have yet to be defined (Wynn 2008). Isolated fibroblasts of IPF patients exhibit changes in the expression of genes involved in the ECM proteins production and degradation. For example the altered expression pattern of  $\beta 1$  integrin, which in healthy fibroblasts is responsible for restraining fibroblast proliferation, if it is bound to type 1 collagen. B1 integrin activates PTEN, which further inactivates PI3K-Akt signaling, which supports cell survival (Wynn 2011). In the model of radiation induced pulmonary fibrosis antibody induced blocking of the integrin  $\alpha V\beta 6$  has protective effects; while bleomycin induced pulmonary fibrosis is increased (described below) in integrin  $\alpha V\beta 6$  knockout mice. The integrin  $\alpha V\beta 6$  may influence fibrosis via the activation of latent TGF- $\beta$ , thus the inhibition with antibodies may lead to an reduced amount of TGF- $\beta$  at the site of fibrosis (Sheppard 2008).

Fibroblasts can be activated via PAMPs and PPR, which induces the expression of proinflammatory cytokines and the differentiation into myofibroblasts. Since there are fibrosis disorders triggered by stimuli different from pathogens, additional mechanism of fibroblast activation are proposed. Fibroblast's autocrine TGF- $\beta$ , B-cell derived IL-6, Th2-cytokines and epigenetic changes account for myofibroblast activation (Wynn 2008).

Important mediators of fibroblast attraction and proliferation are macrophages through the production of TGF- $\beta 1$  and platelet derived growth factor (PDGF). In addition they secrete various chemokines and MMPs. It was shown that macrophages differently influence the progress of fibrosis dependent on the stage of the disease. Lacking macrophages in the early inflammatory phase leads to a decrease of myofibroblasts. In contrast in the late phase of remodeling macrophage deficiency results in persistent fibrosis, because subpopulations can induce apoptosis in myofibroblasts, remove cellular

debris and stimulate MMPs. Taken together macrophages are involved in all stages (Wynn 2011). Alternatively activated macrophages are considered as important inducer of fibrosis, because of their elevated expression of Arginase 1. Arginase 1 converts L-arginine into urea and L-ornithine. The enzymes ODC and OAT further use ornithine to produce polyamines and L-proline, which are important for cell growth and are substrates for collagen synthesis, respectively. In this context Arginase 1 expression is associated with increased fibrotic progression. In contrast to NOS, this is thought to reduce fibrogenesis because it uses the same substrate L-arginin, but produces L-hydroxyarginine, L-citrulline and nitric oxide (Wynn 2004). Interestingly Arginase 1 deficiency in myeloid cells induces an increase in inflammation and fibrosis in the model of *Schistosoma mansoni* induced liver fibrosis (Pesce, Ramalingam et al. 2009).

Many cytokines and chemokines participate either in pro- or anti- fibrotic mechanisms. The two most important chemoattractants in fibrogenesis are the macrophage inflammatory protein 1 $\alpha$  (MIP-1  $\alpha$ , CCL3) and the monocyte chemoattractant protein 1 (MCP-1, CCL2) (Wynn 2008). Both chemokines recruit phagocytes and are produced by macrophages and epithelial cells (Wynn 2008; Deshmane, Kremlev et al. 2009). They most likely act pro- fibrotic through the stimulation of IL-4 and IL-13. In addition the chemokine receptors CXCR4 and CCR7 promote fibrosis through the recruitment of fibrocytes (Wynn 2008). Furthermore TLR2 on respiratory epithelial cells can promote fibrosis via the induction of IL-27 and the chemokines MIP-1  $\alpha$ , MCP-1 and the interferon gamma-induced protein 1 (Kim, Go et al. 2011). In addition the blockage of TLR2 attenuates bleomycin induced pulmonary fibrosis and the maturation of DCs (Yang, Cui et al. 2009).

Various fibrotic diseases exhibit increased levels of TNF, mainly produced by macrophages. Controversially, TNF inhibitors trigger benefits, although TNF can hinder the synthesis of collagen in myofibroblasts (Wynn 2011).

Due to the inflammation a great quantity of leukocytes are present, which in turn support T-cell migration toward the origin of inflammation, activating the adaptive immune system. Different kinds of T helper cell subtypes have distinct influences on fibrogenesis. Th1 cells are considered to have anti- fibrotic effects, because they are responsible for acute inflammation rather than wound healing. In this context Th1 cytokines such as INF- $\gamma$  and IL-12 diminish fibrotic progression. In contrast Th2 cells are regarded to enhance fibrosis. Th2 cells mainly participate in the wound healing and tissue repair response and therefore increase fibrotic symptoms through their release of the cytokines IL-4, IL-5, IL-13 and IL-21. In addition Th2- linked genes – such as procollagens I, III and VI, Arginase 1

(Arg-1), lysyl oxidase, MMP-2, MMP-9 and TIMP-1 – are involved in fibrogenesis (Wynn 2008).

Elevated IL-4 expression in the bronchoalveolar lavage and in the interstitium accompanies idiopathic pulmonary fibrosis and cryptogenic fibrosing alveolitis, respectively. IL-4 acts on the IL-4 receptor on fibroblast subtypes, inducing the expression of collagen type I and III and fibronectin *in vitro* (Wynn 2008). Studies with IL-4 knockout mice demonstrated different IL-4 mediated effects on fibrosis development. Administration of a lethal dose of bleomycin leads to a higher mortality rate of IL-4 deficient mice compared to wild-type mice due to lung fibrosis. This effect was accompanied with an elevated infiltration of T cells in the knockout. In contrast 21 and 28 days post bleomycin treatment IL-4 knockout mice exhibit lower amounts of collagen (Huaux, Liu et al. 2003).

The central effector molecule in fibrosis is IL-13, which operates via the same IL-4R $\alpha$ / Stat6 pathway like IL-4, but with different consequences. Blocking IL-13 depletes collagen deposition, although IL-4 synthesis is maintained. In contrast, over-expression of IL-13 induces subepithelial airway fibrosis without additional inflammatory mediators. However IL-13 can additionally act via IL-13R $\alpha$ 2 chain, which was thought to be only a decoy receptor, and induce TGF- $\beta$ 1. The production of latent TGF- $\beta$ 1 in macrophages can be promoted by IL-13, as well as the synthesis of proteins which activate TGF- $\beta$ 1. In contrast IL-13 can also support collagen deposition independent of TGF- $\beta$ , due to results of MMP-9- , SMAD3- and TGF- $\beta$ 1- deficient mice (Wynn 2008). However the importance of IL-13 also varies in different fibrosis models. While mice deficient in IL-13 show attenuated liver fibrosis in response to *Schistosoma mansoni* compared to wild-type mice, the deficiency has no significant protective effect during bleomycin induced pulmonary fibrosis (Wilson, Madala et al. 2010).

The Th2 cytokine IL-5 recruits and activates eosinophils. It boosts fibrogenesis by promoting the expression of IL-13 and TGF- $\beta$ . Another Th2 cytokine IL-21 stimulates fibrogenesis through the induction of Th2-cell migration and survival. In addition it leads to a greater expression of IL-4 and IL-13 receptors on macrophages (Wynn 2008).

TGF- $\beta$  belongs to the most important contributors in fibrosis. The isoform TGF- $\beta$ 1 participates more than the two other isoforms TGF- $\beta$ 2 and TGF- $\beta$ 3. Monocytes in the blood and tissue macrophages are the main producer and secrete TGF- $\beta$  as a homodimer, which is bound to the latency-associated protein (LAP). LAP inactivates TGF- $\beta$  and has to be removed for the activation of TGF- $\beta$ . For example by integrin  $\alpha$  $\beta$ 6 or MMPs can cleave LAP, which enables TGF- $\beta$  to bind its receptor, which in turn phosphorylates the transcription factors SMAD 2 and 3. As a complex with SMAD 4, they

can adjust transcription of target genes, including procollagen I and III. In addition TGF- $\beta$ 1 is a putative inducer of the differentiation of epithelial cells into myofibroblasts and stimulates the activity of fibroblasts and their collagen synthesis. However TGF- $\beta$ / SMAD signaling pathways independent of collagen production are also proposed (Wynn 2008).

Macrophages and neutrophils can additionally contribute to fibrogenesis via the production of reactive oxygen species (ROS). ROS are created by ROS-generating mitochondria and members of the NADPH oxidase family. For instance NOX4 is elevated in IPF and mediates myofibroblasts differentiation and ECM protein synthesis. Moreover ROS, together with TNF and IL-1 $\beta$ , stimulate the expression of plasminogen activator inhibitor 1, which inhibits plasmin/ plasminogen activator systems. This system is capable to degrade ECM components and induce the production of anti-fibrotic functioning prostaglandin E2 (Wynn 2011).

#### **4.3.3. Bleomycin Induced Lung Fibrosis**

The antibiotic bleomycin (BLM) from actinobacteria *Streptomyces verticillus* is used to induce pulmonary fibrosis in mice. First the drug was identified to eradicate cell carcinomas and skin tumors (Moore and Hogaboam 2008), because it is able to break the DNA double helix (Azambuja, Fleck et al. 2005). Bleomycin is composed of two major structures, namely the bithiazole and the pyrimidine and imidazole structure. The first structure allows bleomycin to intercalate into the DNA double helix. The second forms an activated complex with iron and oxygen, which generates reactive oxygen species (ROS). These ROS mediate strand scission and the loss of DNA bases. In addition bleomycin provokes lipid peroxidation and in this context leads to cell damage, which results in the formation of oedema, infiltration of immune cells and in the end to collagen deposition. The adverse effect of causing pulmonary fibrosis is the limiting factor for a cancer therapy (Hay, Shahzeidi et al. 1991). Degradation of BLM is performed by the bleomycin hydrolase. The low expression of this inactivating enzyme in the respiratory tract is may be the reason for the great susceptible of the lung (Moore and Hogaboam 2008). About 50% of bleomycin is egested by the kidney within four hours (Azambuja, Fleck et al. 2005). Due to these findings the drug is used as model for lung fibrosis in different animal models – such as mice, rats, rabbits – which showed a dose dependent lung fibrosis induction after injecting bleomycin intraperitoneal (i.p.), intravenous (i.v.), subcutaneous or intratracheal (i.t.). May be due to variations in the expression of bleomycin hydrolase, different mice strains react different to bleomycin. For example C57Bl/6 mice are more prone to bleomycin induce lung fibrosis than Balb/c mice (Moore and Hogaboam 2008).

In this study we used the intratracheal route, but modified the application by administering bleomycin through the nose leading to a local application (described in material and methods). For the i.t. or intranasal (i.n.) induction of fibrosis a single administration is efficient, in contrast to an i.v. injection. The etiopathology is characterized by a peak after 21 days and is followed by resolution of the pathology. This transient nature of the model differs from the human character of the disease (Moore and Hogaboam 2008).

#### **4.4. Aim of the Study**

The aim of this study was to address more precisely the contribution of the PI3K and PTEN pathway to the development of bleomycin induced pulmonary fibrosis.

The first purpose was the establishment and the characterization of the phenotype of the bleomycin induced lung fibrosis disease model in mice. Subsequently we investigated mice with a myeloid cell specific PTEN deficiency based on the Cre/loxP system. Therefore the expression of the site-specific DNA recombinase Cre (cyclization recombination) was set under the control of the lysozyme M (LysM) gene promoter, which is used for the generation of conditional knockout in macrophages and DCs (Hume 2010). Based on previously published data, by our group, it can be concluded that myeloid PTEN deficient mice show improved survival during *Streptococcus pneumoniae* infection with reduced levels of TNF- $\alpha$  and elevated levels of IL-10 (Schabbauer, Matt et al. 2010).

Because of that we were interested in the effects in a chronic inflammatory lung disease model. Therefore we investigated the collagen deposition and fibrotic progression. Expression of cytokines was analyzed to identify variations in their expression patterns and their influence on the development of the disease. Additionally we wanted to determine if PTEN deficiency modulates alternative activation of macrophages and if this consequence contributes to pulmonary fibrosis.

## 5. Materials and Methods

### 5.1. Mice

In this study eight to twelve week old, sex matched mice were used and were compared with a control group of wild-type littermates. The genotype was determined via direct polymerase chain reaction (PCR) of in PCR-lysis buffer lysed murine tissue. All animal research studies were approved and were confirm with the institutional guidelines (BMWF-66.009/0103-C/GT/2007).

T.W. Mak (Cancer Institute at Princess Margaret Hospital, University Health Network, Toronto, Ontario, Canada) kindly supplied floxed PTEN mice (Suzuki, Yamaguchi et al. 2001). Floxed Arginase 1 mice were purchased from Jackson Laboratory (Maine, USA). The LysM Cre recombinase transgenic mice were a kind gift from R. Johnson (University of California San Diego, La Jolla, CA) (Peyssonnaud, Datta et al. 2005). The intercrossed mice were backcrossed to a C57BL/6J background for at least eight generations.

### 5.2. Genotyping

#### 5.2.1. Murine Tissue Lysis

##### Materials

- For all experiments requiring dH<sub>2</sub>O was generated by the Deionizer Milli-Q Plus PF, Millipore, MA, USA
- Ear-tag punch (Fisher Scientific, Pittsburg, PA, USA)
- Lysis Buffer  
12.11 g (100 mM) Tris-Cl [pH 8.0], 18.61 g (5 mM) EDTA [pH 8.0], 0.2 g (0.2%) SDS, 11.69 g NaCl (200 mM) were dissolved in 100 ml dH<sub>2</sub>O.
- Proteinase K, PCR grade (Roche Diagnostics, Mannheim, Germany)

### Procedure

To be able to perform littermate controlled experiments we cross-bred wild-type and conditional knockout mice. The genotype of the offspring was determined by taking murine tissue from the ear, which brought along the possibility to recognize the mouse again, because holes were punched in the ears and depending on its localization it signified a different number. The murine tissue was lysed in 95  $\mu$ l PCR-lysis buffer and 5 $^{\circ}$  $\mu$ l proteinase K. The samples were put into a thermo block (Mixing Block MB-102|BIOER, Biozym Scientific GmbH, Hess. Oldendorf, Germany) at a temperature of 55°C and the samples were shook with 650 rpms for 3 hours. After vortexing (Vortex-Genie 2, Scientific Industries Inc., NY, USA) the samples 1 ml dH<sub>2</sub>O was added and the lysis was stopped by heating the samples up to 99°C for 5 min. Afterwards the lysed tissue was centrifuged at 15 000 rpm for 5 min at 4°C (Centrifuge 5417c, Eppendorf AG, Hamburg, Germany) and the chromosomal DNA was stored at 4°C.

### 5.2.2. Polymerase Chain Reaction PCR

#### Materials

- 5x GoTaqR<sup>®</sup> Flexi Buffer (Promega, Madison, WI, USA)
- dNTPs (deoxyribonucleotide triphosphate) (Fermentas, St. Leon-Rot, Germany)
- GoTaqR<sup>®</sup> Flexi DNA Polymerase (Promega, Madison, WI, USA)
- Magnesium Chloride Solution, 25 mM (Promega, Madison, WI, USA)
- PCR adhesive sealing sheets (Eppendorf AG, Hamburg, Germany)
- Twin.tec PCR 96 well plate (Eppendorf AG, Hamburg, Germany)

#### Procedure

Out of the lysed murine tissue direct PCR was carried out. Therefore a master mix was prepared by mixing 12.875  $\mu$ l dH<sub>2</sub>O, 5  $\mu$ l 5x Green GoTaq<sup>®</sup> Reaction Buffer, 2.5  $\mu$ l dNTPs [2 mM], 2.5  $\mu$ l MgCl<sub>2</sub> [25 mM], 1  $\mu$ l primer mix and 0.125  $\mu$ l GoTaq<sup>®</sup> DNA Polymerase [5  $\mu$ g/ $\mu$ l] per each sample. The primer mix was composed of the forward and reversed primer with a concentration of 10 pM/ $\mu$ l each and the sequences can be seen in table 1. 2  $\mu$ l of the lysate were mixed with the master mix. The PCR was completed by the Mastercycler egradient S (Eppendorf AG, Hamburg, Germany) by using the gene specific program from table 2.

**Table 1: Sequences of the PCR primers for genotyping**

Gene	Forward primer (5' → 3')	Reverse primer (5' → 3')
<b>PTEN</b>	CTC CTC TAC TCC ATT CTT CCC	ACT CCC ACC AAT GAA CAA AC
<b>Arg 1</b>	TGC GAG TTC ATG ACT AAG GTT	AAA GCT CAG GTG AAT CGG
<b>Cre</b>	TCG CGA TTA TCT TCT ATA TCT TCA G	GCT CGA CCA GTT TAG TTA CCC

**Table 2: Description of the PCR programs**

PTEN/ Cre		Arginase 1		Steps
Temperature [°C]	Time [s]	Temperature [°C]	Time [s]	
94	180	94	180	Activation of polymerase
94	45 (x35)	94	30 (x35)	Denaturing
60	45 (x35)	60	60 (x35)	Annealing
72	60 (x35)	72	60 (x35)	Extending
72	300	72	120	Last extension
4	∞	4	∞	Cool down

### 5.2.3. Gel Electrophoresis

#### Materials

- 50 x TAE buffer  
242 g Tris base, 71.1 ml Glacial acetic acid and 100 ml 0.5 M EDTA [pH 8.0] were mixed and filled up with dH<sub>2</sub>O to 1000 ml.
- Agarose (Biozym LE Agarose, Biozym Scientific GmbH, Hess. Oldendorf, Germany)

- Ethidium Bromide (Ethidium Bromide Solution 10 mg/ml, Invitrogen Corporation, CA, USA)
- Gene Ruler™ 1 kb DNA Ladder (Fermentas, St. Leon-Rot, Germany)

### **Procedure**

A 0.2% agarose gel was prepared by dissolving 5 g agarose in 250 ml 1x TAE buffer, by heating in the micro wave oven (ELIN). After cooling down 25 µl ethidium bromide was added and the gel was poured into a gel electrophoresis plate and combs were stuck into (peqlab Biotechnologie GmbH, Erlangen, Germany). After the polymerization of the gel the samples and the marker were applied and the gel ran at 120 V for 80 min. The UV-imager (peqlab Biotechnologie GmbH, Erlangen, Germany) was used to take pictures of the gel.

## **5.3. In Vivo Experiments**

### **5.3.1. Anesthesia**

- Forane® (Isoflurane, Abott Laboratories Ltd., Queenborough, GB)
- Ketaminol® (Intervet International GmbH, Unterschleißheim, Germany)
- Xylasol® (Dr. E. Gräub AG, Bern, CH)
- Ringer's Solution (B|Braun Medical Inc., Bethlehem, PA, USA)

Forane® is an inhalation narcotic and was used to euthanize by an overdose. The sedative was dropped on a tissue paper, which was put into a glass container together with a mouse.

For anesthetizing mice a mixture of Ketaminol® and Xylasol®, known as Hellabrunner mixture, was prepared according to table 3. 5 mg/kg Xylasol® and 50 mg/kg Xylasol® were injected intraperitoneally.

**Table 3: Hellabrunner mixture**

Hellabrunner Mixture	
Ketaminol® (100 mg/ml)	2 ml
Xylasol® (20 mg/ml)	1 ml
Ringer's Solution	17 ml

### 5.3.2. Fibrosis Induction

#### Materials

- Bleomycin Sulfate, Streptomyces verticillus (Calbiochem®, Merck KGaA, Darmstadt, Germany)
- Natrium chloratum physiologicum 0.9% „Meditrade“-Infusionslösung (Meditrade Medicare Medizinprodukte GmbH & Co KG, Kufstein. Austria)

#### Method

Mice were anesthetized with 5 mg/kg Xylasol® and 50 mg/kg Ketaminol® intraperitoneally. Bleomycin sulfate was diluted in sterile 0.9% saline solution to a concentration of 0.1 iu BLM per 50 µl. Mice were treated with 0.004 iu bleomycin per one gram body weight. An intranasal application was achieved by a pipette, and drop per drop was applied on the nose of the mouse, which got inhaled immediately.

### 5.3.3. Clinical Fibrosis Scoring

To monitor the fibrotic progression the body weight of the mice were documented. The first time they were weight in the morning before they were treated with bleomycin. Subsequently mice were weight every morning during the experiment. The body weight of the first day was used as reference value.

### 5.3.4. Bronchoalveolar Lavage

#### Materials

- 10 x PBS

400 g NaCl, 10 g KCl and 10g KH<sub>2</sub>PO<sub>4</sub> were dissolved in 5000 ml dH<sub>2</sub>O and the pH was adjusted to 7.4.

- BD Venflon™ 20g A1.26/N (BD Biosciences, Franklin Lakes, NJ, USA)
- Forane® (Isoflurane, Abott Laboratories Ltd., Queenborough, GB)
- Syringe 1 ml (VWR International, Vienna, Austria)

### Method

Mice were euthanized by an overdose of isofluran. The skin and the thyroid gland were removed to reveal the trachea. Afterwards the trachea was jabbed with a 20 g venflon and the needle of the venflon was removed and a 1 ml syringe was connected. For the isolation of cytokines two times 0.5 ml PBS were squirted into the lung with the syringe and recollected by gentle pulling of the plunger. Subsequently the bronchoalveolar lavage fluid (BALF) was centrifuged at 1200 rpm for 5 min at 4°C. The supernatant containing the cytokines was stored at -20°C and analyzed by ELISA (enzyme-linked immunosorbent assay). The cell pellet was either lysed in two fold SDS PAGE sample buffer and stored at -20°C or resuspended in TRIzol and preserved at -70°C, the samples were examined by western blot or by real time PCR, respectively.

### 5.3.5. Lung Homogenization

#### Materials

- 2 x Greenberger Lysis Buffer

The Greenberger lysis buffer was made by mixing 150 mM NaCl, 15 mM Tris base, 1 mM MgCl<sub>2</sub> x 6 H<sub>2</sub>O, 1 mM CaCl<sub>2</sub> x 2 H<sub>2</sub>O in 200 ml dH<sub>2</sub>O. Subsequently the pH was adjusted to 7.4, 1% Triton was added and the buffer was filled up to 250 ml with dH<sub>2</sub>O.

- Protease inhibitor (Roche Diagnostics, Vienna, Austria)

Complete protease inhibitor cocktail tablets, EDTA free were used and directly solved in Greenberger lysis buffer.

- Screw-cap tubes (Peqlab Biotechnologie GmbH, Erlangen, Germany)
- Screw-caps (Peqlab Biotechnologie GmbH, Erlangen, Germany)
- Stainless Steel Beads 5 mm (Quiagen Vertriebs GmbH, Vienna Austria)

## Procedure

After extraction of the four right pulmonary lobes, they were weighed unfrozen. Four fold of the weight in mg saline ( $\mu\text{l}$ ) was added. Subsequently the tissue was homogenized by the Precellys 24 (Bertin technologies, Aix-en-Provence, France) with stainless steel beads with a diameter of 5 mm. The homogenization was performed with 5000 rpm 4 times for 20 sec. 100  $\mu\text{l}$  of the homogenate was mixed with 300  $\mu\text{l}$  TRIzol and RNA isolation was completed. 600  $\mu\text{l}$  homogenate were merged with 600  $\mu\text{l}$  Greenberger lysis buffer and protease inhibitor. After incubating 20 min on ice the samples were centrifuged at 1200 rpm at 4°C for 15 min. Afterwards the supernatant was stored at -20°C and used for ELISA.

### 5.3.6. Preparation of Single Cell Suspensions of Murine Lungs

#### Materials

- Cell strainer 70  $\mu\text{m}$  and 40  $\mu\text{m}$  BD Falcon (BD Biosciences, Franklin Lakes, NJ USA)
- Collagenase I (Gibco®, Grand Island, NY, USA)
- DNase I ((Gibco®, Grand Island, NY, USA)
- Fetal calf serum (Invitrogen, Karlsruhe, Germany)
- Serum-free GIBCO™ RPMI Medium-1640 (Invitrogen, Karlsruhe, Germany)
- Trypan Blue solution (Sigma Chemicals, Balcatta, Australia)

#### Method

Mice were euthanized by cervical dislocation. The lungs and the heart were revealed by opening the chest. Afterwards the peritoneum was opened to intersect the vena cava. Subsequently the lungs were perfused through the heart with 1 x PBS, by pricking into the right ventricle with a 27 g needle. Once the pulmonary lobes turned white, the lungs were taken out of the thorax. The lungs were dissected in small pieces and incubated in RPMI + 5% FCS with dose DNase I (50 iu/ml) and dose collagenase I (150 iu/ml) at 37°C for one hour. The digested lungs were pressed through a 70  $\mu\text{m}$  cell strainer and centrifuged at 1250 rpm, 4 °C, for 10 min. The pellet was resuspended in PBS containing 2% FCS and cells were passed through a 40  $\mu\text{m}$  cell strainer two times

with an end volume of 15 ml. Finally the viable cells were distinguished from dead cells by trypan blue staining and the viable cells were counted by the means of Bürker-Türk counting chamber.

#### **5.4. In Vitro Experiments**

##### **Materials**

- 96-well plates (Iwaki<sup>®</sup>, Iwaki Europe GmbH, Willich, Germany)
- BD Connecta Leur-Lok 3 Way Stopcock Blue (BD Biosciences, Franklin Lakes, NJ USA)
- BD Venflon<sup>™</sup> 20g A1.26/N (BD Biosciences, Franklin Lakes, NJ USA)
- Fetal calf serum (Invitrogen, Karlsruhe, Germany)
- Forane<sup>®</sup> (Isoflurane, Abott Laboratories Ltd., Queenborough, GB)
- L-glutamine (Invitrogen, Karlsruhe, Germany)
- 1 x PBS
- PSF (100 U/ml penicillin, 100 g/ml streptomycin, 0.25 g/ml amphotericin)
- Recombinant Mouse IL-4 (R&D Systems, Minneapolis, USA)
- Recombinant Mouse IL-13 (R&D Systems, Minneapolis, USA)
- Serum-free GIBCO<sup>™</sup> RPMI Medium-1640 (Invitrogen, Karlsruhe, Germany)
- Syringe 5 ml and 10 ml (VWR International, Vienna, Austria)

##### **5.4.2. Isolation of Alveolar Macrophages**

In order to isolate alveolar macrophages, mice were euthanized with an overdose of isoflurane and the lungs were flushed with PBS. Therefore the trachea was revealed, by removing the skin and the thyroid gland. A venflon was used to prick into the trachea and the needle of the venflon was detached. The venflon was connected to a three-way stopcock, which was further attached to a 10 ml syringe filled with PBS and an empty 5 ml syringe. 1 ml PBS was injected into the trachea and in the alveolar space and recollected in the 5 ml syringe. This step was repeated ten times.

The collected BALF was centrifuged at 1500 rpm for 7 min at 20°C with a brake of 4. The supernatant was discarded and the cell pellet resuspended in GIBCO™ RPMI Medium.

### **5.4.3. Stimulation of Alveolar Macrophages *In Vitro***

Alveolar macrophages were isolated by a bronchoalveolar lavage described above. After counting the cells with the Bürker-Türk counting chamber  $10^5$  cells per well were plated in a 96 well plate. As media GIBCO™ RPMI Medium was used and dosed with 10% fetal calf serum, 1% PSF and L-glutamine. The cells were incubated overnight at 37°C and 5% CO<sub>2</sub> in the Steri Cycle CO<sub>2</sub> Incubator (Thermo Electron Corp., MN 55359, USA). On the following day the cells were stimulated with 5 µg/ml IL-4 and 5 µg/ml IL-13. Different stimulation times were applied dependent on the experiment. After the stimulation the supernatant was collected for cytokine determination and the cells were lysed with 2 x sample buffer for SDS-PAGE.

## **5.5. Analytical Methods**

### **5.5.1. Histology**

#### **Materials**

- 1 x PBS
- Cover Glass 24 x 24 mm (VWR Vienna, Austria)
- Ethanol (Merck Merck KGaA, Darmstadt, Germany)
- Forane® (Isoflurane, Abbott Laboratories Ltd., Queenborough, GB)
- Objective slides Superfrost®/plus (Carl Roth GmbH, Karlsruhe, Germany)
- Paraformaldehyd (Carl Roth GmbH, Karlsruhe, Germany)
- Paraffin wax (Sigma Aldrich Handels GmbH, Wien, Austria)
- Roticlear® for histology (Carl Roth GmbH, Karlsruhe, Germany)

## Procedure

The left pulmonary lobe was taken for histological section. First the mice were euthanized by an overdose of isoflouran. To be able to extract the lung first the skin above the chest was removed. Subsequently the peritoneum was opened and the diaphragm was removed. Then the chest was opened on the left and right side, so that it could be tilt up. Finally the lobes were released by cutting off the blood vessels. After extraction the left lobe was fixed with 10% paraformaldehyd in one fold PBS for two days at room temperature. Afterwards the lungs were dehydrated, by putting them into 75% ethanol overnight, then in 95% ethanol for two hours followed by incubation overnight in 100% ethanol. On the following day the tissue samples were put into 100% ethanol at 37°C for 30 min. The next incubation was in 100% roticlear at 37% for half an hour and then the temperature was raised to 60°C and the samples were let there for 30 min. Afterwards the tissue was incubated in a mixture composed of roticlear and paraffin wax at a ratio of 1:1 for 24 hours at 60°C. Finally the bottle was opened for 48 hours at 60°C to let the isopropanol evaporate. Subsequently the tissue was embedded in paraffin by the means of an embedding machine (HistoStar, Thermo Fischer Scientific, Waltham, USA). The precision rotary microtome (Finesse E+, Shandon, Thermo Fischer Scientific, Waltham, USA) was used to slice the paraffin blocks. The sections were made with a diameter of 2 µm.

### 5.5.2. Hematoxilin and Eosin Stain

#### Materials

- Eosin Y solution 0.5% in water (Carl Roth GmbH, Karlsruhe, Germany)  
2 ml 10% eosin was mixed with 198 ml 80% ethanol and 500 ml acetic acid
- Ethanol (100%, 96%, 80%, 70%, 50%) Ethanol (Merck Merck KGaA, Darmstadt, Germany)
- Hamalaum solution acidic acc. to Mayer (Carl Roth GmbH, Karlsruhe, Germany)
- Hydrochloric acid 37% (Carl Roth GmbH, Karlsruhe, Germany)
- Mounting Medium Roti®-Mount (Carl Roth GmbH, Karlsruhe, Germany)
- Roticlear® for histology (Carl Roth GmbH, Karlsruhe, Germany)

## Procedure

The slides with the paraffin slices of the lungs were first deparaffinized by two incubations in Roticlear for 20 min. Afterwards the slides were rehydrated by incubating them in 100%, 96%, 80%, 70%, 50% ethanol for 30 sec each. Then the samples were rinsed in distilled water for 5 min, followed by the staining with hamalaun solution, which was diluted 1:2 with distilled water, for 10 min. Subsequently the sections were washed in running tap water for 7 min. The staining was controlled under the microscope and then the samples were dipped 2 times in 75% ethanol with 0.4% HCl for the decolorization. Then the samples were rinsed in tap water for 7 min and the tissues were dehydrated by incubations in 50% (30 sec), 70% (30 sec) and 80% (20 sec) ethanol consecutively. Then the eosin stain for 2.5 min followed. Afterwards the slides were incubated for 30 sec in 96% ethanol, then for 2 min in 100% ethanol and cleaned in Roticlear. Finally the tissue was mounted with Roti Mount and cover slips were placed on the tissue sections.

### 5.5.3. Sirius Red Stain

#### Solutions

- Acidified water  
5 ml acetic acid (glacial) (Sigma-Aldrich Handels GmbH, Wien, Austria) was added to 1000 ml of distilled water.
- Mounting Medium Roti®-Mount (Carl Roth GmbH, Karlsruhe, Germany)
- Picro-sirius red solution  
0.5 g Sirius red F3B (C.I. 35782) were solved in 500 ml saturated aqueous solution of picric acid. A little amount of solid picric acid was added to ensure saturation.
- Roticlear® for histology (Carl Roth GmbH, Karlsruhe, Germany)

#### Method

First the paraffin sections on the slides were deparaffinized by two incubations in Roticlear for 20 min each. Subsequently the slides were incubated in 100%, 96%, 80%, 70%, 50% ethanol for 30 sec each to rehydrate the tissue. After washing the tissue samples in distilled water for 5 min, they were stained in picro-sirius red for one hour. Afterwards they were washed in acidified water two times for 1 min each. The remaining water was removed by filter papers. Then the samples were incubated three times in

100% ethanol for 5 min. The last step was the clearance with roticlear for 5 min. Finally the tissue sections were mounted with Roti®-Mount and cover slips were put on the top of the slide.

#### **5.5.4. Quantification of Histological Sections**

Pictures of the stained histological sections were taken with the microscope (Olympus, Vienna, Austria). The collagen deposition according to the Sirius red stain was quantified with ImageJ (Abramoff, Magalhaes et al. 2004). First blood vessels were excluded to eliminate false positive collagen deposition due to the collagen of the adventitia. Then the picture was converted from a RGB format to 8-bite format. For the elimination of the background noise the same threshold was set for every picture. The amount of particles were quantified by the analyze particles tool, which were compared.

#### **5.5.5. Hydroxyproline Measure**

##### **Solutions**

- Acetate citrate buffer  
120 g N acetate trihydrate, 46 g citric acid, 12 ml acetic acid and 34 g NaOH were dissolved in 1000 ml dH<sub>2</sub>O and the pH was adjusted to 6.5.
- Chloramine T solution  
635 mg chloramines T was dissolved in 10 ml 50% N-propanol. Afterwards 40 ml acetate citrate buffer and 1.11 ml 10 M NaOH were added.
- Ehrlich's reagent  
1.5 g 4-dimethylamino benzaldehyde was added to a mixture of 6.7 ml N-propanol and 3.3 ml perchloric acid.
- Hydroxypoline standards  
Out of the stock solution with a concentration of 1 mg/ml standards were prepared by diluting the stock solution with 6 M HCl. The standard curve consisted of the standard points: 500, 250, 125, 62.5, 31.5, 15.63, 0 µg/ml hydroxyproline.

## Procedure

The four frozen right pulmonary lobes were weighed and 900  $\mu\text{l}$  prechilled  $\text{dH}_2\text{O}$  was added. With the tissue homogenizer (INULA, OMNI TH International, Kennesaw, GA, USA) the lungs were homogenized. Between the samples the homogenizer was rinsed in distilled water, 96% ethanol and again in distilled water. The homogenate was transferred into screw top tubes and 125  $\mu\text{l}$  50% TCA (trichloroacetic acid) were added, vortexed and incubated for 20 min on ice. After the precipitation of the protein the samples were centrifuged at 6000 rpm for 10 min at 4°C. The supernatant was discarded and 1000  $\mu\text{l}$  ice-cold ethanol were added and vortexed. Subsequently the samples were spun 6000 rpm for 10 min at 4°C again. This washing step was repeated two times. After discarding the supernatant the tubes were opened and dried up side down for 10 min. Afterwards 800  $\mu\text{l}$  of 6 M HCl were added and incubated for 18 hours at 95°C. Subsequently the samples were cooled down to room temperature and then vortexed. After a centrifugation at 14000 rpm for 10 min at room temperature the supernatant was withdrawn by using a 1 ml syringe needle and volume was documented. 40  $\mu\text{l}$  of the supernatant were mixed with 460  $\mu\text{l}$  Chloramine T solution. In addition 460  $\mu\text{l}$  Chloramine T solution was added to the hydroxyproline standards. Both were incubated for 30 min. Afterwards 500  $\mu\text{l}$  Ehrlich's reagent was added and incubated at 65°C for 20 min. After the samples reached room temperature the coloring was measured at 550 nm.

The amount of hydroxyproline ( $\mu\text{g}/\text{ml}$ ) per pulmonary lobe was calculated as follows. The concentration ( $\mu\text{g}/\text{ml}$ ) was divided by 1000 multiplied by the documented volume ( $\mu\text{l}$ )

### 5.5.6. RNA Isolation with TRIzol

#### Materials

- Isopropanol waterfree (Fischer Scientific, Waltham, MA, USA)
- RotiPhenol/ Chloroform (Carl Roth GmbH, Karlsruhe, Germany)
- TRIzol® Reagent (Invitrogen Corporation, CA, USA)
- UltraPure DEPC-treated Water (Invitrogen Corporation, CA, USA)

### **Method**

In order to isolate RNA from tissue samples homogenized tissue samples in TRIzol were centrifuged at 12000 g for ten minutes at 4°C and with the supernatant the protocol was continued. To the supernatant and direct to the cell samples in TRIzol a fifth of the initial volume of TRIzol were added and the samples were mixed for 5 sec and incubated for 3 min at room temperature (RT). Subsequently the samples were spun with 12000 g for 15 min at 4°C. The water phase was taken and the same amount of isopropanol was added, mixed by pipetting and incubated overnight at -20°C. On the next day the samples were centrifuged at 12000 g for 10 min at 4°C. The supernatant was discarded and 500 µl 75% EtOH was added, incubated for 2 h at -70°C and then spun with 12000 g for 10 min at 4°C. Afterwards the supernatant was discarded and 500 µl 75% EtOH was added and then centrifuged with 12000 g for 10 min at 4°C. The supernatant was removed and the pellet was dried at RT. The pellet was dissolved in nuclease free water and solved for 10 min at 55°C.

The RNA concentration was measured with the Nano-Drop machine (NanoPhotometer® Pearl, IMPLEN, Munich, Germany) and the RNA samples were stored at -70°C.

### **5.5.7. Reverse Transcription**

#### **Materials**

- High-Capacity cDNA Reverse transcription Kits, Applied Biosystems, US
- UltraPure DEPC-treated Water (Invitrogen Corporation, CA, USA)

#### **Method**

First a master mix was prepared, by mixing 2 µl RT buffer, 0.8 µl dNTP Mix (100 mM), 2.0 µl RT random primers, 1 µl RNase Inhibitor and 3.2 µl nuclease-free water. 10 µl of the master mix were added to 10 µl RNA. RNA samples were diluted and 1 µg RNA was transcribed. Subsequently the samples were incubated for ten min at 25°C; afterwards they were allowed to stand for 120 min at 37°C. By rising the temperature to 85°C the reaction was stopped and then cooled down to 4°C. The cDNA was stored at -20°C.

### 5.5.8. Quantitative Polymerase Chain Reaction (qPCR)

#### Materials

- Adhesive PCR foil (Sarstedt, Nümbrecht, Germany)
- Ethanol 70% and 96% (Merck Merck KGaA, Darmstadt, Germany)
- Fast SYBR® Green Master Mix (Applied Biosystems, Life Technologies Corporation, Carlsbad, California, USA)
- Multiply PCR-Plates 96 well (Sarstedt, Nümbrecht, Germany)
- UltraPure DEPC-treated Water (Invitrogen Corporation, CA, USA)

**Table 4: Sequences of the used primers for Real time PCR.**

<b>Gene</b>	<b>Forward primer (5'→ 3')</b>	<b>Reverse primer (5'→ 3')</b>
<b>KC</b>	CCA CAC TCA AGA ATG GTC GC	TCT CCG TTA CTT GGG GAC AC
<b>IL-6</b>	TGC AAG TGC ATC ATC GTT GTT C	CCA CGG CCT TCC CTA CA
<b>Arg 1</b>	AGA GAT TAT CGG AGC GCC TT	TTT TTC CAG CAG ACC AGC TT
<b>FIZZ</b>	CTG GAT TGG CAA GAA GTT CC	CCC TTC TCA TCT GCA TCT CC
<b>YM1</b>	TTT CTC CAG TGT AGC CAT CCT T	TCT GGG TAC AAG ATC CCT GAA
<b>MRC1</b>	CAG GTG TGG GCT CAG GTA GT	TGG CAT GTC CTG GAA TGA T
<b>CCL17</b>	TGC TTC TGG GGA CTT TTC TG	ATA GGA ATG GCC CCT TTG AA
<b>CCL22</b>	TCT GGA CCT CAA AAT CCT GC	TGG AGT AGC TTC TTC ACC CA
<b>iNOS</b>	TGA AGA AAA CCC CTT GTG CT	TTC TGT GCT GTC CCA GTG AG
<b>HPRT</b>	TCC TCC TCA GAC CGC TTT T	CAT AAC CTG GTT CAT CAT CGC

### Procedure

The master mix was prepared as described in table 5. 13.5  $\mu$ l master mix were put into a well with 1.5  $\mu$ l cDNA. All steps were performed on ice and protected from light. As reference gene hypoxanthine phosphoribosyltransferase (HPRT) was applied. Sequences of the primers were either looked up in the qPrimer Depot (<http://mouseprimerdepot.nci.nih.gov/>) or were designed with Ensembl ([www.ensembl.org](http://www.ensembl.org)) and verified via NCBI Blast (<http://blast.ncbi.nlm.nih.gov/Blast.cgi>). The sequences of the used primers can be seen in table 4.

The PCR was achieved by the StepOne™ Real-Time PCR System (Applied Biosystems, Foster City, CA, USA).

**Table 5: Composition of the qPCR mastermix**

Mastermix	
Reagents	$\mu$ l /sample
Master mix	7.5
Forward primer	0.375
Reverse primer	0.375
DEPC water	5.25

### 5.5.9. SDS-PAGE

#### Materials

- 96% Ethanol (Merck Merck KGaA, Darmstadt, Germany)
- Anti-Chicken IgY HRP Conjugate (Promega, Madison, WI, USA)
- Anti-Rabbit IgG HRP-linked Antibody (Cell Signaling Technology, Danvers, MA, USA)
- Bio-Rad Filter Papers (Bio-Rad Laboratories Inc., Hercules, CA, USA)
- Gel Pouring Rack (Bio-Rad Laboratories Inc., Hercules, CA, USA)
- Immobilion-P PVDF Transfer Membrane (Millipore, Bedford, MA, USA)
- PlusOne Tween-20 (GE Healthcare, Bio-Science AB, Uppsala, Sweden)

- Running chamber and Western Blot Apparatus (Bio-Rad Laboratories Inc., Hercules, CA, USA)
- Skim Milk Powder (Sigma-Aldrich Handels GmbH, Wien, Austria)
- SuperSignal<sup>®</sup> West Femto Maximum Sensitivity Substrate (Thermo Fisher Scientific, Waltham, USA)
- TEMED (Roth GmbH+Co. KG, Karlsruhe, Germany)

### **Stocks**

- APS (10% ammonium persulfate in dH<sub>2</sub>O.)
- 10 x PBS
- PBS-T

PlusOne Tween 20 (GE Healthcare, Bio-Science AB, Uppsala, Sweden) was added to 1x PBS in a concentration of 0.5%.

### **Solutions**

- Solution A  
30 g acrylamide and 0.8 g methylenbisacrylamide were dissolved in 100 ml dH<sub>2</sub>O.
- Solution B  
18.2 g tris(hydroxymethyl)aminomethane and 0.4 g SDS were dissolved in dH<sub>2</sub>O and the pH was adjusted to 8.8.
- Solution C  
6.06 g Tris base and 0.4 g SDS were filled up to 100 ml dH<sub>2</sub>O. The pH was adapted to 6.8.

### **Buffers**

- 2x Sample Buffer  
12.5 ml Solution C, 5 ml mercaptoethanol, 11.5 ml 87% glycerol, 2 g SDS and 5 mg bromphenol blue were filled up to a total volume of 50 ml with dH<sub>2</sub>O.
- 4x Running Buffer  
12 g Tris base, 57.6 g and 4 g SDS were solved in 1000 ml dH<sub>2</sub>O

- **Blotting Buffer**  
250 ml 4 x running buffer and 200 ml methanol were filled up to a total volume of 1000 ml with dH<sub>2</sub>O.
- **Stripping Buffer**  
12.5 ml Solution C, 350 µl β-mercaptoethanol and 1 g SDS were filled with dH<sub>2</sub>O up to 50 ml.

### **Antibodies**

- Phospho-Akt (Ser473) (D9E) XP™ Rabbit mAb (Cell Signaling Technology, Inc.)
- Phospho-GSK-3β (Ser9) (5B3) Rabbit mAb (Cell Signaling Technology, Inc.)
- Arginase I (C-2): sc-166920 (Santa Cruz Biotechnology, INC.)
- Anti-Actin antibody produced in rabbit (Sigma-Aldrich Handels GmbH, Vienna, Austria)

### **Procedure**

The performance of the sodium dodecyl sulfate polyacrylamide gel electrophoresis (SDS-PAGE) was started with the pouring of gels with 10% acrylamide content by the means of a gel pouring rack. Therefore for each gel 1.65 ml solution A, 0.8 ml dH<sub>2</sub>O and 2.5 ml solution B were mixed. For the induction of the polymerization 10 µl TEMED and 20 µl APS were added. After pouring the liquid gel between two glass plates 96% EtOH helped to remove air bubbles and to smooth the surface. The EtOH was eliminated after the polymerization. Then the stacking gel was used to fill up the remaining space between the glass plates and a comb was put into it. The stacking gel contained 0.35 ml solution A, 0.9 ml dH<sub>2</sub>O and 1.25 ml solution C. 7.5 µl TEMED and 12.5 µl APS induced the polymerization.

The samples were previously suspended in 2x sample buffer and before applying the samples on the gel, they were cooked at 99°C for 10 min at 650 rpm. The gel run at 30 mA until the marker started to separate and subsequently the run was continued with 60 mA. The run took place in a chamber filled with 1 x running buffer.

### 5.5.10. Western Blot

Following the protein separation via SDS-PAGE western blot was performed. In this context a sponge, 3 filter papers, the gel, a PVDF membrane, 3 filter papers and a sponge were placed above each other. Before the membrane was employed, it was equilibrated with methanol and then put into blotting buffer. The sandwich was assembled that the gel was close to the negative pole and the membrane near the positive pole to allow the proteins to move toward the membrane due to their negative charge. The blotting was executed in blotting buffer at 4°C and 150 mA for two hours. Afterwards the membrane was blocked in 5% skim milk powder dissolved in 0.5% PBS-T for one hour. Then the primary antibody was diluted with 5% milk solution and applied overnight at 4°C on the shaker.

On the following day the membrane was washed 5 times with 0.5% 1x PBS-T for 5 minutes each. Subsequently the secondary antibody, diluted in 5% milk solution, was put on the membrane and incubated shaking at room temperature for two hours. After washing the membrane 5 times with 0.5% 1x PBS-T for 5 minutes the blot was treated with SuperSignal<sup>®</sup> West Femto Maximum Sensitivity Substrate. The FluorChem<sup>®</sup> HD2 Chemiluminescence Imager (Alpha Innotech Corp., San Leandro, CA, USA) was used to develop the blot.

To analyze additional proteins the blot was stripped. Therefore the blot was incubated for 35 min at 55°C in stripping buffer. After washing the blot 5 times with 0.5% 1x PBS-T for 5 minutes it was blocked with 5% milk solution. The following steps of antibody incubation and development were performed similar as described before.

### 5.5.11. Enzyme Linked Immunosorbent Assay (ELISA)

#### Materials

- Mouse Interleukin-4 ELISA Ready-Set-Go!<sup>®</sup> Kit (eBioscience Inc., San Diego, USA)
- Mouse Interleukin-6 ELISA Ready-SET-Go!<sup>®</sup> Kit (eBioscience Inc., San Diego, USA)
- Mouse Interleukin-12 / Interleukin-23 ELISA Ready-SET-Go!<sup>®</sup> Kit (eBioscience Inc., San Diego, USA)
- Mouse Interleukin-17A (homodimer) ELISA Ready-Set-Go!<sup>®</sup> Kit (eBioscience Inc., San Diego, USA)
- Mouse Interleukin-33 (IL-33) Ready-Set-Go!<sup>®</sup> Kit (eBioscience Inc., San Diego, USA)

## Materials and Methods

- Mouse Interferon-gamma (INF- $\gamma$ ) Ready-SET-Go!<sup>®</sup> Kit (eBioscience Inc., San Diego USA)
- Mouse CXCL 1/KC Mab (Clone 48415), Rat IgG2A (R&D Systems, Minneapolis, USA)
- Mouse CXCL 1/KC Biotinylated Affinity Purified PAb, Goat IgG (R&D Systems, Minneapolis, USA)
- Recombinant Mouse CXCL 1/KC (R&D Systems, Minneapolis, USA)
- Anti-Mouse TNF alpha Biotin (eBioscience Inc., San Diego, USA)
- Anti-Mouse TNF alpha (eBioscience Inc., San Diego, USA)
- Mouse TNF alpha Recombinant Protein (eBioscience Inc., San Diego, USA)
- MIP-2 Douset ELISA (R&D, Systems, Minneapolis, USA)
- 0.05% PBS-T  
1 x PBS was mixed with PlusOne Tween-20 (GE Healthcare, Bio-Science AB, Uppsala, Sweden)
- Blocking solution  
BSA dissolved in 1 x PBS to reach an 1 % solution
- TMB 2-Component Microwell Peroxidase Substrate Kit (VWR International, Vienna, Austria)
- 2 N H<sub>2</sub>SO<sub>4</sub>
- Streptavidin-HRP (R&D Systems, Minneapolis, USA)
- F8 Maxisorb Loose Nunc-Immuno Module (Thermo Scientific-Nunc A/S, Roskilde, Denmark)

### Procedure

The enzyme linked immunosorbent assay was started with the coating with the coating antibody of the 96-well-plate. The antibody was applied in the concentration according to the manufacturer's manual. The immune globulin was diluted in PBS and incubated overnight at 4°C on a plate shaker.

On the next day the plate was washed with 0.05% PBS-T three times and then the unspecific binding sites of the antibodies were blocked with the blocking solution for one

hour at room temperature. In the meanwhile the standard curve and the samples were prepared. As highest point of the standard curve was 2 µg/ ml and a serial dilution was performed by diluting the highest point 1:2 with the blocking solution. The only exception was IL-33, which standard curve started with 8 µg/ ml. The samples were either applied undiluted or diluted with blocking solution. After three washing steps with 0.05% PBS-T the standards and the samples were put on the plate and incubated overnight at 4°C.

On the following day the ELISA plate was washed again three times and then the capture antibody was added, diluted with blocking solution as referred in the manufacturer's protocol. After two hours incubation at room temperature and four washing steps streptavidin labeled with horseradish peroxidase was diluted in the same concentration as the capture antibody in the blocking solution. The plate was incubated with streptavidin for 20 min at room temperature and washed for five times. Subsequently the TMB substrate was added for 10 min. Afterwards the enzymatic reaction was stopped by adding 2 N H<sub>2</sub>SO<sub>4</sub> and the intensity of the color was measured with the Bio-Tek EL808 Ultra Microplate Reader (Bio-Tek Instruments, Winooski, VT, USA) at 450 nm and 540 nm and a 4 Parameter log-log curve was created to calculate the concentrations of the samples.

#### **5.5.12. Cytospin**

First a bronchoalveolar lavage was performed and the obtained cells were counted with the Bürker-Türk counting chamber. The solution was diluted to achieve a suspension with  $6 \times 10^5$  cells per ml.

Primary the object slides were mounted with a paper pad and the cuvette in the methal holder and placed in the cytocentrifuge (Shandon cytopsin® 4, Thermo Fischer Scientific, Waltham, MA, USA). Then the paper pads were wet by pipetting 50 µl PBS into the cuvette and the first run with 550 rpm for 1 min was started. Afterwards 50 µl of the cells suspension were filled into the cuvette and were centrifuged at 550 rpm for 2 min. Therefore 30 000 cells were applied on the slide. After the spin the slide, the paper and the cuvette were detached and the cytopsin was dried at room temperature overnight. The prepared cytopsin were stained with hematoxylin and eosin.

### 5.5.13. Antibody Staining for Flow Cytometry

#### Materials

- FACS Buffer  
1 x PBS was mixed with FCS to achieve a solution of 2%.
- Viability dye eFluor 780 (eBioscience, Inc. San Diego, CA USA)
- Permeabilizing agent: FIX&PERM® Solution A (ADG. Vienna, Austria)

**Table 6: List of antibodies used for flow cytometry.**

Antibody	Conjugate	Isotype	Clone	Company
CD3e	V500	hamster IgG2 K	500A2	BD Biosciences, Franklin Lakes, NJ USA
CD45	V500	rat IgG2b K	30-F11	BD Biosciences, Franklin Lakes, NJ USA
CD8	FITC	rat IgG2a K	53-6.7	eBioscience Inc. San Diego, CA USA
CD11c	FITC	IgG1, lambda2	HL3	BD Biosciences, Franklin Lakes, NJ USA
MRC1	FITC	rat IgG2a K	MR5D3	Biologend, London, UK, London, UK
MHCII	FITC	rat IgG2a,k	2G9	BD Biosciences, Franklin Lakes, NJ USA
F4/80	FITC	Rat IgG2a,k	BM8	eBioscience Inc. San Diego, CA USA
CD11c	AF647	IgG	N418	Biologend, London, UK
MGL2	AF647	rat IgG2a	ERMP23	BD Biosciences, Franklin Lakes, NJ USA
CD19	PE	rat IgG2a	PeCa1	
Ly6G	PE	rat IgG2a K	1A8	Biologend, London, UK
CD80	PerCP Cy5.5	Arm ham IgG	16-10A1	Biologend
B220	PerCP Cy5.5	rat IgG2a K	RA3-6B2	eBioscience Inc. San Diego, CA USA
F4/80	PerCP Cy5.5	rat IgG2a K	BM8	Biologend, London, UK
CD11b	AF700	rat IgG2b K	M1/70	eBioscience Inc. San Diego, CA USA
CD4	AF700	rat IgG2a K	RM4-5	eBioscience Inc. San Diego, CA USA
NK1.1	eFluor 450	mouse IgG2a K	PK136	eBioscience Inc. San Diego, CA USA
CD90.2	eFluor 450	rat IgG2a K	53-2.1	eBioscience Inc. San Diego, CA USA
Ly6C	BV 570	IgG2c,k	HK1.4	Biologend, London, UK

## **Method**

Dilution of antibodies and the washing of cells during this procedure were performed with FACS buffer.

A single lung cells suspension was prepared as described above and  $10^6$  cells were taken out per staining. The cells were centrifuged at 1250 rpm, 4°C, for 5 min (these conditions was applied to all subsequent centrifugation steps) and the supernatant was discarded. To block unspecific binding sites cells were incubated 15 min with 6 µg normal mouse IgG in 30 µl FACS buffer at room temperature. The 50 µl antibody solution per staining was added and the cells were incubated for 30 min at 4°C (surface staining). Cells were washed three times (two last with PBS only) followed by viability staining using fixable viability dye eFlour 780 for 30 min at 4°C. After the final washing step cells were resuspended in 300 µl FACS buffer and analyzed using the flow cytometer LSR Fortessa (BD Biosciences, Franklin Lakes, NJ USA).

### **5.6. Statistical Analysis**

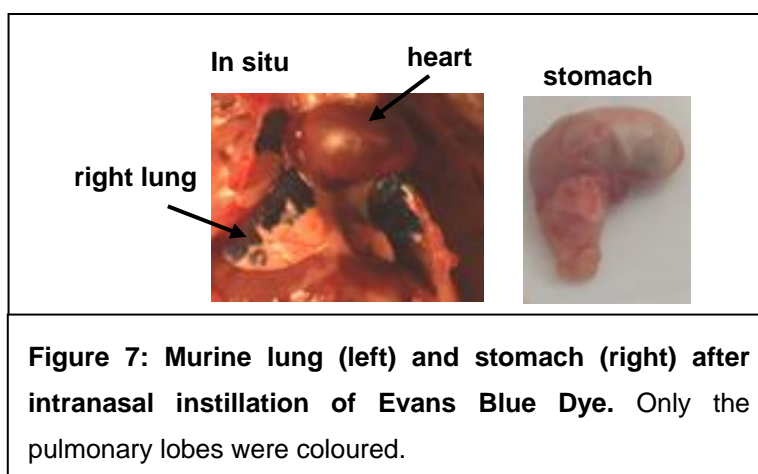
The gained values were evaluated with GraphPad Prism 4 software (GraphPad, San Diego, CA, USA) by the means of unpaired Student t test. Critical for significant differences was a p-value smaller than 0.05 for all experiments.



## 6. Results

### **6.1. Establishment and Validation of the Bleomycin Induced Pulmonary Fibrosis Model**

In the literature the bleomycin induced pulmonary fibrosis model (BIPF) is one of the most well characterized fibrosis models. The drug can be administered i.v., i.p., i.t. and i.n. Systemic (i.v. or i.p.) application leads to subpleural scarring, while local application (i.t.) results in bronchiolocentric changes, which more resembles pulmonary fibrosis in humans. We therefore decided to apply bleomycin locally. Using single application is sufficient. Since intranasal application route is less invasive than intratracheal, it was the preferred route of application. To test if intranasal administration is equivalent to intratracheal we first tested the distribution of intranasally instilled fluids. To address this we treated the mice with Evans Blue Dye and monitored the localization of the dye. We could detect the dye in the left and right lungs, but the stomach was unstained (Figure 7).



After showing that the intranasal treatment localizes only to the lung we compared the outcome of intranasally and intratracheally induced pulmonary fibrosis. C57Bl/6J wild-type mice were treated with BLM and the left lung was harvested after 21 days. To assess the collagen content 2  $\mu\text{m}$  lung sections were stained with Sirius Red. While the untreated lung exhibited collagen deposition only around blood vessels, the BLM treated lungs were streaked with collagen instead of alveoli. Comparing both routes of BLM application no differences were observed (Figure 8). In addition two different concentrations 0.05 iu and 0.15 iu BLM were examined and a dose dependent collagen deposition was monitored

Results

(Figure 9). The collagen content was quantified by ImageJ and demonstrated that both application routes lead to a comparable outcome.

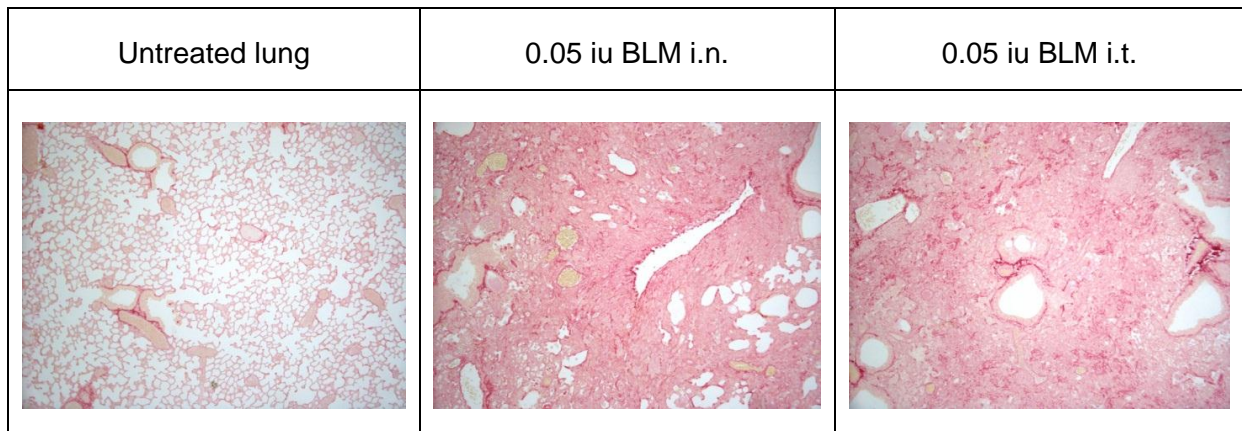


**Figure 8: Sirius red stained lung sections 21 d post bleomycin instillation.** The left lung represents a healthy mouse, while in the middle and the right the lung originate from mice treated with bleomycin intranasally (i.n.) and intratracheally (i.t.), respectively.

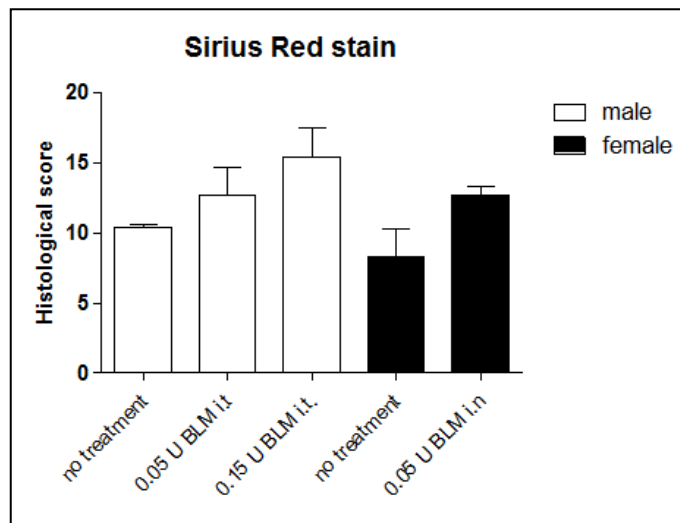


**Figure 9: Quantification of the area of collagen deposition.** Different routes (intratracheally (i.t.) and intranasally (i.n.)) and different concentrations (0.05 iu and 0.15 iu) were tested.

Due to our interest in the involvement of immune cells and their effector mechanisms in the development of pulmonary fibrosis, we measured different cytokines in lung tissue. To examine this we treated wild-type mice with 0.5 iu BLM intranasally and a bronchoalveolar lavage was performed after 7 days to measure the cytokines of the bronchoalveolar space. Secondly the lungs were removed and homogenized for the cytokine measure of the whole lung tissue. In the lung homogenate we found increased levels of IL-17, IL-6, MIP-2 and KC, while there were no significant changes in the

expression of INF- $\gamma$ , IL-4, IL-12 and TNF $\alpha$  (Figure 10). Augmented levels of IL-17, KC and IL-6 were found in the bronchoalveolar lavage fluid (Figure 11). The increase of IL-17 is confirmed in the literature, where it is described that IL-17 may induce neutrophilia and the expression of MMP-1 (Wynn and Ramalingam 2012). In addition neutrophil attracting chemokines KC and MIP-2 are elevated (Wynn 2011). IL-6 can support fibroblasts and together with TGF- $\beta$  promote differentiation of T helper cells toward TH17 cells (Wynn and Ramalingam 2012).

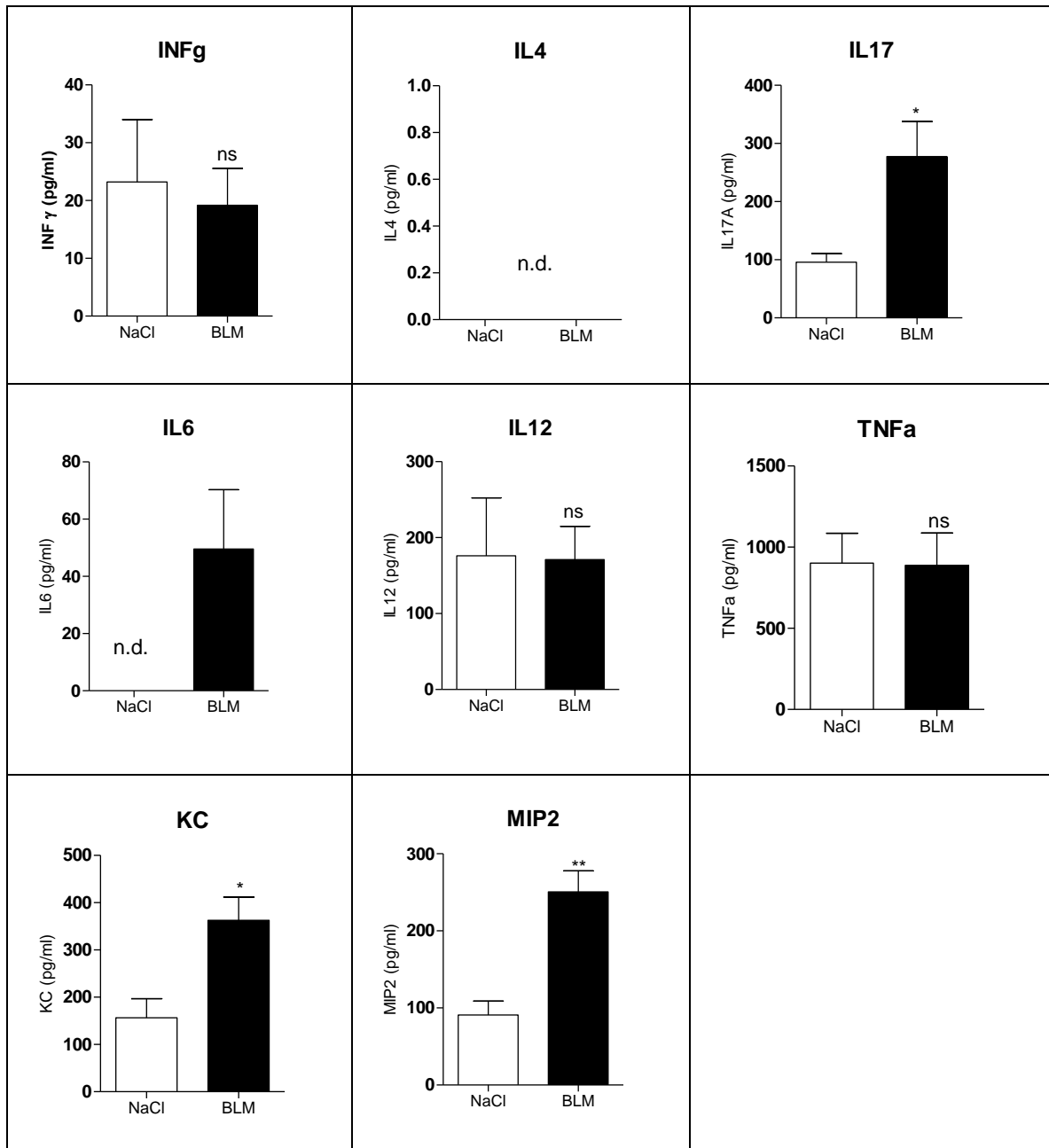


**Figure 10: Comparison of the cytokine levels between healthy mice and bleomycin treated mice.** Whole lung tissue was homogenized and cytokines were measured by ELISA. Error bars show the standard deviations of the mean. (n.d...not determined)

Results

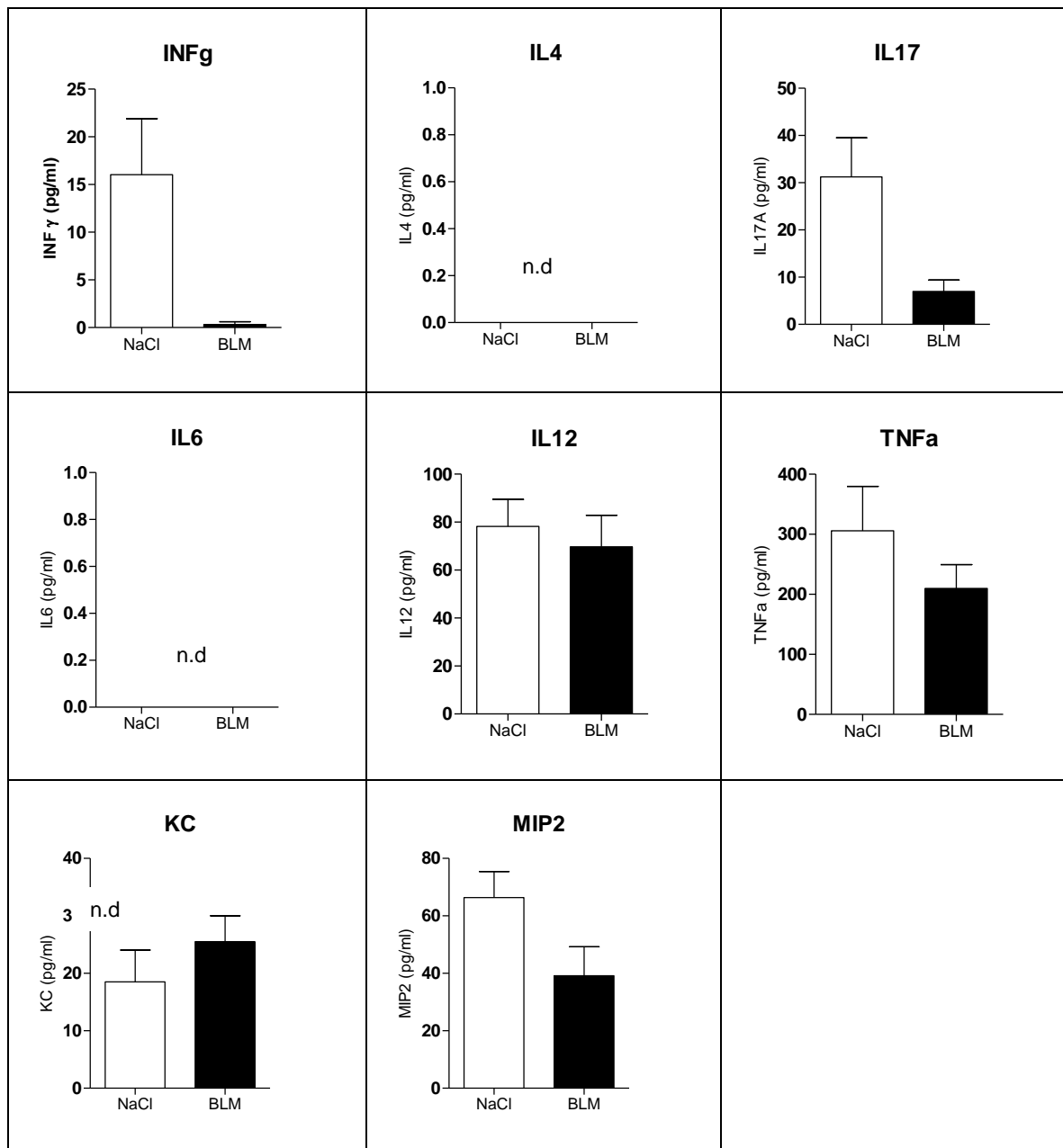


**Figure 11: Comparison of the cytokine levels between healthy mice and bleomycin treated mice.** The cytokines of the bronchoalveolar lavage fluid were measured by ELISA. Error bars show the standard deviations of the mean.

## **6.2. PTEN Deficient Alveolar Macrophages Display a Decreased Inflammatory Response**

The main aim of this study was to figure out if myeloid cell PTEN has a role in pulmonary fibrosis. To address this issue we used mice with homozygote floxed PTEN alleles and the Cre recombinase under the promoter of lysozyme M leading to a conditional *pten* knockout. LysM expression is specific for myeloid cells, such as macrophages or dendritic cells. In figures myeloid PTEN deficient mice are referred as MyPTEN<sup>-/-</sup> or MyPTEN KO and their wild-type littermates as WT.

To elucidate the influence of the lack of myeloid cell derived PTEN on immune responses, alveolar macrophages were isolated via a bronchoalveolar lavage and stimulated with LPS for 10, 30 and 60 minutes *in vitro*. Actually the deletion of PTEN caused an increase in the baseline activity of the PI3K. This result was indicated by the detection of phosphorylated Akt and phosphorylated GSK-3 $\beta$ , two downstream kinases of the PI3K (Figure 12). The time course analysis demonstrated that PI3K activity was enhanced in PTEN deficient alveolar macrophages and that the maximum was reached after ten minutes stimulation, while WT macrophages achieved a PI3K activity maximum after 60 minutes. Despite the unequal loading the western blot clearly indicates hyperactive PI3K signaling.

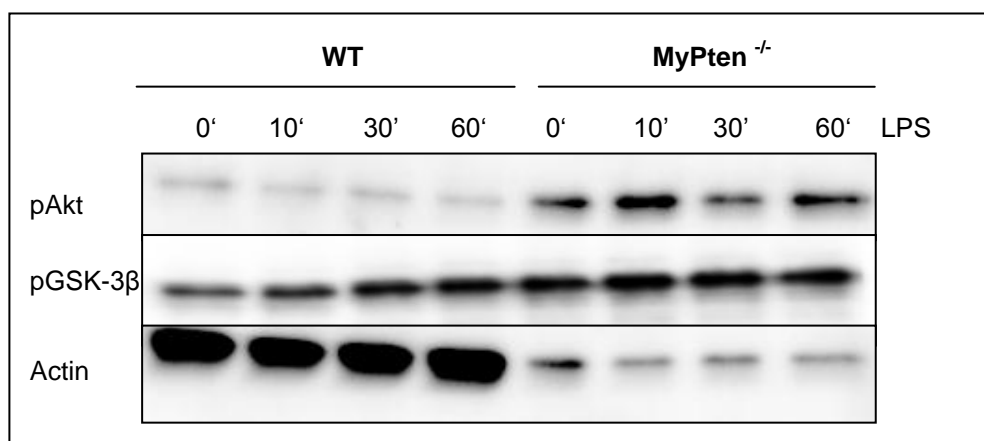


**Figure 12: Wild-type and PTEN deficient alveolar macrophages were stimulated with LPS.** The PI3K activity was examined by the phosphorylation of the two downstream kinases Akt and GSK-3 $\beta$ . Determination of actin was used as loading control.

PTEN activity is associated with the expression of pro-inflammatory cytokines, shown by previously published data by our group 2010 in the Journal of Immunology (Schabbauer, Matt et al. 2010). To rule out if PTEN deletion leads to a down regulation of inflammatory genes PTEN deficient alveolar macrophages were stimulated with LPS or heat killed *Streptococcus pneumoniae* for 16 hour *in vitro*. The conditional knock out led to a reduced release of TNF $\alpha$  (Figure 13). In addition the amount of nitric oxide declined, indicating a diminished activity of iNOS (Figure 13). This analysis of the data led to the question how myeloid cell specific PTEN influences chronic diseases.

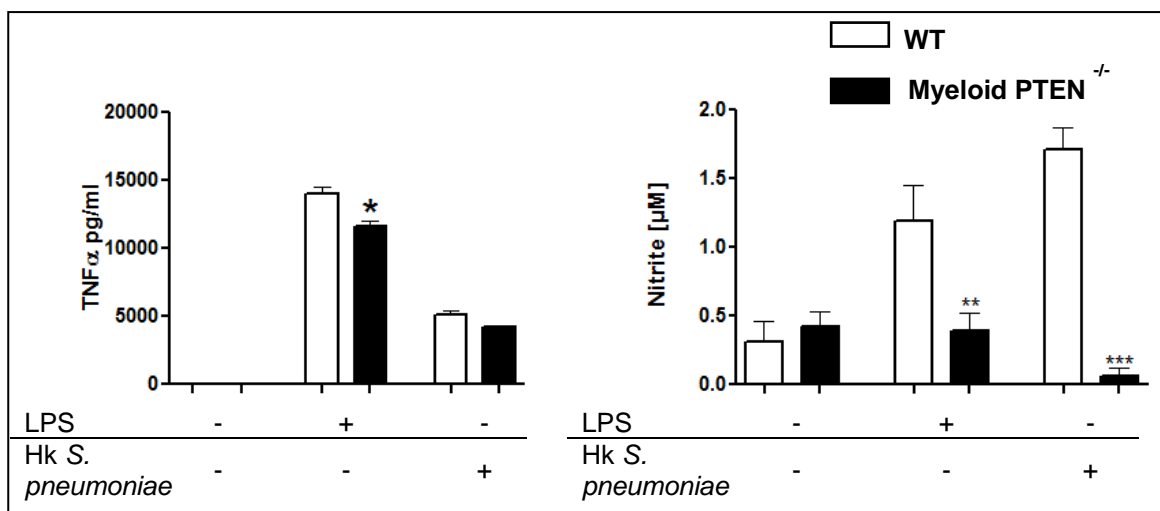


**Figure 13: Stimulation of wild-type and PTEN deficient alveolar macrophages with LPS or heat killed (hk) *S. pneumoniae*.** TNF- $\alpha$  was determined by ELISA and nitrite via the NO generation assay. Error bars show the standard deviations of the mean. (Schabbauer, Matt et al. 2010)

### **6.3. Myeloid PTEN Deficiency Promotes Fibrotic Response in Bleomycin Induced Lung Injury**

To investigate whether myeloid PTEN deficiency influence chronic diseases we chose bleomycin (BLM) induced pulmonary fibrosis as chronic disease model. Wild-type and myeloid PTEN deficient mice were treated with BLM as described in materials and methods. The body weight of the treated mice was determined every day for 21 days and expressed as percentage of the weight of day zero. The saline treated groups gained weight, while the two other groups, suffering from BLM, lost weight (see Figure 14A). The strongest decrease in weight was eight days post BLM application. The myeloid PTEN deficient mice had a greater response than their wild-type littermates. According to the literature the greatest collagen deposition is noticed 21 days post BLM treatment and that

the mice can reach their original weight again during this period. During the three weeks both genotypes failed to recover their initial weight, they had on the day of the treatment.

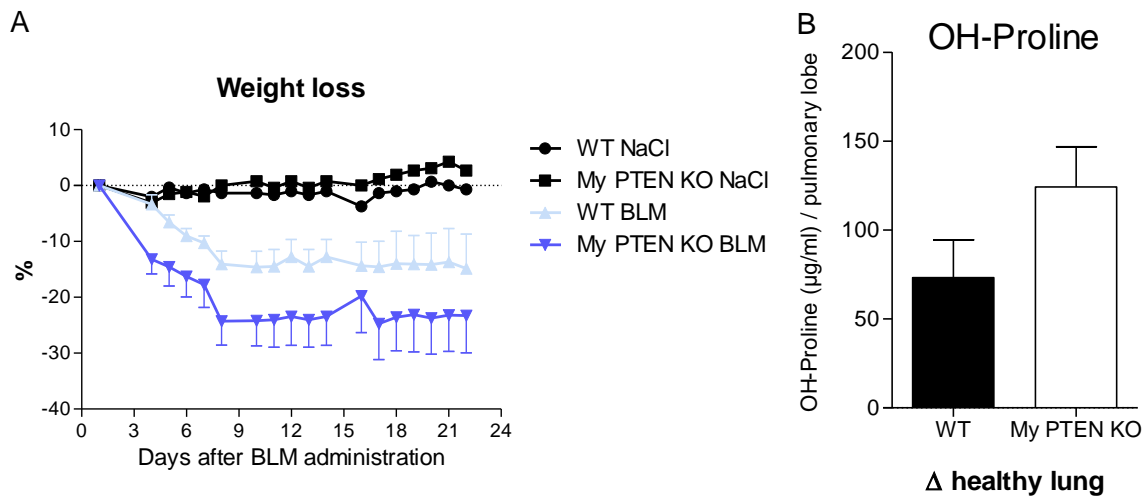


**Figure 14: Comparison of fibrotic markers between WT and myeloid PTEN KO mice.** A) Body weight loss of mice after bleomycin administration. B) Hydroxyproline (OH-Proline) content in murine lungs 21 day post bleomycin treatment. Error bars show the standard deviations of the mean.

21 days after the BLM treatment the left lung was removed and prepared for histological analysis. The pathological changes were examined via hematoxylin and eosin (H&E) staining to differentiate immune cells (see Figure 15). In addition Sirius Red staining was applied to visualize collagen deposition. The H&E staining displayed an enormous infiltration of immune cells, such as macrophages and neutrophils. Collagen deposition was induced by bleomycin and was increased in the group of myeloid PTEN KO mice (see Figure 15). In addition the right lung was used for measuring the hydroxyproline levels. Hydroxyproline is the main component of collagen and in mammals it is only found in collagen and elastin. In this context the content of hydroxyproline indicates the collagen content. Hydroxyproline was elevated in the lungs of myeloid PTEN deficient mice after pulmonary fibrosis induction (see Figure 14B).

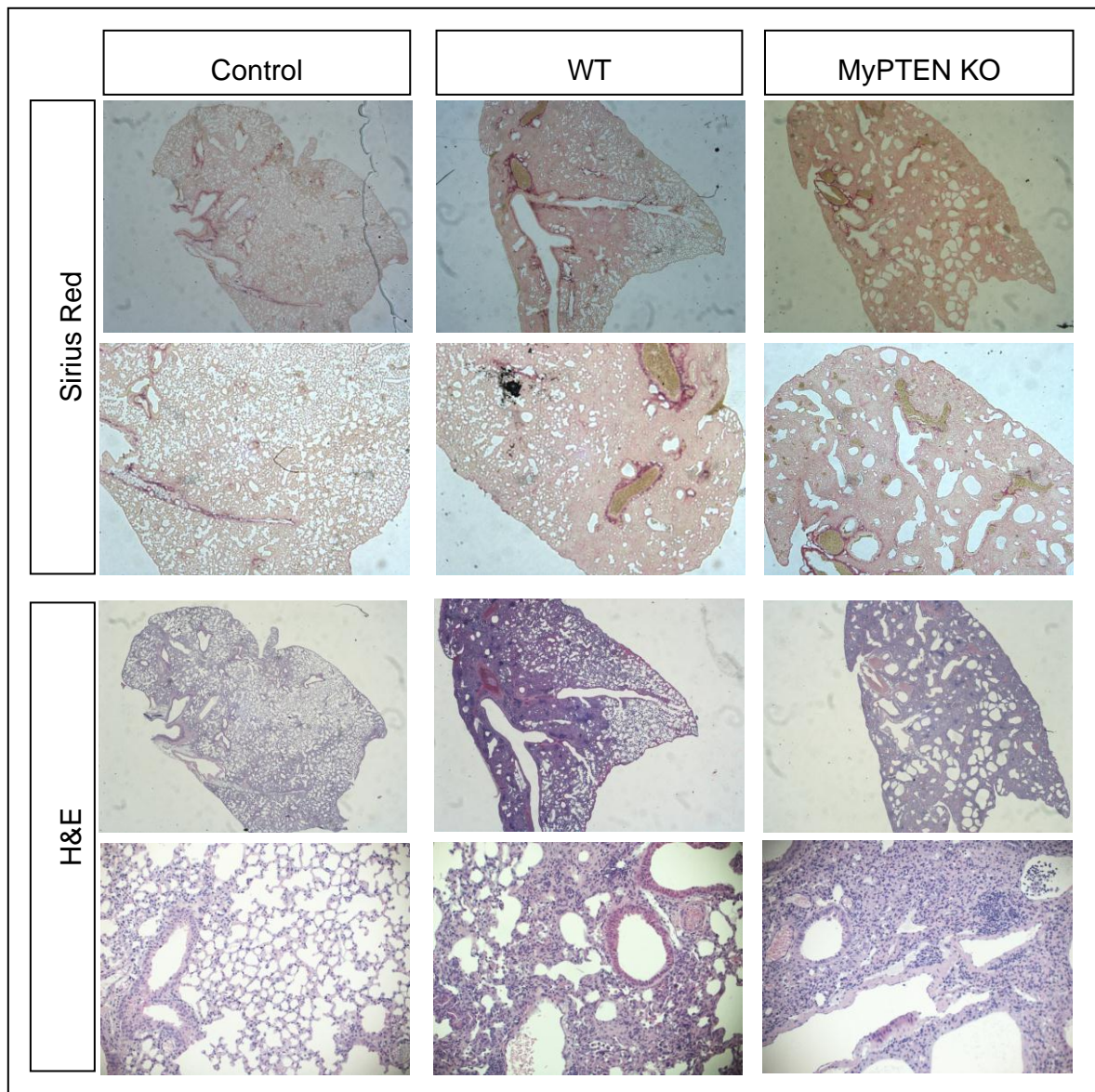
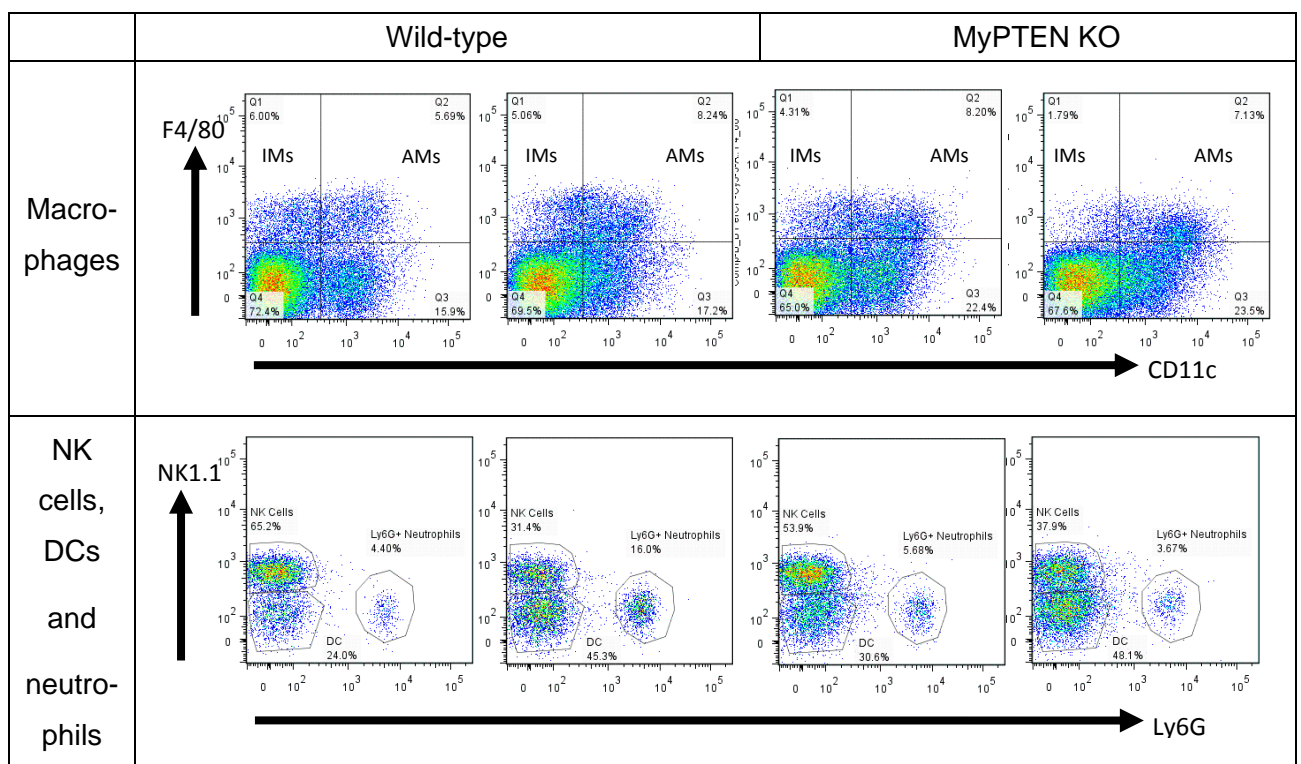


**Figure 15: Histological specimen of murine lung tissue.** The left column present the control lung treated with saline, the middle column demonstrates the lung of a wild-type mouse 21 day post bleomycin treatment and the right one covers the bleomycin treated lung of a myeloid PTEN knockout mouse. The two upper rows display the collagen deposition via Sirius Red staining. The third and fourth rows demonstrate the hematoxylin and eosin staining. Images of each row top-down are shown at 12.5, 40, 12.5 and 200 x magnification. Tissue was embedded in paraffin and 2  $\mu$ m sections were prepared.

We were further interested if this pathological outcome is may linked to differences in the amount of immune cell populations. In this context we took mice seven days after BLM application and prepared a single cell suspension of the lungs for flow cytometry analysis. Therefore the lungs were flushed through the heart, cut in small pieces and digested by collagenase 1 and DNase 1. The cell suspension was harvested by filtering

the homogenate through a cell strainer. Afterwards the cells were stained with antibodies for flow cytometry analysis. The results were evaluated by the following gating strategy: first the viable cells were selected according to the viability dye; secondly single cells were picked in accordance with the forward and side scatter (Figure 16). This population was used for further analysis. To identify B-cells a CD45 positive population was separated according to their expression of B220 and CD19. Double positive cells were recognized as B-cells and between wild-type and myeloid PTEN deficient mice no differences were noticed. CD45 positive, CD90.1 positive and CD3 positive cells were referred as T-cells. In myeloid PTEN deficient mice this population was decreased compared to wild-type mice seven days after BLM treatment. In contrast, we made the observation that the ratio of CD4+ T helper cells and CD8+ cytotoxic T cells was similar. Moreover CD45 positive, F4/80 positive and CD11c negative cells, probably interstitial macrophages, and F4/80 positive and CD11c positive cells, most likely alveolar macrophages, were found to be present at similar extent. NK cells were tried to be identified via the expression of CD45, CD11c and NK1.1 and exhibited no significant differences. In addition we failed to identify any variation between the wild-type and myeloid PTEN deficient mice in the infiltration of neutrophils, which were characterized by the expression of CD45, CD11c, and Ly6G. Similar amounts of CD45 positive and CD11c positive DCs lacking the expression of NK1.1 or Ly6G were noticed. Further no differences were detected in the population expressing the T<sub>REG</sub>-cell marker CD25.



Results

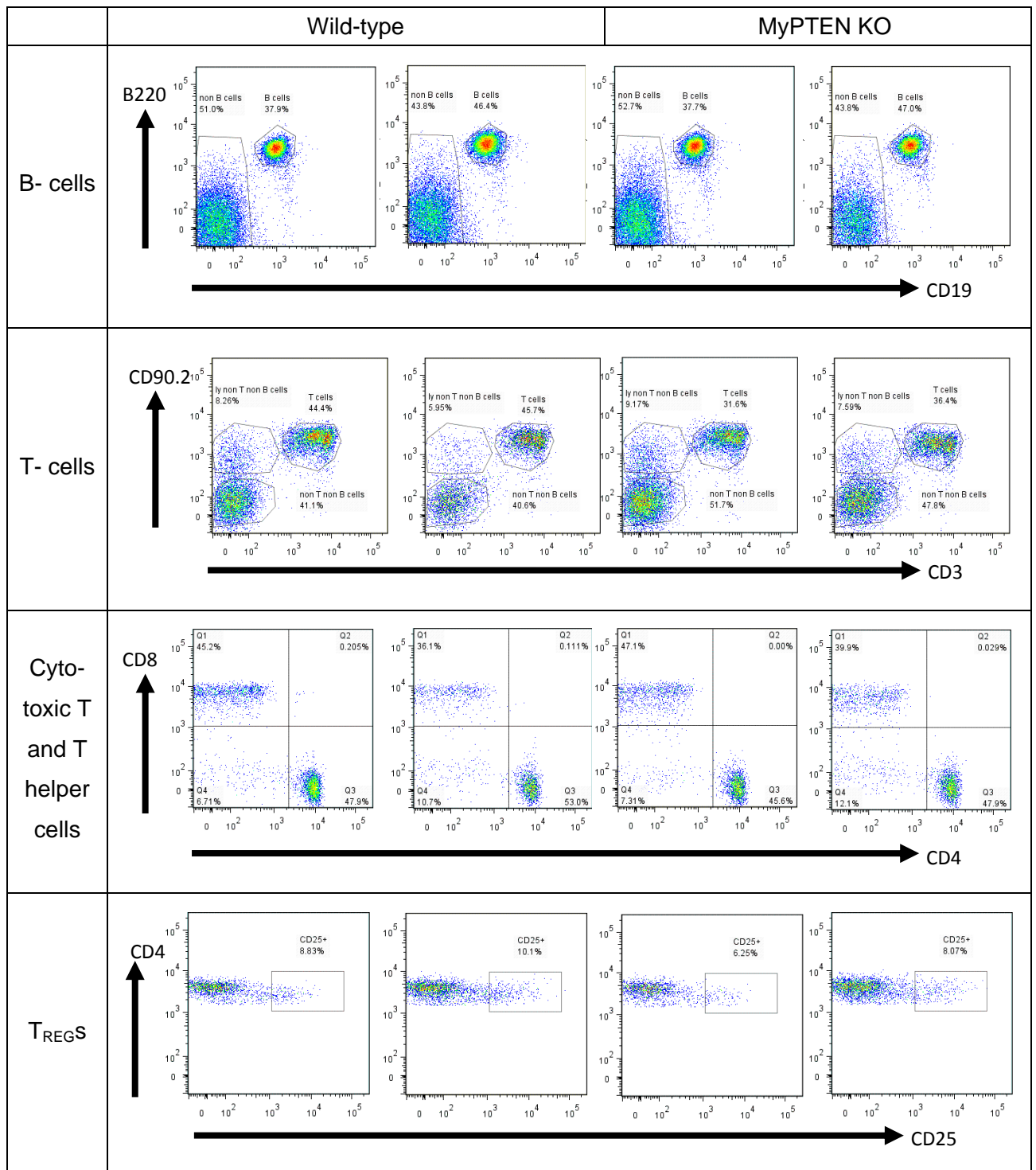


**Figure 16: Flow cytometric analysis of murine lung cell suspension 7 days post bleomycin treatment.** Wild-type mice were compared with myeloid PTEN deficient mice. Each genotype is represented by two mice. Different markers were applied to identify macrophages, DCs, NK-cells, B-cells, T-cells, Th cells, cytotoxic T-cells and T<sub>REG</sub>-cells.

#### **6.4. Cytokines Linked to Inflammation and Fibrosis are Partly Elevated in Myeloid PTEN Deficient Mice**

Next we measured cytokines associated with inflammation and fibrosis on protein level with ELISA and on mRNA level with Real Time PCR. BALF and lung homogenates were used for ELISA, and RNA was isolated from the lung homogenate. The real time PCR demonstrated that IL-6 and the chemokine KC were stronger induced in the conditional PTEN knockout mice 7 days post BLM treatment (Figure 17). As reference gene HPRT was measured. Further we could show that the cytokines INF- $\gamma$ , IL-4 and IL-17, IL-12, IL-6, TNF- $\alpha$ , IL-33 were elevated in myeloid deficient mice in the lung tissue (Figure 18). In addition the cytokines of the bronchoalveolar lavage fluid were examined (Figure 19). The outcome showed that INF- $\gamma$ , IL-4, IL-17, IL-6 and TNF- $\alpha$  were increased similar to the result of the analysis of the whole lung tissue. In contrast decreased levels of IL-12 and KC were observed.

IL-33 is released by damaged epithelial cells and promotes the differentiation of T helper cells toward TH2 cells (Wynn and Ramalingam 2012). INF- $\gamma$  and IL-12 are the main cytokines of the TH1 response and are believed to diminish fibrotic progression (Thannickal, Toews et al. 2004), in contrast IL-12 stimulates, in addition to the TH1 response, TH17 cells with profibrotic characteristics (Wilson, Madala et al. 2010). Further an over-expression of TNF- $\alpha$  is associated with a severer fibrotic disease (Wynn 2011). Nevertheless the inflammatory chemokine KC was not differentially expressed on protein level. All together the variations in the cytokine profiles of the two different genotypes might indicate that the myeloid PTEN deficient mice developed a more serious inflammatory response promoting fibrosis.

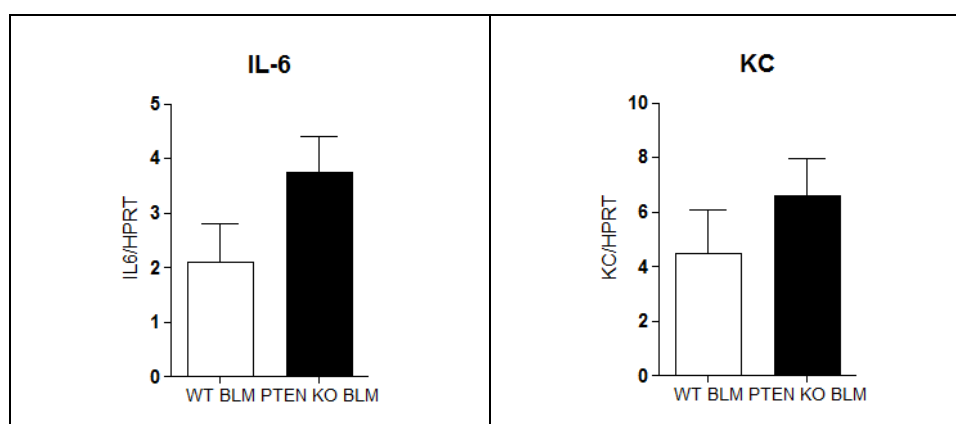


**Figure 17: IL-6 and KC expression 7 days post bleomycin treatment.** RNA was isolated from lungs of myeloid PTEN knockout mice and wild-type littermates. Error bars show the standard deviations of the mean.

## Results

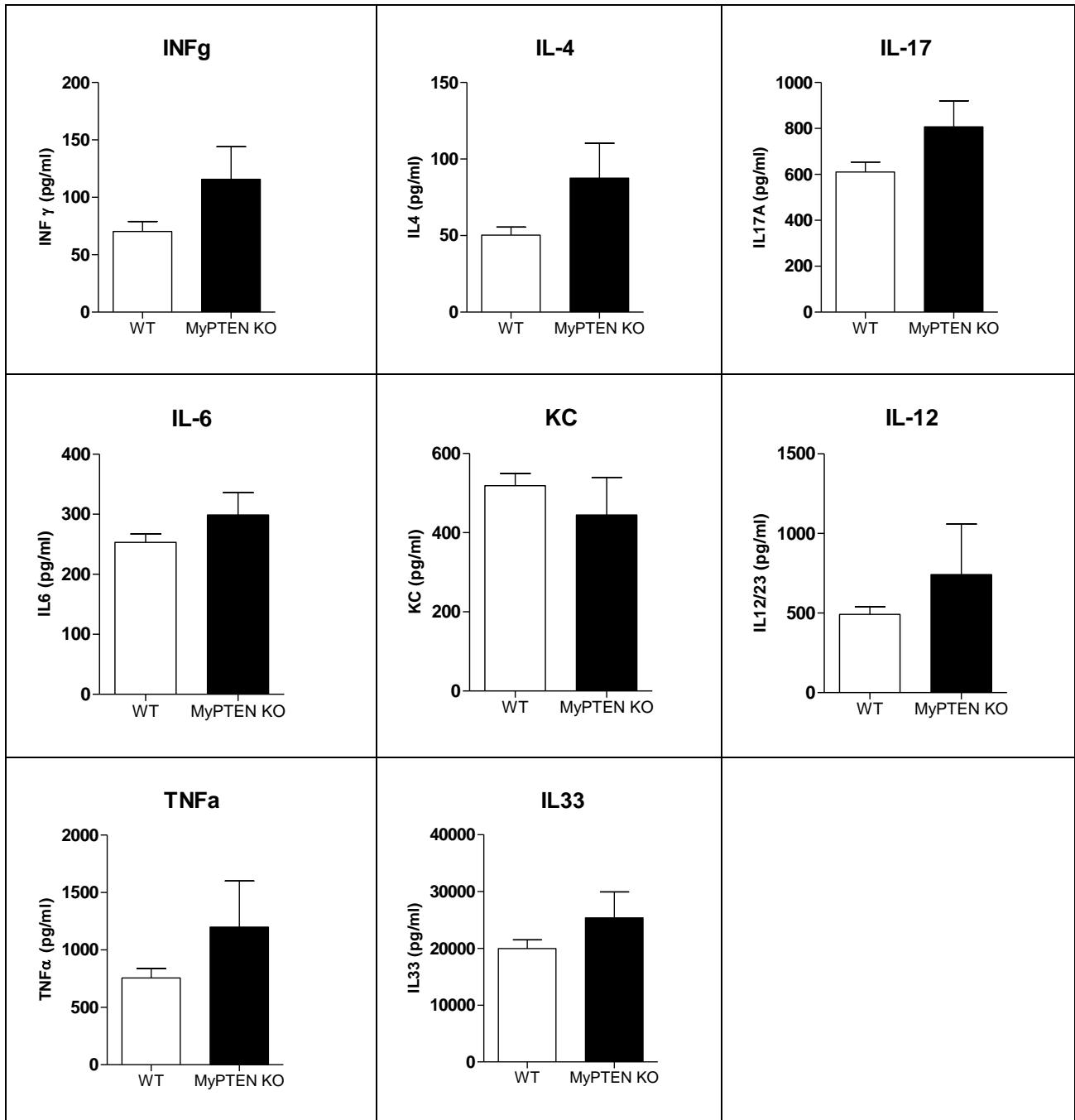


**Figure 18: Wild-type and myeloid PTEN deficient mice were treated with bleomycin for 7 days and subsequently their lungs were homogenized and analyzed by ELISA. Error bars show the standard deviations of the mean.**

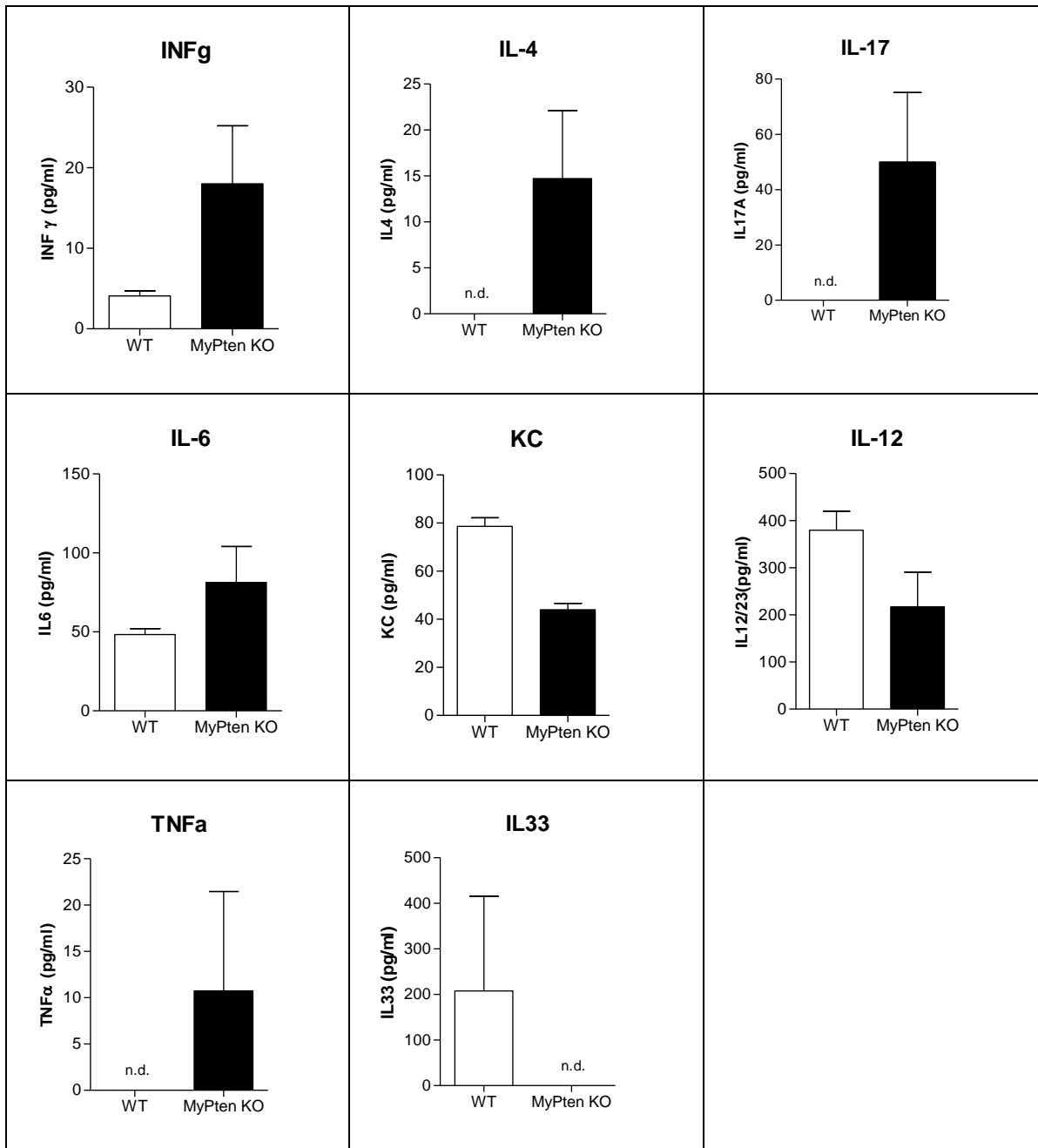


**Figure 19: Wild-type and myeloid PTEN deficient mice were treated with bleomycin, at day 7 the bronchoalveolar lavage fluid was collected and analyzed by ELISA. Error bars show the standard deviations of the mean. (n.d...not determined)**

### **6.5. IL-4/ IL-13 Stimulation Leads to Enhanced PI3K Activity in PTEN Deficient Alveolar Macrophages**

Due to the importance of IL-4 and IL-13 in the pathogenesis of lung fibrosis, we elucidated whether these type 2 cytokines are potent to activate PI3K signaling. In this context we isolated alveolar macrophages and stimulated them with IL-4 and IL-13 *in vitro*. The time course analysis with the time points: 10, 30 and 60 minutes, showed that the two cytokines stimulated the activity of the PI3K albeit at a lower level as compared to other activators of the PI3K pathway. This effect was demonstrated by western blotting, at which we made the observation that the downstream kinases Akt and GSK-3 $\beta$  of the PI3K were phosphorylated in response to the stimulation (Figure 20). Phosphorylation of Akt and GSK-3 $\beta$  denotes PI3K signaling.

Wild-type macrophages exhibited the greatest PI3K activity after 60 minutes. In comparison PTEN deficient macrophages displayed activity, that was even higher after ten minutes than in wild-types after 60 minutes. The activity seemed to be constantly high for the 60 minutes. This result indicated that IL-4 and IL-13 were able to trigger PI3K action, but to a lower extent as compared to LPS (Figure 12).

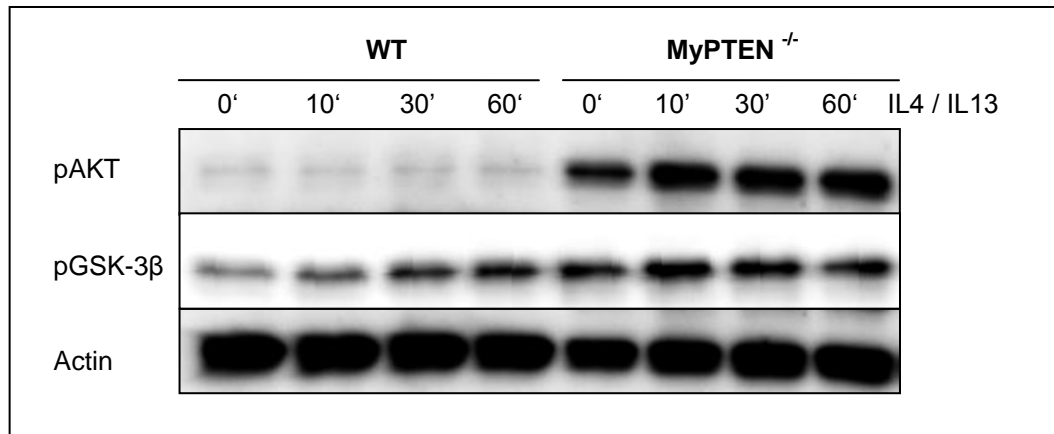


**Figure 20: Western Blot analysis of wild-type and myeloid deficient alveolar macrophages after 10, 30 or 60 minutes stimulation with IL-4 and IL-13.** As target the phosphorylation state of the PI3K downstream kinases Akt and GSK-3 $\beta$  were investigated. Actin was used as loading control.

### **6.6. The Phenotypic Analysis of Naïve Lung Macrophages Deficient for PTEN**

Since IL-4 and IL-13 are known to induce a M2 activation state in macrophages and the observation that these type 2 cytokines are potent inducers of the PI3K, we were

interested if there are baseline differences in the M2 phenotype between wild-type and conditional PTEN knockout mice. For that purpose lung cell suspensions of naïve mice were generated. After flushing the lung via the heart to remove erythrocytes, the lungs were sliced, digested with collagenase 1 and DNase 1 and homogenized with cell strainers. The cells were stained with fluorescently labeled antibodies specific for M1 and M2 markers. On the one hand we investigated MHCII, the costimulatory molecule CD80 and Ly6C as surface molecules specific for a M1 phenotype and on the other hand the mannose receptor MRC1 and the macrophage galactose N-acetyl-galactosamine specific lectin 2 (MGL2) were used to characterize a M2 phenotype. Additionally the cells were labeled for viability to be able to exclude dead cells, which would maybe triggered false positive signals. For the evaluation of the results following gating strategy was used: first the dead cells were excluded via the viability dye and secondly doublets were eliminated according to the forward and side scatters. In order to display a macrophage population, the next gating step was to take the CD45 positive cells and to separate this population according to their expression of CD11b and CD11c. These two markers enabled the differentiation between alveolar macrophages, interstitial macrophages and dendritic cells. Autofluorescent cells, which were double positive for CD11c and CD11b, were further gated for F4/80 and considered as alveolar macrophages. Cells, which expressed CD11c but did not express CD11b, were further selected for the presence of Ly6G and assumed to be dendritic cells. Non-autofluorescent cells only positive for CD11b were thought to be interstitial macrophages. These three populations were examined for their expression of the above named M1 and M2 markers. The analysis showed no differences in the relative numbers of interstitial macrophages, alveolar macrophages and dendritic cells.

In addition the comparison of the above mentioned surface markers between the wild-type and PTEN deficient alveolar macrophages showed no alterations (Figure 21). However the dendritic cells seemed to have also similar expression patterns. In contrast the interstitial macrophages differed slightly in their expression of MGL2 and Ly6C. Both markers were reduced in mice with a deletion of PTEN in myeloid cells, indicating a change in the phenotype of the macrophages, but not a shift toward M1 or M2, because markers for both phenotypes were diminished. Since these data are based on a single experiment observation, the results need to be further analyzed.

Moreover we compared the cell composition of wild-type and myeloid PTEN deficient mice. The amount of B-cells, characterized by the expression of CD45, B220 and CD19, and T-cells, typified by the expression of CD3 out of the B220 and CD19 negative population, were comparable. Furthermore the ratio between CD4 T helper cells and CD8 cytotoxic T cells was similar (data not shown).

Results

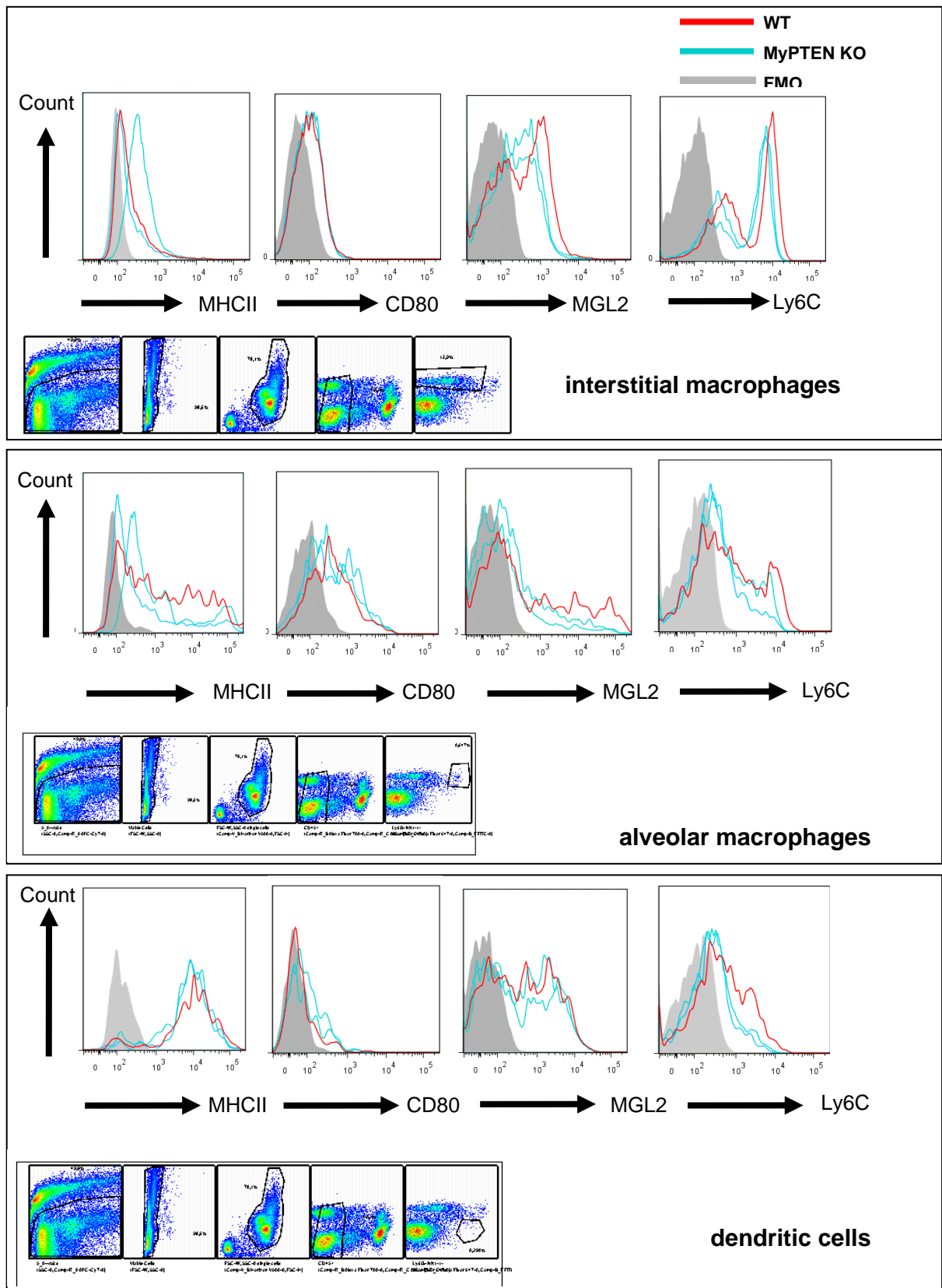


**Figure 21: Flow cytometry analysis of murine lungs for M1 and M2 markers.** Interstitial, alveolar macrophages and dendritic cells were examined. Gating strategy: excluding of the dead cells via the viability dye, elimination of the doublets according to the forward and side scatters, taking of the CD45<sup>+</sup> cells and separating them according to CD11b and CD11c expression

### **6.7. IL-4 or IL-13 Stimulated PTEN Deficient Macrophages Display a M2 like Phenotype**

To further clarify differences in the phenotype of wild-type and PTEN deficient macrophages, we analyzed the effects of typical M2 inducing cytokines and *S. pneumoniae*. Alveolar macrophages were isolated and *in vitro* stimulated with IL-4, IL-13 or heat-killed bacteria. After 16 hours stimulation the cells were harvested and RNA was isolated for Real Time PCR analysis. mRNAs of representative alternative activation markers were investigated to identify the functional activation state of these macrophages. As reference gene HPRT was used.

The first gene we examined was Arginase 1. Unchallenged macrophages, independent of PTEN expression or deletion, did not express Arginase 1. In contrast the stimulation with IL-4 led to its expression and the results showed a tendency of Arginase 1 to be higher expressed in PTEN deficient macrophages. A significant increased expression of Arginase 1 in phagocytes with conditional PTEN knockout was induced by IL-13. This was shown by a fold change of 1.056 in contrast to a fold exchange of 0.739 in wild-types, compared with unstimulated macrophages. The treatment with heat killed *S. pneumoniae* did not affect the expression profile of this gene.

As second step we analyzed the expression of FIZZ also referred as Relm- $\alpha$ . PTEN deficient macrophages challenged with IL-4 exhibited significantly increased levels of FIZZ mRNA (Figure 22). A similar ratio was seen by the stimulation with IL-13, but the induction was reduced compared to the IL-4 treatment. Stimulation of alveolar macrophages with *S. pneumoniae* failed to stimulate the expression of FIZZ.

Furthermore differences of the mRNA levels of YM1 also known as Chi3l3 were examined. Investigation of baseline levels of YM1 mRNA indicated that absence of PTEN lead to a down regulation of the protein (Figure 22). Although the stimulation with IL-4 and with IL-13 initiated the transcription of the *ym1* gene, the levels were reduced compared to wild-type cells. The bacterial challenge failed to induce YM1 expression and similar to the naïve macrophages, PTEN deficient cells had diminished transcription.

Additionally the expression of the mannose receptor 1 (MRC-1) was studied. Unchallenged alveolar macrophages displayed an expression of MRC-1 with a similar extent between wild-type and PTEN deficient macrophages (Figure 22). In both genotypes the stimulation with IL-4 or with IL-13 lead to the induction of the receptor, but no significant differences in the expression were noticed. Similar to the other M2 markers *S. pneumoniae* was unsuccessful in inducing MRC-1 expression.

## Results

Additionally we analyzed the levels of the two chemokines CCL17 and CCL22 (macrophage derived chemokine), which participate in the M2 immune response. Naive macrophages lacked the expression of CCL17 and only had small levels of CCL22 (Figure 22). Confronting these immune cells with IL-4 or IL-13 induced the expression of both chemokines. The PTEN knockout caused a significantly reduced amount of CCL17 and CCL22 after IL-4 treatment, similar to the challenge with IL-13. *S. pneumoniae* promoted only a slightly increase of CCL17 with a tendency that PTEN deficiency diminished CCL17 expression. CCL22 was additionally stimulated by *S. pneumoniae*, but no differences could be seen between the two genotypes.

In addition to the M2 markers we also analyzed the expression of iNOS, the counteracting enzyme of Arginase 1 and a marker for classically activated macrophages (M1). Stimulation of alveolar macrophages with LPS or heat killed *S. pneumoniae* led to the expression of iNOS (Figure 23). The PTEN deficiency triggered a significantly reduce in in the expression compared to the wild-type macrophages.

All these results indicated that the PI3K / PTEN axis influences the phenotype of activated macrophages. PTEN deficiency led to an increase of Arginase 1 and FIZZ, but in contrast MRC-1 was unchanged and YM1 together with the chemokines CCL17 and CCL22 were diminished. Moreover the M1 marker iNOS was also decreased in the conditional PTEN knockout cells.

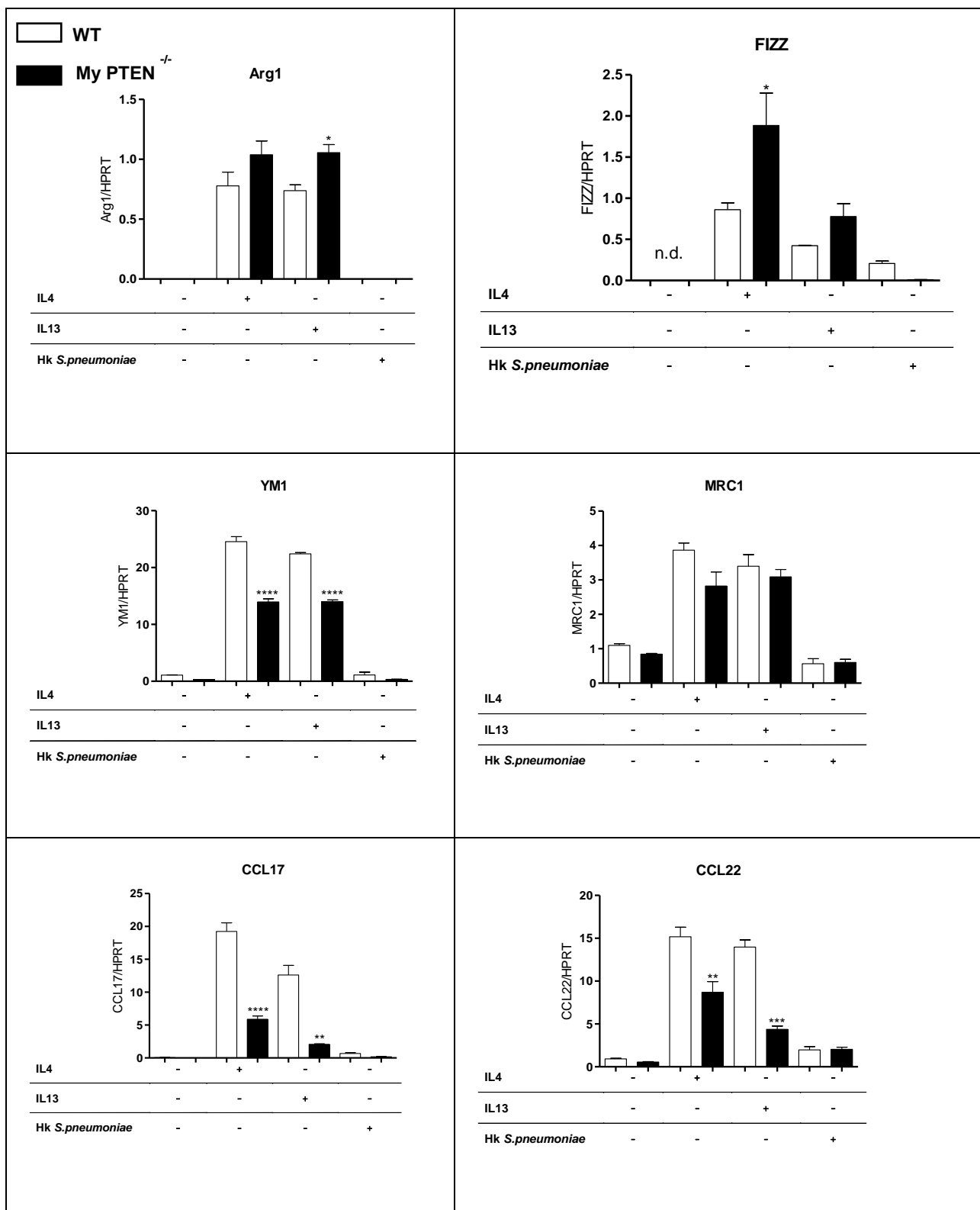


**Figure 22: mRNA levels of M2 markers of WT and PTEN deficient alveolar macrophages after stimulation with IL-4, IL-13 or heat killed *S. pneumoniae*.** The levels are expressed as fold change of the untreated control. Error bars show the standard deviations of the mean. Not determined (n.d.).

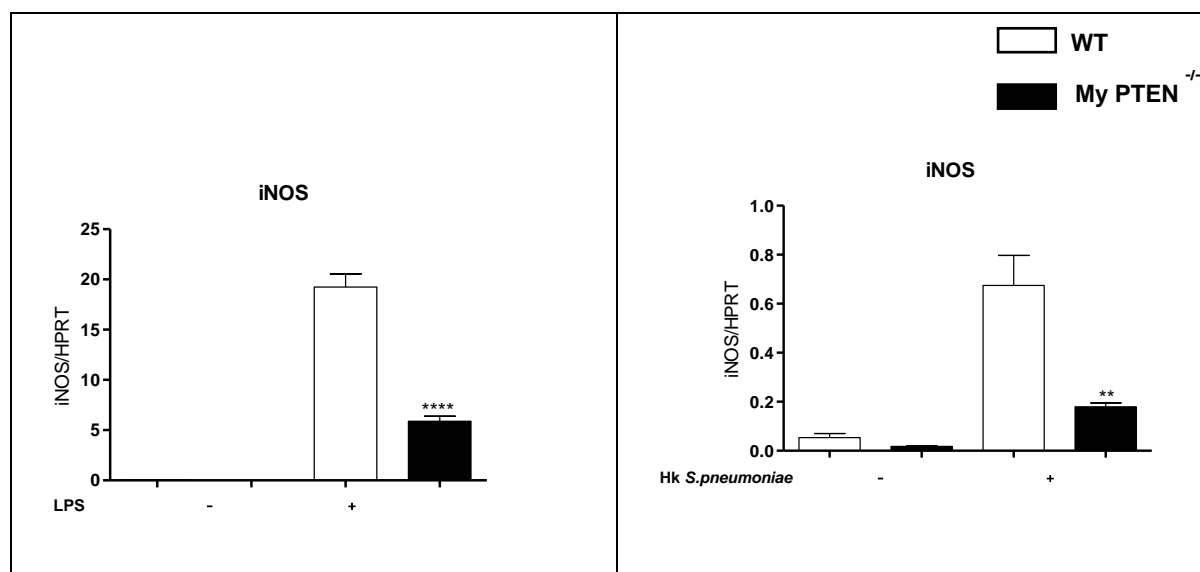


**Figure 23: Expression of iNOS of alveolar macrophages in response to LPS or heat killed *S. pneumoniae*.** Wild-type mice were compared with myeloid PTEN deficient mice. The levels are expressed as fold change of the untreated control. Error bars show the standard deviations of the mean.

### **6.8. In Vitro Stimulation with IL-4/ IL-13 Leads to Increased Levels of Arginase 1 in PTEN Deficient Alveolar Macrophages**

Due to the importance of Arginase 1 in collagen synthesis, we further wanted to proof if the increase in Arginase 1 mRNA can be reflected on the protein level. In order following on that idea we took alveolar macrophages of wild-type mice and myeloid PTEN deficient mice and stimulated the cells with IL-4 and IL-13 overnight. The cells were harvested and lysated in 2 x sample buffer. After the protein separation via SDS PAGE and western blotting Arginase 1 was detected with a specific antibody. The experiment showed that the cytokines IL-4/ IL-13 induced the expression of Arginase 1 in alveolar macrophages (Figure 24). Lack of PTEN caused increased amounts of Arginase 1. Therefore this result supported the data about increased Arginase 1 mRNA in PTEN deficient alveolar macrophages.

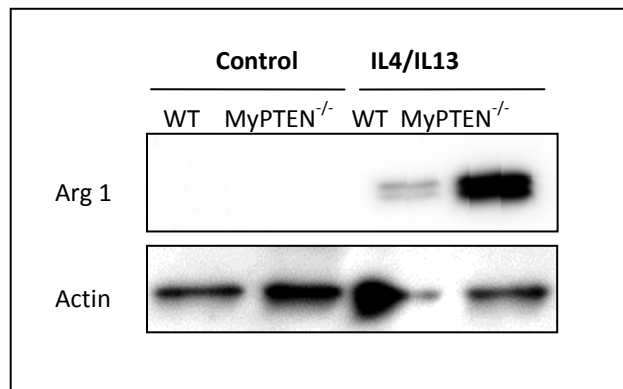


**Figure 24: Expression of Arginase 1 in wild-type and PTEN deficient alveolar macrophages after stimulation with IL4/IL13 overnight *in vitro*.** As loading control actin was applied.

### **6.9. Arginase 1 Expression is Increased in Myeloid PTEN Deficient Mice Post BLM Treatment**

To figure out the importance of alternative activation of macrophages and in particular the role of Arginase 1 we examined the expression of Arginase 1 during pulmonary fibrosis. Arginase 1 is part of the main markers for alternatively activated macrophages, which are considered as drivers of fibrosis (Wynn 2004). The enzyme is important for the generation of L-proline, which in turn is required for the collagen synthesis by fibroblasts (Wynn 2004). In this perspective wild-type and myeloid PTEN deficient mice were treated with bleomycin. After 7 days we isolated cells from treated animals, which entered the bronchioles and alveoli, via a bronchoalveolar lavage. Examination of H&E stained cytopins indicated that these cells were mainly composed of macrophages, neutrophils, basophils and in lower extent lymphocytes (Figure 25).

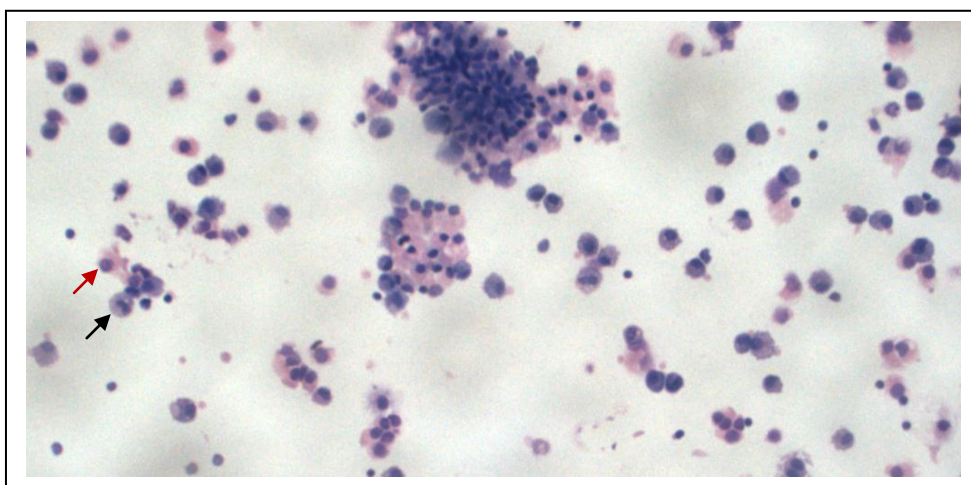


**Figure 25: Cytopsin of the bronchoalveolar lavage fluid.** One example of a macrophage and a neutrophil are indicated by a red and black arrow, respectively.

These BAL cells were directly lysated in sample buffer for SDS-PAGE and western blotting was performed. In saline treated mice of both genotypes Arginase 1 expression was undetectable. In contrast, BLM treatment leads to the expression of the enzyme after seven days (Figure 26). Three days post BLM application Arginase 1 was not detected (data not shown). To further analyze why PTEN deficiency in myeloid cells led to an increase in fibrosis, we compared the expression between wild-type and the conditional PTEN knockout mice. The western blot showed that mice lacking PTEN in myeloid cells produced enhanced levels of Arginase 1 seven days post BLM treatment.

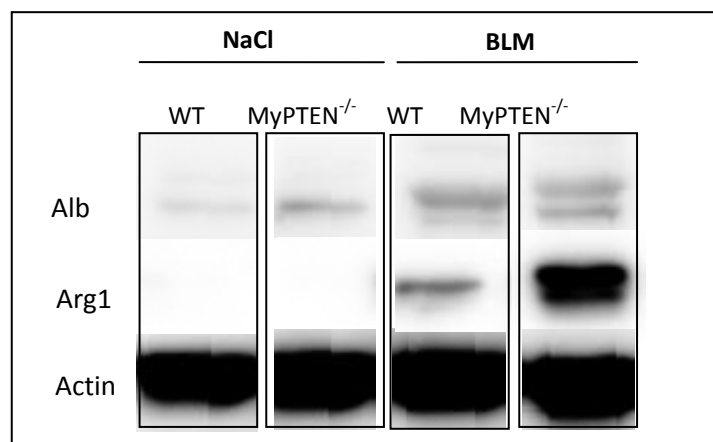


**Figure 26: Western blot analysis of the expression of Arginase 1 and the release of albumin 7 days post bleomycin treatment.** The expression was compared between myeloid PTEN deficient mice and their wild-type littermates. Actin was used as loading control.

### **6.10. Myeloid Cells are Responsible for the Expression of Arginase 1 in BLM Induced Pulmonary Fibrosis**

To elucidate the importance of myeloid derived Arginase 1 during pulmonary fibrosis, we used mice with floxed Arginase 1 alleles and created a conditional knockout with the Cre recombinase under expression of the LysM promoter. These genetic modifications led to a deficiency of the *arginase 1* gene only in myeloid cells. Mice with the expression of Cre are referred as MyArg1<sup>-/-</sup> or MyArg1 KO mice in figures. We wanted to identify if the Arginase 1 expression during pulmonary fibrosis was due to myeloid cells. In this context we treated wild-type and myeloid Arginase 1 deficient mice with 0.1 iu BLM intranasally. Seven days after the application the lungs were lavaged via the trachea to collect cytokines and cells of the bronchus and the alveoli. The BALF was centrifuged to

separate the cells from the fluid and the pellet was resuspended in SDS PAGE sample buffer. Western blot analysis showed that Arginase 1 was strongly reduced in the myeloid Arginase 1 deficient mice (Figure 27). The little expression was possible due to the incomplete knockout. This result indicated that the main producers of Arginase 1 during pulmonary fibrosis were myeloid cells.

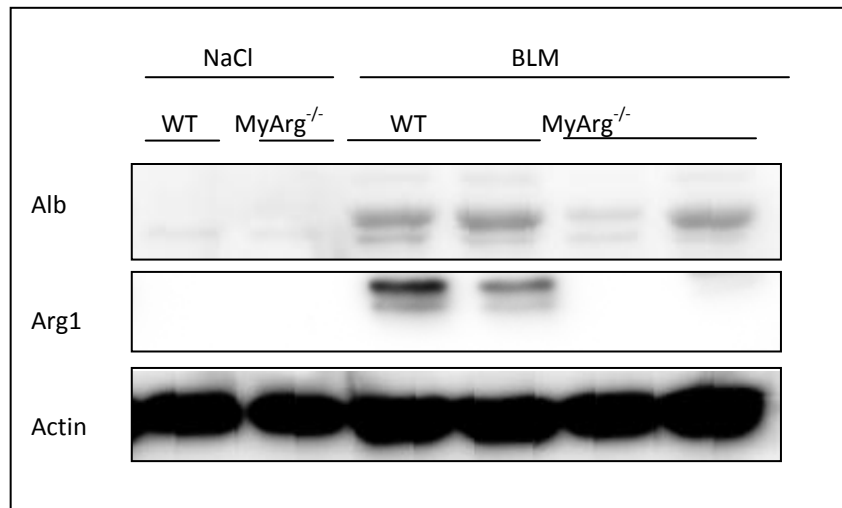


**Figure 27: Illustration of the expression of Arginase 1 and release of albumin by western blot analysis 7 days after the bleomycin treatment.** In this figure wild-types were compared with myeloid Arginase 1 deficient mice. The loading control was actin.

### **6.11. Myeloid Arginase 1 deficient mice have a reduced loss of weight due to BLM application**

Following the idea that myeloid PTEN deficient mice suffered from a severer fibrosis due to the elevated Arginase 1 expression, we assumed that the myeloid specific deletion of this enzyme may comprise protective features, specifically in our fibrosis model. To elucidate this question fibrosis was induced by bleomycin. One parameter for the progression of pulmonary fibrosis is the weight and accordingly its loss throughout the illness. During the first and the second day after the bleomycin instillation, myeloid Arginase 1 deficient mice had a significantly lower weight loss than their wild-type littermates (Figure 28). In this experiment we used a dose of 0.3 iu BLM which was too high, because the response was too strong that after five days both genotypes had a similar weight loss.

The additional fibrosis parameters such as the concentration of hydroxyproline have to be measured again, because the first experiment, in which it was planned to

characterize the fibrotic phenotype of myeloid Arginase 1 deficient mice failed due to the activity loss of BLM. In that experiment the induction of fibrosis was unsuccessful.

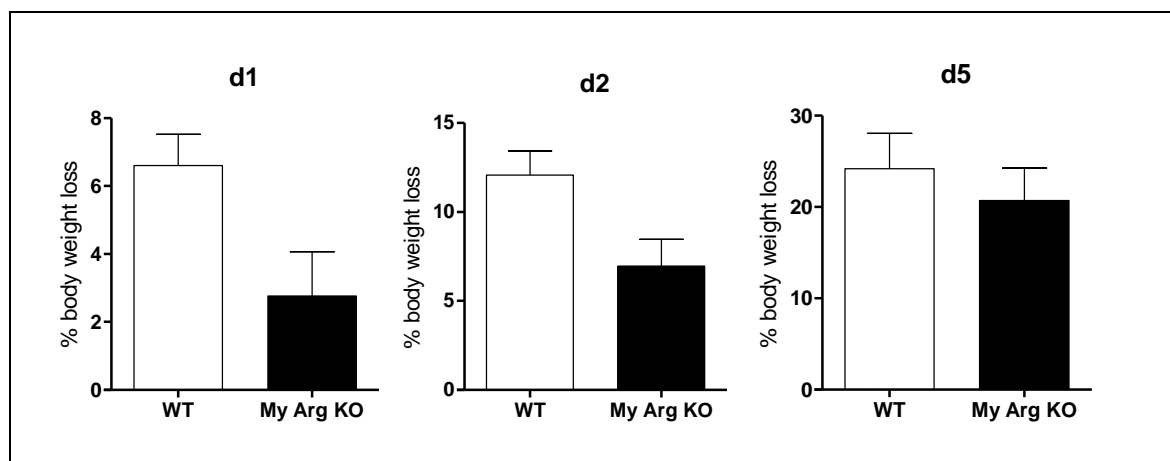


**Figure 28: Percentage of body weight loss due to bleomycin treatment. The differences of the weights were shown from the days one, two and five post bleomycin instillation (from left to right) and wild-types and myeloid Arginase 1 deficient mice were compared. Error bars show the standard deviations of the mean.**

### **6.12. Cytokine Profile of Myeloid Arginase 1 Deficient Mice in Pulmonary Fibrosis**

To characterize the influence of the deletion of Arginase 1 in myeloid cells on pulmonary fibrosis, cytokines were determined seven days post BLM treatment. Due to low dose or low bleomycin efficiency and the limited number of mice only a tendency could be seen. Bronchoalveolar lavage fluid and homogenized lungs were investigated for their cytokine profile.

No differences were noticed between lung homogenates of wild-type and conditional Arginase 1 knockout mice in the levels of IL-12, KC, IL-6 and INF- $\gamma$  (Figure 29). A small trend could be seen in the production of IL-4 and TNF- $\alpha$ , which seemed to be increased, while IL-17 gave the impression to be reduced in the lung homogenate of myeloid Arginase 1 mice. In the BALF only KC and IL-12 showed a tendency to be reduced in the conditional knockout mice, while IL-6 and INF- $\gamma$  seemed to be produced to a similar extent (Figure 30). The amount of IL-17, IL-4, TNF- $\alpha$  and IL-33 were below the detection limit of the ELISA. To investigate the potential effects mediated by Arginase 1 deficiency the experiments have to be repeated with a larger sample size and maybe with a slightly increased dose of BLM.

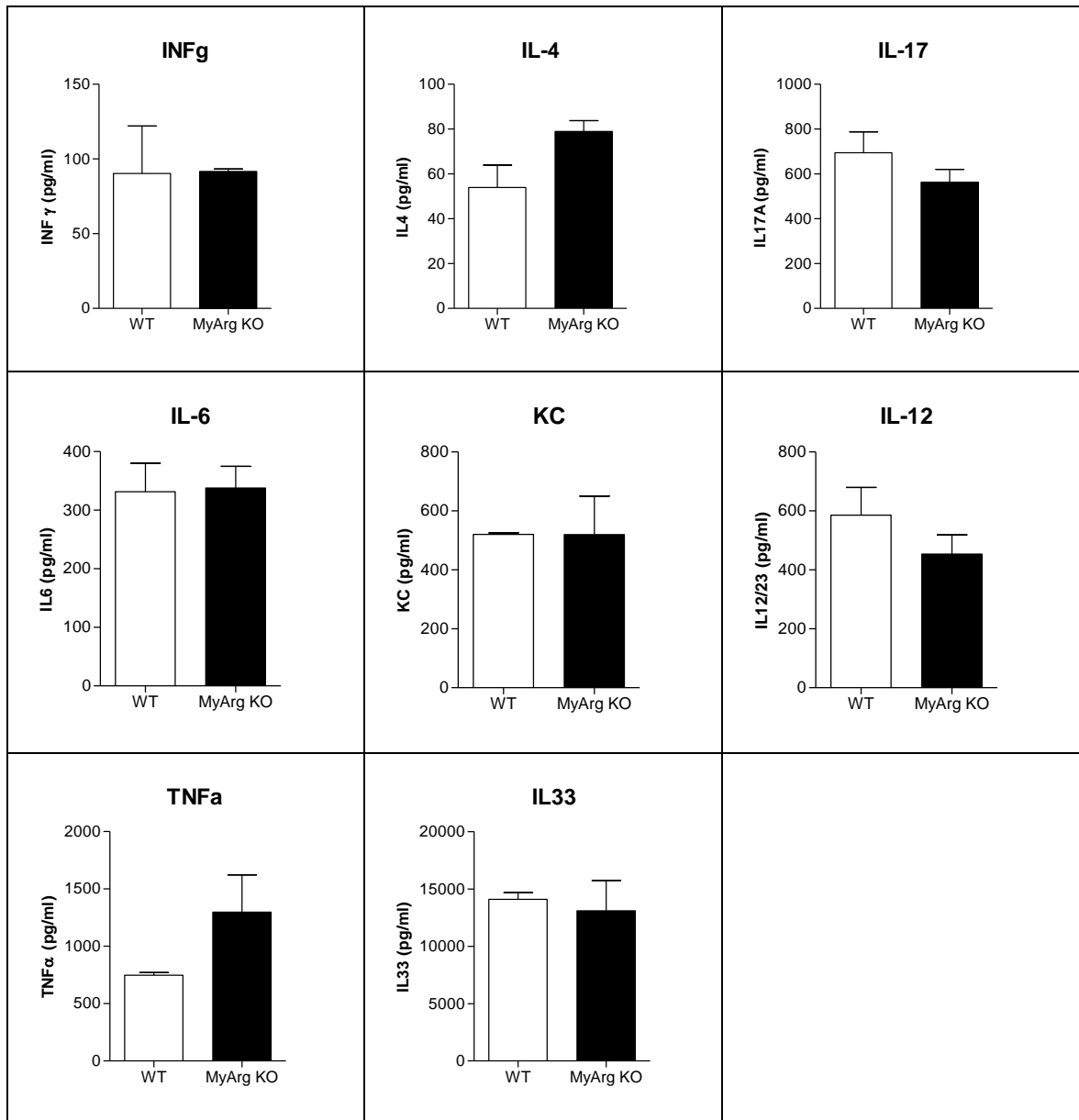


**Figure 29: Cytokine levels of lung homogenates of myeloid Arginase 1 deficient mice and wild-type littermates 7 days post bleomycin treatment. Error bars show the standard deviations of the mean.**

Results

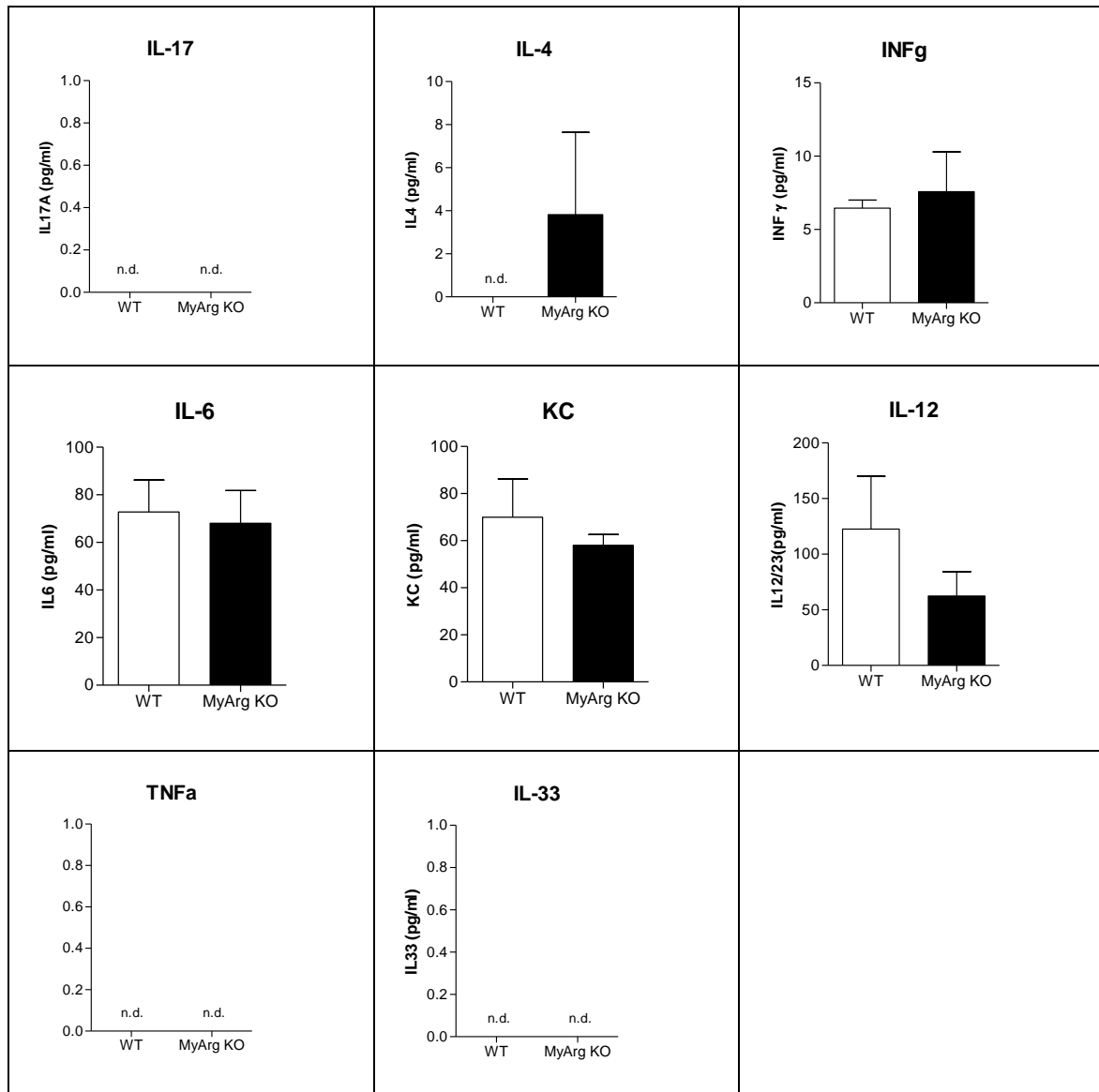


**Figure 30: Cytokines of the bronchoalveolar lavage fluid of myeloid Arginase 1 deficient mice were compared with the cytokines of wild-type littermates.** The mice were treated with bleomycin and after 7 days the lavage was performed. Error bars show the standard deviations of the mean.

## 7. Discussion and Perspectives

Increasing evidence of the influence of the innate immunity and alternatively activated macrophages in the pathogenesis of fibrosis triggered our interest, if myeloid PTEN contributes to fibrogenesis.

Previously published data by our group (Schabbauer, Matt et al. 2010) showed that myeloid knockout of PTEN leads to a reduced inflammatory response. We showed that LPS challenged alveolar macrophages produce lower levels of the pro-inflammatory cytokine TNF- $\alpha$  and NO if PTEN is absent. Moreover myeloid PTEN deletion increases the survival rate during *S. pneumoniae* infection. Based on this beneficial effect of increased PI3K activity in acute inflammation, we were interested in its influence on chronic inflammation. As model we decided to establish the bleomycin induced pulmonary fibrosis model. The advantages of this disease model are the high reproducibility, the histological analogy to human IPF and the simple application. Due to the clinical use of BLM in some cancer therapies, the model adds clinical relevance. In contrast the transient character of this model is dissimilar with the human pathogenesis and leads to differences in the persistence, which are the limitations of the bleomycin induced pulmonary fibrosis model. Moreover this model makes it difficult to discriminate between anti-inflammatory or anti-fibrotic effects (Moeller, Rodriguez-Lecompte et al. 2006). In this study we slightly modified this disease model. Instead of an intratracheally or intravenous application, we administered BLM intranasally in anesthetized mice. As proof of feasibility using Evans Blue showed that this application route only gave rise to pulmonary distribution of the fluid and that the gastrointestinal tract was unaffected. Moreover an equal collagen deposition was achieved by an intranasal BLM instillation compared with an injection into the trachea. These results reveal that this is a feasible and proper method, with the advantage to avoid surgical intervention and an increased survival during the application.

As mentioned before we wanted to characterize the role of innate immunity in pulmonary fibrosis, in this context we intended to target macrophages. Therefore we used conditional PTEN and Arginase 1 knockout mice with the genetic background of the Cre/lox system. The *cre* (cyclization recombination) gene of the bacteriophage P1 encodes for the site-specific DNA recombinase Cre. Cre recognizes the 34 bp long loxP (locus of X-over of P1) sites and removes DNA fragments between two directly repeated loxP sites. The excised DNA fragment forms a covalently closed circle. A common method to induce gene ablation only in macrophages is the administration of Cre expression under the regulation of the promoter of lysozym M, a rather specific protein for macrophages, and other myeloid cells. In mice two isotopes are known the LysM and

LysP, which are found in myeloid cells and in Paneth cells of the gut, respectively. Although LysM was recognized as a major constitutive secreted protein of inflammatory macrophages, it is also expressed and stored by granulocytes (Gordon 2003). Moreover the expression of LysM was detected in non-hematopoietic cells, the alveolar type II cells and the precursor cells of the interventricular septum of the heart (Stadtfeld, Ye et al. 2007). In contrast tissue macrophages and most other cell types, such as T- and B lymphocytes, lack LysM expression (Hume 2010).

A disadvantage of the Cre/lox system is that random monoallelic inactivation can lead to variation in the target gene down regulation among individual mice and even bone marrow derived macrophage populations (Faust, Varas et al. 2000). Apart from that the Cre/lox system provides a great possibility to generate animals with a partial knockout, thus avoiding lethality due to a complete knockout in all cell types. An additional benefit of the Cre/lox system is that properties of gene products of specific cell types can be determined. In our trial we are interested in the role of myeloid PTEN in pulmonary fibrosis. A loss of function mutation of *pten* leads to embryonic death after embryonic day (E) 7.5 (Di Cristofano, Pesce et al. 1998). Consequently a conditional knockout provides the option to create PTEN deficiency, without developmental failure (Hume 2010).

First we wanted to figure out if myeloid PTEN has an influence on pulmonary fibrosis. In that regard our primary aim was to characterize differences in the development of fibrosis between wild-type and myeloid PTEN deficient mice. The outcome of the BLM induced pulmonary fibrosis indicated that the ablated myeloid PTEN expression triggered a more severe outcome of fibrosis. Observations of increased loss of body weight, elevated hydroxyproline values in the lung and histological sections were the basis for this hypothesis. Collagen deposition displayed by Sirius Red staining and infiltration of immune cells demonstrated by H&E staining point out that the loss of PTEN in myeloid cells exacerbates pulmonary fibrosis. This leads to the suggestion that hyperactivity of PI3K, due to the lack of its inhibitor PTEN, may mediate effector mechanisms that could promote fibrosis.

To elucidate the possible effector functions of the PI3K various fibrosis and inflammation related cytokines were determined after BLM treatment. Surprisingly we found pro-inflammatory cytokines, such as IL-17, IL-6, MIP2 and KC elevated in myeloid PTEN deficient mice. This may demonstrate that BLM induced pulmonary fibrosis is elicited by different mechanism than *S. pneumoniae* or activation of macrophages by LPS. The important cell membrane molecule of gram negative bacterial LPS is known to trigger the immune response via TLR4, while gram positive bacteria *S. pneumoniae* induce the

inflammatory response mainly via the binding of lipoteichoic acid to TLR2. Both TLRs mediate a decrease in pro-inflammatory cytokines via the inhibition of GSK-3 $\beta$  and the consequently diminished activation of CREB (Martin, Rehani et al. 2005). One attempt to explain this phenomenon could be that other signaling pathways are strongly induced and lead to the augmented pro-inflammatory cytokines and dominate the anti-inflammatory effects of PTEN deficiency during pulmonary fibrosis. Another possibility could be that, in the early immune response pro-inflammatory cytokines are still decreased in conditional myeloid PTEN knockout mice compared to wild-types, but maybe persistent stimuli of the pulmonary disease trigger cytokine expression through different downstream pathways.

Inflammation often triggers and accompanies fibrosis. The great number of various cytokines, chemokines and immune cells makes it difficult to identify the precise role of inflammation. For example on the one hand overexpression of TNF can lead to fibrosis. Based on this knowledge there were many trials to use antagonists against TNF as therapeutic invention. Unlike the expectations this attempt failed, inhibition of TNF via its antagonists directed an even severer outcome of fibrosis. This effect is traced to the finding that TNF can slow down collagen synthesis and thereby attenuate the level of the disease (Wynn 2011).

Wynn proposes that a strong inflammatory response at the beginning and a diminished inflammation at later time points contribute to fibrotic progression. Our observation was that mice lacking PTEN in the myeloid cell lineage demonstrated more inflammation and fibrosis at day 7 after BLM application, hence we assume that the time point is an important factor and crucial for the development of the disease. The different stages of fibrosis offer possibilities for explanation. Based on the idea that immune cells increase the levels of IL-13 and TGF- $\beta$  at the beginning of the medical condition, they promote pathogenesis. In contrast due to the character of inflammatory cells, they can down regulate fibrosis at later stages, by the clearance of cell debris and controlling of cell proliferation (Wilson and Wynn 2009). In contrast immune cells could also produce pro-fibrotic cytokines at later stages of fibrosis and therefore contribute to the disease. The expression pattern of pro- or anti-inflammatory cytokines seems to change during disease progression and should be addressed in further experiments.

Another possibility could be that PI3K activity in immune cells is not mediated by TLRs but by cytokines and therefore comprises different effects. In fibrosis IL-4 and IL-13 are augmented (Wynn 2004), for that reason we analyzed *in vitro* if these cytokines are able to initialize PI3K signaling. By means of western blot analysis we could show that the downstream kinases Akt and GSK-3 $\beta$  got phosphorylated after IL-4 and IL-13 stimulation,

which pointed out that they influence PI3K activity. This effect was strongly increased in myeloid PTEN deficient macrophages. Possibly these cytokines stimulate the PI3K to induce cell survival in macrophages via the inhibition of caspase 9 and Bcl-2-associated death promoter (BAD) during tissue remodeling (Marone, Cmiljanovic et al. 2008). In this context PI3K maybe thwart macrophage clearance. To elucidate this issue macrophage numbers of wild-type and PTEN deficient mice have to be compared for example via flow cytometry or H&E staining of cytopins of the cells of the bronchoalveolar lavage.

Furthermore IL-4 and IL-13 are important cytokines for the alternatively activation of macrophages, in contrast to INF- $\gamma$ , which endorses classical activation. These different stimuli of macrophage activation trigger diverse phenotypes. In consequence of the observation that IL-4 and IL-13 raise PI3K activity, we wanted to assay if the M2 phenotype is altered by elevated PI3K signaling. In this perspective we investigated, if myeloid PTEN deficient macrophages exhibit a different phenotype due to IL-4 or IL-13 stimulation *in vitro*. Markers of M2 polarization were checked on mRNA level. The experiment made obvious that there were differences in the M2 expression pattern. The alternative activation marker YM1 was significantly decreased in the absent of PTEN, similar the M2 chemokines CCL17 and CCL22 were diminished after stimulation with the type 2 cytokines, while baseline levels are constant. In contrast FIZZ was increased, especially due to IL-4 stimulation, although untreated macrophages lacking PTEN had significantly reduced amount of this M2 marker. To further elucidate their phenotype we analyzed Arginase 1 and its counter actor iNOS, which are indicators for a M2 and M1 functional phenotype, respectively, and we found out that they were differentially expressed. In PTEN deficient macrophages Arginase 1 was increased and iNOS decreased. Moreover we could confirm this data on protein level. Western blot analysis showed in addition that PTEN deficient alveolar macrophages have increased levels of Arginase 1 in response to IL-4 and IL-13 stimulation. These dissimilarities of the M2 expression profile showed that the PI3K/PTEN axis influences the M2 polarization and that the absence of PTEN promotes a M2 like phenotype. Maybe the PI3K can activate the transcription factor STAT6 or C/EBP $\beta$  (El Kasmi, Qualls et al. 2008) and thus induce Arginase 1. Perhaps in a similar way as IL-4 and IL-13 activate STAT6 and therefore lead to the activation of M2 genes, such as Arginase I (Welch, Escoubet-Lozach et al. 2002). Maybe reporter assays will help to clarify this question.

IL-4 and IL-13 are famous for their action on macrophages to polarize them toward a M2 phenotype (Gordon 2003) and in addition they play an important role in the development of pulmonary fibrosis. Due to the finding of varieties in the expression pattern of macrophages after alternative activation, it could be possible that the release of

IL-4 and IL-13 during lung fibrosis has different effects in the myeloid PTEN deficient mice than in the wild-type mice. With this background it could be that the negative effects of IL-4 and IL-13 on progression of the disease are even worse in conditional PTEN knockout mice. To identify more precisely if alteration in the M2 phenotype of macrophages could play a role during pulmonary fibrosis we examined the expression of Arginase 1 during the disease.

Interestingly we found out that BLM induced the expression of Arginase 1 in wild-type and myeloid PTEN deficient mice and similar to the *in vitro* studies the concentration was elevated in the conditional knockout mice. Arginase 1, which is a urea cycle enzyme, converts L-arginine into L-ornithine and urea; L-ornithine is further converted into L-proline and polyamines. L-proline is a very important compound of collagen and in this context Arginase 1 is implicated as a driver of collagen deposition and fibrosis (Wynn 2004). Augmented Arginase activity induces a depletion of L-arginine in the microenvironment, which leads to the failure of T-cells to express the  $\zeta$ -chain of the TCR, and the lack of L-ornithine impairs the cell proliferation and differentiation (Baniyash 2004). This effect could be the reason for the diminished number of T-cells in myeloid PTEN deficient mice during pulmonary fibrosis seen by flow cytometry. The reduced number of T-cells can either promote or inhibit fibrosis dependent on their differentiation towards TH2 or TH1 cells, respectively. To elucidate their cytokine expression profile ELISAs were performed indicating that INF- $\gamma$ , IL-4 and L-17 were increased in myeloid PTEN deficient mice, leading to the suggestion that these cytokine differences may be driven by innate immune cells. To verify this idea intracellular staining of these cytokines and flow cytometry analysis would be helpful.

Furthermore the increased Arginase 1 concentration could induce higher L-proline levels. After hydroxylation L-proline becomes hydroxyproline, which is a main component of collagen. In this context Arginase 1 may support collagen deposition by myofibroblasts and therefore the development of fibrosis. To find out if myeloid cells mediate the Arginase 1 expression during pulmonary fibrosis, we treated myeloid Arginase 1 deficient mice with bleomycin and investigated the Arginase 1 expression. We could demonstrate that myeloid Arginase 1 deficient mice had no or a strongly reduced Arginase 1 expression post BLM instillation. The little Arginase 1 expression is probably due to the incomplete knockout of Arginase 1 or due to other unidentified Arginase 1 expressing cells, which contribute to the disease. This result shows that Arginase 1 in pulmonary fibrosis is mainly produced by myeloid cells, including an important role of these cells during the disease.

Mice, which lack Arginase 1 expression in myeloid cells exhibit a protective phenotype within the first two days, suggesting a pro-fibrotic role of Arginase 1. Due to the concentration of BLM (0.5 iu) we failed to examine additional differences between the two genotypes after day 5 post BLM application. Since we could not detect Arginase 1 in the bronchoalveolar lavage fluid three days after BLM treatment; maybe interstitial macrophages rather than alveolar macrophages trigger the protective phenotype on the first two days. Flow cytometry analysis indicated differences in the M2 phenotype of interstitial macrophages between myeloid PTEN deficient and wild-type mice differs, thus maybe interstitial macrophages effect fibrotic progression.

An experiment with a lower dose of BLM (0.1 iu) did not show any differences in the cytokine levels between the myeloid Arginase 1 deficient mice and wild-types, except TNF- $\alpha$  and IL-4. This effect could be due to the possible protective downstream effect of Arginase 1 activity. The experiment will be repeated with an adequate concentration of BLM. Pesce and colleagues showed that Arginase 1 deficiency in myeloid cells lead to more severe schistosomias mediated liver fibrosis. They argued that Arginase 1 activity leads to a depletion of L-arginine, which is important for T helper cell proliferation and therefore down regulates their effector function. Additionally they think that myeloid Arginase 1 competes with Arginase 1 of myofibroblasts for L-arginine and therefore reduce the collagen synthesis of myofibroblasts. Another proposed possibility was that mitochondrial Arginase 2 converts L-arginine instead of Arginase 1 and promotes L-proline synthesis, because of its colocalization with L-ornithine decarboxylase (ODC) (Pesce, Ramalingam et al. 2009). Taking these results together Arginase 1 has a pro-fibrotic as well as a protective character and that possibly the concentration is crucial for its effects. Moreover Arginase 1 can have contradictory effects on fibrosis dependent on the time point. Additionally the balance between Arginase 1 and iNOS may be important for efficient wound healing. Treatment of wild-type mice with recombinant Arginase 1 during BLM induced fibrosis may facilitate the clarification of the amount of Arginase 1 with beneficial characteristics.

Many open questions still remain and have to be elucidated. The next main aim is the establishment of a cytokine profile that accompanies fibrosis, by measuring cytokines and chemokines at various time points. This will be helpful to establish possible expression differences between wild-types and conditional knockout mice and to figure out which consequences the lack of PTEN implicates and how it may manipulate the

development of fibrosis. Additionally, it is planned to re-stimulate T-lymphocytes of the lung with anti-CD3 / CD28 antibodies to amplify T-cell cytokines and to intensify differences.

Moreover, one important experiment will be to characterize the phenotype of myeloid Arginase 1 deficient mice after BLM administration. On that account, it is planned to treat myeloid Arginase 1 knockout mice and littermate controls with BLM for three weeks and to measure the hydroxyproline levels of the lungs and figure out if there are differences in the collagen deposition depicted by histological staining.

In order to identify how PI3K signaling may alter the M2 phenotype and the outcome of fibrosis, we want to characterize if this signaling pathway changes the expression of transcription factors. In this regard, mRNA levels can be examined and then verified by western blotting.

According to the clarifying of the effector mechanisms, rescue experiments are scheduled. In this context, myeloid PTEN deficient mice will be treated with the Arginase 1 inhibitor N (omega)-hydroxyl-L-arginine (NOHA) and monitored if the phenotype can be recovered. In addition, double knockout mice with a lack of PTEN and Arginase 1 in myeloid cells can be tested for fibrosis development.



## 8. List of Figures

- Figure 1: Phosphoinositide 3-kinase pathway. Modified from (Gunzl and Schabbauer 2008)..... 17
- Figure 2: L-arginine conversion by Arginase versus iNOS in murine myeloid cells (Munder 2009).20
- Figure 3: Phenotypical characterization of M1 macrophages and its communication with Th1 cells and NK cells. Reactive nitrogen intermediates (RNI), reactive oxygen intermediates (ROI). (Biswas and Mantovani 2010).....22
- Figure 4: Phenotypical characterization of M2 macrophages and its communication with TH2 cells, basophils and innate lymphoid cells. (Biswas and Mantovani 2010).....24
- Figure 5: Differentiation pathways of dendritic cells. (Kushwah and Hu 2011) .....27
- Figure 6: Phases of wound healing response and their possible contribution to fibrosis. (Wynn 2011) .....31
- Figure 8: Sirius red stained lung sections 21 d post bleomycin instillation. The left lung represents a healthy mouse, while in the middle and the right the lung originate from mice treated with bleomycin intranasally (i.n.) and intratracheally (i.t.), respectively. ....62
- Figure 9: Quantification of the area of collagen deposition. Different routes (intratracheally (i.t.) and intranasally (i.n.)) and different concentrations (0.05 iu and 0.15 iu) were tested.....62
- Figure 10: Comparison of the cytokine levels between healthy mice and bleomycin treated mice. Whole lung tissue was homogenized and cytokines were measured by ELISA. Error bars show the standard deviations of the mean. (n.d...not determined) .....63
- Figure 11: Comparison of the cytokine levels between healthy mice and bleomycin treated mice. The cytokines of the bronchoalveolar lavage fluid were measured by ELISA. Error bars show the standard deviations of the mean.....64
- Figure 12: Wild-type and PTEN deficient alveolar macrophages were stimulated with LPS. The PI3K activity was examined by the phosphorylation of the two downstream kinases Akt and GSK-3 $\beta$ . Determination of actin was used as loading control. ....65
- Figure 14: Comparison of fibrotic markers between WT and myeloid PTEN KO mice. A) Body weight loss of mice after bleomycin administration. B) Hydroxyproline (OH-Proline) content in murine lungs 21 day post bleomycin treatment. Error bars show the standard deviations of the mean. ....67
- Figure 15: Histological specimen of murine lung tissue. The left column present the control lung treated with saline, the middle column demonstrates the lung of a wild-type mouse 21 day post bleomycin treatment and the right one covers the bleomycin treated lung of a myeloid PTEN knockout mouse. The two upper rows display the collagen deposition via Sirius Red staining. The third and fourth rows demonstrate the hematoxylin and eosin staining. Images of

## List of Figures

- each row top-down are shown at 12.5, 40, 12.5 and 200 x magnification. Tissue was embedded in paraffin and 2  $\mu$ m sections were prepared. ....68
- Figure 16: Flow cytometric analysis of murine lung cell suspension 7 days post bleomycin treatment. Wild-type mice were compared with myeloid PTEN deficient mice. Each genotype is represented by two mice. Different markers were applied to identify macrophages, DCs, NK-cells, B-cells, T-cells, Th cells, cytotoxic T-cells and T<sub>REG</sub>-cells. ....70
- Figure 17: IL-6 and KC expression 7 days post bleomycin treatment. RNA was isolated from lungs of myeloid PTEN knockout mice and wild-type littermates. Error bars show the standard deviations of the mean. ....71
- Figure 18: Wild-type and myeloid PTEN deficient mice were treated with bleomycin for 7 days and subsequently their lungs were homogenized and analyzed by ELISA. Error bars show the standard deviations of the mean. ....72
- Figure 19: Wild-type and myeloid PTEN deficient mice were treated with bleomycin, at day 7 the bronchoalveolar lavage fluid was collected and analyzed by ELISA. Error bars show the standard deviations of the mean. (n.d...not determined) ....73
- Figure 20: Western Blot analysis of wild-type and myeloid deficient alveolar macrophages after 10, 30 or 60 minutes stimulation with IL-4 and IL-13. As target the phosphorylation state of the PI3K downstream kinases Akt and GSK-3 $\beta$  were investigated. Actin was used as loading control. ....74
- Figure 21: Flow cytometry analysis of murine lungs for M1 and M2 markers. Interstitial, alveolar macrophages and dendritic cells were examined. Gating strategy: excluding of the dead cells via the viability dye, elimination of the doublets according to the forward and side scatters, taking of the CD45+ cells and separating them according to CD11b and CD11c expression .76
- Figure 22: mRNA levels of M2 markers of WT and PTEN deficient alveolar macrophages after stimulation with IL-4, IL-13 or heat killed *S. pneumonia*. The levels are expressed as fold change of the untreated control. Error bars show the standard deviations of the mean. Not determined (n.d.).....79
- Figure 23: Expression of iNOS of alveolar macrophages in response to LPS or heat killed *S. pneumonia*. Wild-type mice were compared with myeloid PTEN deficient mice. The levels are expressed as fold change of the untreated control. Error bars show the standard deviations of the mean. ....80
- Figure 24: Expression of Arginase 1 in wild-type and PTEN deficient alveolar macrophages after stimulation with IL4/IL13 overnight *in vitro*. As loading control actin was applied. ....81
- Figure 25: Cytospin of the bronchoalveolar lavage fluid. One example of a macrophage and a neutrophil are indicated by a red and black arrow, respectively. ....81

- Figure 26: Western blot analysis of the expression of Arginase 1 and the release of albumin 7 days post bleomycin treatment. The expression was compared between myeloid PTEN deficient mice and their wild-type littermates. Actin was used as loading control.....82
- Figure 27: Illustration of the expression of Arginase 1 and release of albumin by western blot analysis 7 days after the bleomycin treatment. In this figure wild-types were compared with myeloid Arginase 1 deficient mice. The loading control was actin. ....83
- Figure 28: Percentage of body weight loss due to bleomycin treatment. The differences of the weights were shown from the days one, two and five post bleomycin instillation (from left to right) and wild-types and myeloid Arginase 1 deficient mice were compared. Error bars show the standard deviations of the mean.....84
- Figure 29: Cytokine levels of lung homogenates of myeloid Arginase 1 deficient mice and wild-type littermates 7 days post bleomycin treatment. Error bars show the standard deviations of the mean. ....85
- Figure 30: Cytokines of the bronchoalveolar lavage fluid of myeloid Arginase 1 deficient mice were compared with the cytokines of wild-type littermates. The mice were treated with bleomycin and after 7 days the lavage was performed. Error bars show the standard deviations of the mean. ....86

## 9. List of Tables

Table 1: Sequences of the PCR primers for genotyping .....	39
Table 2: Description of the PCR programs .....	39
Table 3: Hellabruner mixture.....	41
Table 4: Sequences of the used primers for Real time PCR.....	51
Table 5: Composition of the qPCR mastermix.....	52
Table 6: List of antibodies used for flow cytometry.....	58

## 10. Curriculum Vitae

### Personal Information:

Name: Julia Kral  
 Date of Birth: 21.11.1988  
 Place of Birth: 1180 Vienna  
 Nationality: AUSTRIAN

### Education:

2010 to 2012 Master studies "Genetic and Molecular Pathology" at the University of Vienna, Vienna I  
 2007 to 2010 Bachelor studies "Molecular Biotechnology" at the University of Applied Sciences, Vienna III  
 6<sup>th</sup> June 2007 Allgemeine Reifeprüfung (equivalent to the A levels in England)  
 1999 to 2007 Realgymnasium Rosasgasse (similar to a secondary school)

### Work Experience:

November 2011 to September 2012      **Master Thesis**  
"Investigation of the Role of PTEN and the Alternative Activation of Macrophages in Pulmonary Fibrosis"  
 Medical University of Vienna, Department of Physiology  
 Research group: Protective signalling pathways in acute and chronic disease, Gernot Schabbauer, Ph.D.

September and October 2011      **Practical**  
"The role of Lcn2 and IL-17 during pneumococcal pneumonia"  
 Medical University of Vienna, Department of Medicine 1  
 Research group: The innate immune response to bacterial infections, Silvia Knapp, M.D., Ph.D.

January to May 2010

**Bachelor Thesis**

“Evaluation of the capability of a panel of analytical methods to detect intentionally modified/degraded human coagulation factor IX”

Octapharma Produktionsgesm.b.H.

Katharina Pock, Ph.D.

## 11. Literature

- Abramoff, M., P. Magalhaes, et al. (2004). "Image processing with ImageJ." Biophotonics International.
- Azambuja, E., J. F. Fleck, et al. (2005). "Bleomycin lung toxicity: who are the patients with increased risk?" Pulm Pharmacol Ther **18**(5): 363-6.
- Bachman, M. A., V. L. Miller, et al. (2009). "Mucosal lipocalin 2 has pro-inflammatory and iron-sequestering effects in response to bacterial enterobactin." PLoS Pathog **5**(10): e1000622.
- Baniyash, M. (2004). "TCR zeta-chain downregulation: curtailing an excessive inflammatory immune response." Nat Rev Immunol **4**(9): 675-87.
- Bataller, R. and D. A. Brenner (2005). "Liver fibrosis." J Clin Invest **115**(2): 209-18.
- Beutler, B. (2004). "Innate immunity: an overview." Mol Immunol **40**(12): 845-59.
- Biswas, S. K. and A. Mantovani (2010). "Macrophage plasticity and interaction with lymphocyte subsets: cancer as a paradigm." Nat Immunol **11**(10): 889-96.
- Boutard, V., R. Havouis, et al. (1995). "Transforming growth factor-beta stimulates arginase activity in macrophages. Implications for the regulation of macrophage cytotoxicity." J Immunol **155**(4): 2077-84.
- Bronte, V. and P. Zanovello (2005). "Regulation of immune responses by L-arginine metabolism." Nat Rev Immunol **5**(8): 641-54.
- Cantley, L. C. (2002). "The phosphoinositide 3-kinase pathway." Science **296**(5573): 1655-7.
- Chaplin, D. D. (2003). "1. Overview of the immune response." J Allergy Clin Immunol **111**(2 Suppl): S442-59.
- Deshmane, S. L., S. Kremlev, et al. (2009). "Monocyte chemoattractant protein-1 (MCP-1): an overview." J Interferon Cytokine Res **29**(6): 313-26.
- Desjardins, M., J. E. Celis, et al. (1994). "Molecular characterization of phagosomes." J Biol Chem **269**(51): 32194-200.
- Di Cristofano, A., B. Pesce, et al. (1998). "Pten is essential for embryonic development and tumour suppression." Nat Genet **19**(4): 348-55.
- Domin, J. and M. D. Waterfield (1997). "Using structure to define the function of phosphoinositide 3-kinase family members." FEBS Lett **410**(1): 91-5.

## Literature

- El Kasmi, K. C., J. E. Qualls, et al. (2008). "Toll-like receptor-induced arginase 1 in macrophages thwarts effective immunity against intracellular pathogens." Nat Immunol **9**(12): 1399-406.
- Faust, N., F. Varas, et al. (2000). "Insertion of enhanced green fluorescent protein into the lysozyme gene creates mice with green fluorescent granulocytes and macrophages." Blood **96**(2): 719-26.
- Fruman, D. A. and L. C. Cantley (2002). "Phosphoinositide 3-kinase in immunological systems." Semin Immunol **14**(1): 7-18.
- Fruman, D. A., F. Mauvais-Jarvis, et al. (2000). "Hypoglycaemia, liver necrosis and perinatal death in mice lacking all isoforms of phosphoinositide 3-kinase p85 alpha." Nat Genet **26**(3): 379-82.
- Galli, S. J., N. Borregaard, et al. (2011). "Phenotypic and functional plasticity of cells of innate immunity: macrophages, mast cells and neutrophils." Nat Immunol **12**(11): 1035-44.
- Gericke, A., M. Munson, et al. (2006). "Regulation of the PTEN phosphatase." Gene **374**: 1-9.
- Gordon, S. (2003). "Alternative activation of macrophages." Nat Rev Immunol **3**(1): 23-35.
- Gordon, S. and F. O. Martinez (2010). "Alternative activation of macrophages: mechanism and functions." Immunity **32**(5): 593-604.
- Gunzl, P. and G. Schabbauer (2008). "Recent advances in the genetic analysis of PTEN and PI3K innate immune properties." Immunobiology **213**(9-10): 759-65.
- Harwood, N. E. and F. D. Batista (2008). "New insights into the early molecular events underlying B cell activation." Immunity **28**(5): 609-19.
- Hay, J., S. Shahzeidi, et al. (1991). "Mechanisms of bleomycin-induced lung damage." Arch Toxicol **65**(2): 81-94.
- Hodge, M. R., H. J. Chun, et al. (1996). "NF-AT-Driven interleukin-4 transcription potentiated by NIP45." Science **274**(5294): 1903-5.
- Huaux, F., T. Liu, et al. (2003). "Dual roles of IL-4 in lung injury and fibrosis." J Immunol **170**(4): 2083-92.
- Hume, D. A. (2010). "Applications of myeloid-specific promoters in transgenic mice support in vivo imaging and functional genomics but do not support the concept of

- distinct macrophage and dendritic cell lineages or roles in immunity." J Leukoc Biol **89**(4): 525-38.
- Kim, H. S., H. Go, et al. (2011). "TLR2-mediated production of IL-27 and chemokines by respiratory epithelial cells promotes bleomycin-induced pulmonary fibrosis in mice." J Immunol **187**(8): 4007-17.
- Kim, J. I., I. C. Ho, et al. (1999). "The transcription factor c-Maf controls the production of interleukin-4 but not other Th2 cytokines." Immunity **10**(6): 745-51.
- Krishnamoorthy, S. and K. V. Honn (2006). "Inflammation and disease progression." Cancer Metastasis Rev **25**(3): 481-91.
- Kushwah, R. and J. Hu (2011). "Complexity of dendritic cell subsets and their function in the host immune system." Immunology **133**(4): 409-19.
- Laird, M. H., S. H. Rhee, et al. (2009). "TLR4/MyD88/PI3K interactions regulate TLR4 signaling." J Leukoc Biol **85**(6): 966-77.
- Lieber, C. S. (1999). "Prevention and treatment of liver fibrosis based on pathogenesis." Alcohol Clin Exp Res **23**(5): 944-9.
- Marone, R., V. Cmiljanovic, et al. (2008). "Targeting phosphoinositide 3-kinase: moving towards therapy." Biochim Biophys Acta **1784**(1): 159-85.
- Martin, M., K. Rehani, et al. (2005). "Toll-like receptor-mediated cytokine production is differentially regulated by glycogen synthase kinase 3." Nat Immunol **6**(8): 777-84.
- McInnes, A. and D. M. Rennie (1988). "Interleukin 4 induces cultured monocytes/macrophages to form giant multinucleated cells." J Exp Med **167**(2): 598-611.
- Medzhitov, R. (2007). "Recognition of microorganisms and activation of the immune response." Nature **449**(7164): 819-26.
- Mehendale, H. M. (2005). "Tissue repair: an important determinant of final outcome of toxicant-induced injury." Toxicol Pathol **33**(1): 41-51.
- Miller, J. C., B. D. Brown, et al. (2012). "Deciphering the transcriptional network of the dendritic cell lineage." Nat Immunol **13**(9): 888-899.
- Moeller, A., J. C. Rodriguez-Lecompte, et al. (2006). "Models of pulmonary fibrosis." Drug Discovery Today: Disease Models **3**(3): 243-2-49.
- Moore, B. B. and C. M. Hogaboam (2008). "Murine models of pulmonary fibrosis." Am J Physiol Lung Cell Mol Physiol **294**(2): L152-60.

## Literature

- Munder, M. (2009). "Arginase: an emerging key player in the mammalian immune system." Br J Pharmacol **158**(3): 638-51.
- Munder, M., K. Eichmann, et al. (1999). "Th1/Th2-regulated expression of arginase isoforms in murine macrophages and dendritic cells." J Immunol **163**(7): 3771-7.
- Munder, M., F. Mollinedo, et al. (2005). "Arginase I is constitutively expressed in human granulocytes and participates in fungicidal activity." Blood **105**(6): 2549-56.
- Nair, M. G., Y. Du, et al. (2009). "Alternatively activated macrophage-derived RELM- $\alpha$  is a negative regulator of type 2 inflammation in the lung." J Exp Med **206**(4): 937-52.
- Okada, T., L. Sakuma, et al. (1994). "Blockage of chemotactic peptide-induced stimulation of neutrophils by wortmannin as a result of selective inhibition of phosphatidylinositol 3-kinase." J Biol Chem **269**(5): 3563-7.
- Pesce, J. T., T. R. Ramalingam, et al. (2009). "Arginase-1-expressing macrophages suppress Th2 cytokine-driven inflammation and fibrosis." PLoS Pathog **5**(4): e1000371.
- Peyssonnaud, C., V. Datta, et al. (2005). "HIF-1 $\alpha$  expression regulates the bactericidal capacity of phagocytes." J Clin Invest **115**(7): 1806-15.
- Ratledge, C. and L. G. Dover (2000). "Iron metabolism in pathogenic bacteria." Annu Rev Microbiol **54**: 881-941.
- Reese, T. A., H. E. Liang, et al. (2007). "Chitin induces accumulation in tissue of innate immune cells associated with allergy." Nature **447**(7140): 92-6.
- Schabbauer, G., U. Matt, et al. (2010). "Myeloid PTEN promotes inflammation but impairs bactericidal activities during murine pneumococcal pneumonia." J Immunol **185**(1): 468-76.
- Schimanski, L. M., H. Drakesmith, et al. (2005). "In vitro functional analysis of human ferroportin (FPN) and hemochromatosis-associated FPN mutations." Blood **105**(10): 4096-102.
- Schluns, K. S. and L. Lefrancois (2003). "Cytokine control of memory T-cell development and survival." Nat Rev Immunol **3**(4): 269-79.
- Sheppard, D. (2008). "The role of integrins in pulmonary fibrosis." European Respiratory Review **17**(109): 157-162.

- Shmagel, K. V. and V. A. Chereshevnev (2009). "Molecular bases of immune complex pathology." Biochemistry (Mosc) **74**(5): 469-79.
- Sica, A. and A. Mantovani (2012). "Macrophage plasticity and polarization: in vivo veritas." J Clin Invest **122**(3): 787-95.
- Stadtfeld, M., M. Ye, et al. (2007). "Identification of interventricular septum precursor cells in the mouse embryo." Dev Biol **302**(1): 195-207.
- Suzuki, A., M. T. Yamaguchi, et al. (2001). "T cell-specific loss of Pten leads to defects in central and peripheral tolerance." Immunity **14**(5): 523-34.
- Szabo, S. J., S. T. Kim, et al. (2000). "A novel transcription factor, T-bet, directs Th1 lineage commitment." Cell **100**(6): 655-69.
- Thannickal, V. J., G. B. Toews, et al. (2004). "Mechanisms of pulmonary fibrosis." Annu Rev Med **55**: 395-417.
- Vanhaesebroeck, B., S. J. Leever, et al. (2001). "Synthesis and function of 3-phosphorylated inositol lipids." Annu Rev Biochem **70**: 535-602.
- Welch, J. S., L. Escoubet-Lozach, et al. (2002). "TH2 cytokines and allergic challenge induce Ym1 expression in macrophages by a STAT6-dependent mechanism." J Biol Chem **277**(45): 42821-9.
- Wilson, M. S., S. K. Madala, et al. (2010). "Bleomycin and IL-1beta-mediated pulmonary fibrosis is IL-17A dependent." J Exp Med **207**(3): 535-52.
- Wilson, M. S. and T. A. Wynn (2009). "Pulmonary fibrosis: pathogenesis, etiology and regulation." Mucosal Immunol **2**(2): 103-21.
- Wong, B. R., D. Besser, et al. (1999). "TRANCE, a TNF family member, activates Akt/PKB through a signaling complex involving TRAF6 and c-Src." Mol Cell **4**(6): 1041-9.
- Wynn, T. A. (2004). "Fibrotic disease and the T(H)1/T(H)2 paradigm." Nat Rev Immunol **4**(8): 583-94.
- Wynn, T. A. (2008). "Cellular and molecular mechanisms of fibrosis." J Pathol **214**(2): 199-210.
- Wynn, T. A. (2011). "Integrating mechanisms of pulmonary fibrosis." J Exp Med **208**(7): 1339-50.
- Wynn, T. A. and T. R. Ramalingam (2012). "Mechanisms of fibrosis: therapeutic translation for fibrotic disease." Nat Med **18**(7): 1028-40.

## Literature

- Yang, H. Z., B. Cui, et al. (2009). "Targeting TLR2 attenuates pulmonary inflammation and fibrosis by reversion of suppressive immune microenvironment." J Immunol **182**(1): 692-702.
- Zhang, D. H., L. Cohn, et al. (1997). "Transcription factor GATA-3 is differentially expressed in murine Th1 and Th2 cells and controls Th2-specific expression of the interleukin-5 gene." J Biol Chem **272**(34): 21597-603.
- Zhu, J. and W. E. Paul (2010). "Heterogeneity and plasticity of T helper cells." Cell Res **20**(1): 4-12.